ISSN 0915-633X

NATIONAL INSTITUTE FOR FUSION SCIENCE

Mean-Field Theory and Self-Consistent Dynamo Modeling

A. Yoshizawa, N. Yokoi, S.-I Itoh and K. Itoh

(Received - Nov. 28, 2001)

NIFS-719 Dec. 2001

RESEARCH REPORT
NIFS Series

TOKI, JAPAN

Mean-Field Theory and Self-Consistent Dynamo Modeling

Akira Yoshizawa,[a] Nobumitsu Yokoi,[a] Sanae-I Itoh,[b] and Kimitaka Itoh[c]

[a]Institute of Industrial Science, University of Tokyo, Komaba, Meguro-ku, Tokyo 153-8505, Japan

[b]Research Institute for applied Mechanics, Kyushu University 87, Kasuga 816-8580, Japan

[c]National Institute for Fusion Science, Toki, Gifu 509-5292, Japan

Abstract. Mean-field theory of dynamo is discussed with emphasis on the statistical formulation of turbulence effects on the magnetohydrodynamic equations and the construction of a self-consistent dynamo model. The dynamo mechanism is sought in the combination of the turbulent residual-helicity and cross-helicity effects. On the basis of this mechanism, discussions are made on the generation of planetary magnetic fields such as geomagnetic field and sunspots and on the occurrence of flow by magnetic fields in planetary and fusion phenomena.

Keywords: turbulent dynamo, magnetohydrodynamics, turbulent theory, planetary magnetic fields, flow dynamo

Contents

1. Introduction
2. One-fluid magnetohydrodynamic approximation
   2.1. Fundamental equations
   2.2. Nondimensional parameters characterizing flows
   2.3. Elsasser's variables and conservation properties
3. Cowling's anti-dynamo theorem
4. Fundamentals of mean-field theory
   4.1. Mean-field equations
   4.2. Turbulence equations
5. Theoretical estimate of turbulence effects on magnetic-field equations
   5.1. Quasi-kinematic method
   5.2. Counter-kinematic method
   5.3. Discussions on dynamo effects from quasi-kinematic and
        counter-kinematic methods
   5.4. Magnetohydrodynamic method
6. One-point dynamo modeling with emphasis on self-consistency
   6.1. Necessity and significance of one-point modeling
   6.2. Modeling policy and procedures
   6.3. Summary of dynamo model
7. Typical magnetic-field generation processes
   7.1. Dominant-helicity dynamo
   7.2. Dominant/cross-helicity dynamo
   7.3. Traditional kinematic dynamo
8. Application to astro/geophysical and fusion dynamo phenomena
   8.1. Solar magnetic fields
   8.2. Geomagnetic fields
   8.3. Collimation of accretion jets
   8.4. Reversed-field pinches of plasmas
   8.5. Plasma rotation in tokamaks
9. Summary

References

Appendix: Statistical theory and modeling of electrically nonconducting turbulence
   A1. Perturbational method to turbulence
   A2. Introduction of Green's function
   A3. Evaluation of Reynolds stress
   References

1. Introduction

Magnetic-field generation in stellar objects such as the earth and the sun is a structure-formation phenomenon in nature. The interiors of the earth and the sun are schematically shown in Figs. 1 and 2 (the radii of the earth and the sun are 6300 km and 700000 km, respectively). The earth consists of the mantle, the outer core, and the inner core, whose primary ingredients are silicon, melted iron, and solid iron, respectively. Earth's magnetic field (the geomagnetic field) occurs from the motion of melted iron in the outer core. There the velocity is inferred to be $O(10^{-4})$ m s^{-1} from some geophysical observations, and the kinematic viscosity of melted iron is of the same order as for water [about $O(10^{-6})$ m^2 s^{-1}]. Then the Reynolds number R_e is estimated to be $O(10^8)$, suggesting that the fluid motion in the outer core is turbulent.

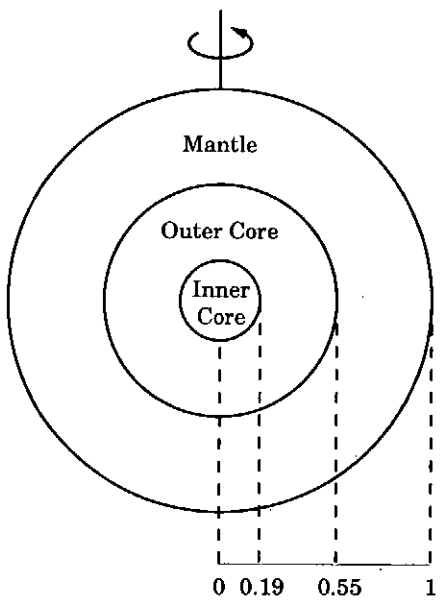

Fig. 1. Interior of the earth.

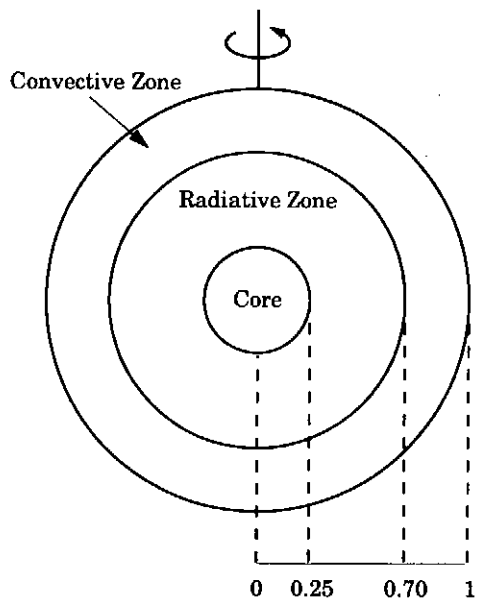

Fig. 2. Interior of the sun.

One of the prominent features of turbulent flow is the enhancement of diffusion or mixing effects. They often destroy distinct global structures of flow. Such a typical instance is a flow in a circular pipe. In the laminar state, the flow is subject to a parabolic velocity profile. With the intensification of velocity fluctuations, this velocity profile is lost. In the fully-developed turbulent state, the flattened mean velocity profile appears except the vicinity of the pipe wall. This change of flow structure may be captured through the enhancement of momentum diffusion across the cross section of the pipe. In the context of the foregoing geomagnetic field, its distinct global profile persists against the enhanced diffusion effect by turbulent motion. This mechanism is generally called

dynamo, and its study from the viewpoint of turbulence theory is one of the primary subjects in this review.

Some typical features of the geomagnetic field are summarized as follows [1, 2]

(E1) The main component of the geomagnetic field observed at the surface is the dipole field whose present axis is nearly along earth's rotation axis. The strength of the field is about a few Gauss (G).

(E2) The toroidal component is not observable at the surface since it is confined below the bottom of the mantle that is electrically nonconducting. The unobservable toroidal component is inferred to be of $O(10) \sim O(10^2)$ G, which is stronger than the dipole one.

(E3) The polarity of the geomagnetic field reverses irregularly in the interval of $O(10^5) \sim O(10^7)$ years, but the time necessary for the reversal is much shorter and is less than $O(10^4)$ years.

The formation of the distinct dipole field in a turbulent fluid motion is a central concern in the study of the generation mechanism of geomagnetic field (geodynamo). The situation that the toroidal field is not observable is a big stumbling block for the study of geodynamo. The magnetic energy of 1 G per unit mass of iron is equivalent to the kinetic energy of velocity $O(10^{-3})$ m s^{-1}. Then the energy of the dipole field of a few G is some hundred times the kinetic energy of the melted iron with an estimated velocity $O(10^{-4})$ m s^{-1}. With the unobservable toroidal component included, the energy of the geomagnetic field is $O(10^4) \sim O(10^6)$ times the kinetic energy of the fluid motion or the generator of the former. This leads us to a rather surprising conclusion that the geomagnetic field is generated quite efficiently by the turbulent fluid motion in the outer core. A proposed geodynamo model needs to address this point adequately. The persistence of one geomagnetic polarity is quite long, compared with the sun referred to below, which indicates that the dipole field along earth's rotation axis is very stable. The clarification of the mechanism for such stableness is also an important theme of geodynamo.

In contrast to the earth, the solar constitution is simple, and its constituents are hydrogen (90 percent) and helium (10 percent). All the solar energy arises from the thermonuclear fusion reaction in the core, and the resulting heat is supplied to the outermost or convective zone through the intermediate or radiative zone. The motion of highly ionized hydrogen gases in the convective zone is strongly turbulent. It is the origin of solar magnetic fields, whose most typical manifestation is sunspots. Inside the zone,

the toroidal field aligned with the equator is generated, and loops of this field rise up owing to buoyancy effects and break through the photosphere above the convective zone. Their cross sections are observed as pairs of sunspots (Fig. 3). The intensity of a large-sunspot magnetic field is a few kG, and the toroidal field with the intensity stronger by one order is inferred to be generated near the bottom of the convective zone.

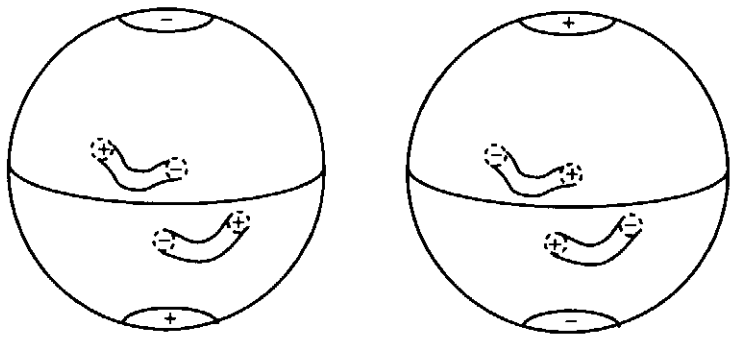

Fig. 3. Sunspot's polarity rule.

Sunspots obey the well-known polarity rule, whose primary parts may be stated as follows [3, 4].

(S1) Sunspots are limited to the middle- to low-latitude region. The polarity reverses quite regularly, that is, in about 11 years.

(S2) The polarity of the leading sunspot is coincident with the polarity of the polar field or the poloidal field near the pole of the hemisphere (Fig. 3). The latter is a few G and is very weak, compared with sunspot's magnetic field.

In the relative intensity of poloidal to toroidal components, the solar poloidal field is very weak than its geomagnetic counterpart, as was noted above. It is important to clarify the relationship of this point with the regular polarity reversal.

At the early stage of the dynamo study, the kinematic approach plays a leading role. There the generation mechanism of magnetic fields is examined using the magnetic induction equation with a properly chosen fixed velocity field [5]. Afterwards, the computer simulation based on a combined system of fluid and magnetic-field equations became feasible with the remarkable advancement of computer capability. In reality, a large amount of information has already been obtained about the generation processes of magnetic fields in the presence of a highly three-dimensional motion of an electrically conducting fluid [6-7].

A computer simulation in the dynamo study does not take the place of an analytical method developing from the kinematic approach. The reason may be stated as follows.

(i) Nondimensional parameters characterizing the fluid motion in stellar objects are very large. They are the Taylor number (T_a), the Rayleigh number (R_a), etc., where T_a is the square of the ratio of Coriolis to molecular viscous forces, and R_a is the product of the Prandtl number (the ratio of kinematic viscosity to thermal diffusivity) and the square of the ratio of buoyancy to molecular viscous forces. In the current study of electrically nonconducting flows such as channel flow, the complete computer simulation capturing energy-dissipative components of motion is limited for $R_e \leq O(10^4)$. Then a computer simulation closely mimicking the situation close to the earth and the sun is not possible in the near future.

(ii) In a computer dynamo simulation, a large amount of numerical data is available in general. Those data are analyzed on the basis of computer graphics, and spatial and temporal properties of magnetic fields are investigated. The current geodynamo simulations may really show that the energy of generated magnetic fields is much larger than the kinetic energy of flow, as is consistent with the foregoing conjecture. These simulations, however, have not yet succeeded in revealing what is the key process in storing such a large amount of magnetic energy.

A representative analytical approach to dynamo is mean-field theory [9-12]. In the approach based on the application of ensemble averaging, attention is focused on global characteristics of magnetic fields at the cost of highly time-dependent properties. As a result, large nondimensional parameters are not a critical stumbling block for mean-field theory. Specifically, the theory is suitable for detecting the properties common to geodynamo, solar dynamo, etc. since the key dynamo processes are explored in a mathematical but not numerical form. From each merit of mean-field theory and a computer simulation, one is complementary to the other in the study of planetary dynamo.

An astronomical instance of distinct global flow profiles in turbulence is the collimation of astronomical jets. High-mass objects such as active galactic nuclei, neutron stars, protostars, etc. are surrounded by gases in the form of a disk [13-15]. The disk is called an accretion disk (Fig. 4). Gases accrete onto the objects while rotating, resulting in the release of the gravitational energy and the angular momentum. The gravitational energy is a primary source of energetic activities of those objects.

The process through which gases release the angular momentum is a great concern in understanding the physics of accretion-disk phenomena. Two mechanisms may be

mentioned for the release of angular momentum. One is the angular-momentum transport by the turbulent motion of gases towards the outer part of the disk. The other is the release by ubiquitously observed bipolar jets that are composed of parts of accreting gases and are driven in the two directions normal to the disk. The jet speed is $O(10) \sim O(10^2)$ km s^{-1} for protostars and several ten percent of light speed for active galactic nuclei, respectively.

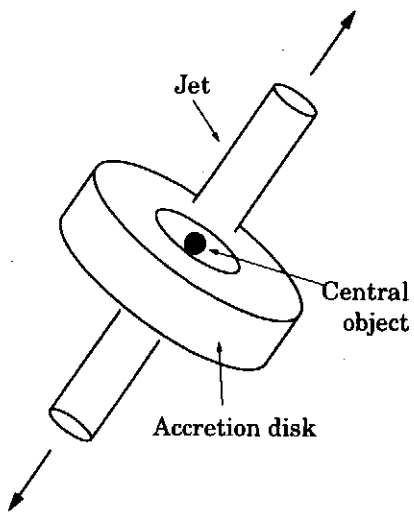

Fig. 4. Accretion disk and bipolar jets.

A noteworthy feature of the foregoing bipolar jets is the high collimation; namely, they keep a straight shape with an extremely small growth of jet width. For the mechanism of high collimation, there are two candidates. One is the suppression of jet growth due to high-Mach-number effects on turbulent flow, and the other is the confinement of gases by magnetic fields since accretion gases are often ionized owing to their high temperature.

The present review is organized as follows. In § 2, we give a brief explanation of a system of one-fluid magnetohydrodynamic (MHD) equations. In § 3, we refer to Cowling's anti-dynamo theorem leading to the introduction of the concept of turbulent dynamo. In § 4, we give the fundamentals of mean field theory. In § 5, we discuss on the dynamo effects by turbulence from three different viewpoints: quasi-kinematic, counter-kinematic, and MHD approaches. In § 6, we make full use of these findings and construct a one-point dynamo model applicable to real-world phenomena, with emphasis put on its self-consistency. In § 7, we discuss on some typical processes of magnetic-field generation and the resulting feedback effects. In § 8, we investigate into the generation of planetary magnetic fields and the flow occurrence by magnetic effects in planetary and fusion phenomena. In § 9, we give a simple summary of this review. In

Appendix, we explain a statistical theory of turbulence that is helpful to the derivation of dynamo effects in the MHD system.

2. One-Fluid Magnetohydrodynamic Approximation

2.1. Fundamental equations

In § 1, we referred to the generation of large-scale magnetic-field structures by fluid motion and the high collimation of bipolar jets from an accretion disk. A useful tool for investigating into these phenomena is the magnetohydrodynamic (MHD) approximation, specifically, the one-fluid approximation [16, 17]. In what follows, we shall give its brief account and refer to the limitation.

The motions of electron and ion gases are governed by

$$\frac{\partial \rho_S^{(M)}}{\partial t} + \nabla \cdot \left(\rho_S^{(M)} \mathbf{v}_S \right) = 0, \tag{2.1}$$

$$\frac{\partial}{\partial t} \rho_S^{(M)} v_{Si} + \frac{\partial}{\partial x_j} \rho_S^{(M)} v_{Sj} v_{Si} = - \frac{\partial p_S}{\partial x_i} + \rho_S^{(C)} \left(\mathbf{e} + \mathbf{v}_S \times \mathbf{b} \right)_i + C_{Si}, \tag{2.2}$$

with subscript S denoting E and I for electron and ion, respectively. Here $\rho_S^{(M)}$ is the mass density, $\mathbf{v}_S$ is the gas velocity, p_S is the gas pressure, $\rho_S^{(C)}$ is the charge density, $\mathbf{e}$ is the electric field, and $\mathbf{b}$ is the magnetic field. On the right-hand side of Eq. (2.2), the second term is the Lorentz force, and $\mathbf{C}_S$ is the force arising from the collision between electron and ion, which is expressed as

$$\mathbf{C}_E = -\mathbf{C}_I = -\rho_E^{(M)} (\mathbf{v}_E - \mathbf{v}_I) \nu_{EI}, \tag{2.3}$$

with ν_{EI} as the collision frequency. The mass density $\rho_S^{(M)}$ and the charge density $\rho_S^{(C)}$ are written as

$$\rho_S^{(M)} = n_S m_S, \tag{2.4}$$

$$\rho_S^{(C)} = n_S e_S, \tag{2.5}$$

with $e_E = -e_0$ and $e_I = Ze_0$, where n_S and m_S are the number density and the mass of ion or electron, respectively, and e_0 is the charge of an electron.

In the one-fluid MHD approximation, we introduce the total mass density ρ, the associated fluid velocity $\mathbf{u}$, the total pressure p, and the electric current density $\mathbf{j}$ as

$$\rho = \rho_E^{(M)} + \rho_I^{(M)}, \tag{2.6}$$

$$\mathbf{u} = \frac{\rho_E^{(M)}\mathbf{v}_E + \rho_I^{(M)}\mathbf{v}_I}{\rho}, \tag{2.7}$$

$$p = p_E + p_I, \tag{2.8}$$

$$\mathbf{j} = -n_E e_0 \mathbf{v}_E + n_I Z e_0 \mathbf{v}_I, \tag{2.9}$$

respectively. Here we note the difference between the masses of electron and ion, that is,

$$\frac{m_E}{m_I} = O\left(10^{-3}\right), \tag{2.10}$$

which signifies

$$\rho \cong \rho_I^{(M)}, \tag{2.11}$$

$$\mathbf{u} = \mathbf{v}_I. \tag{2.12}$$

The key assumption of the one-fluid MHD approximation is the quasi-neutrality of charge density,

$$\rho_C = \rho_E^{(C)} + \rho_I^{(C)} = -n_E e_0 + Z n_I e_0 \cong 0. \tag{2.13}$$

Under Eq. (2.13), Eq. (2.9) is rewritten as

$$\mathbf{j} = -n_E e_0 \left(\mathbf{v}_E - \mathbf{v}_I\right). \tag{2.14}$$

We combine Eq. (2.1) for electron gas with its ion counterpart, and use Eqs. (2.6) and (2.7). Then we have

$$\frac{\partial \rho}{\partial t} + \nabla \cdot (\rho \mathbf{u}) = 0. \tag{2.15}$$

Similarly, the combination of Eq. (2.2) with Eqs. (2.11)-(2.13) results in

$$\frac{\partial}{\partial t}\rho u_i + \frac{\partial}{\partial x_j}\rho u_j u_i = -\frac{\partial p}{\partial x_i} + (\mathbf{j} \times \mathbf{b})_i$$

$$+ \frac{\partial}{\partial x_j}\left(\mu\left(\frac{\partial u_j}{\partial x_i} + \frac{\partial u_i}{\partial x_j} - \frac{2}{3}\nabla \cdot \mathbf{u}\delta_{ij}\right) + \zeta_V \nabla \cdot \mathbf{u}\delta_{ij}\right). \tag{2.16}$$

Here we should note the following two points. One is the disappearance of the electric field $\mathbf{e}$, which arises from the quasi-neutrality assumption, Eq. (2.13). As a result, the study of fusion phenomena closely related to $\mathbf{e}$ effects is beyond the scope of the one-fluid MHD approximation. The other is that the diffusion effect arising from the collision among ions themselves is supplemented as the last part of Eq. (2.16), where μ is the viscosity, and ζ_V is the bulk viscosity.

In this review, we shall pay special attention to the case of constant mass density and discuss on the generation mechanism of magnetic fields as well as their feedback effects. Density-variation effects will be partially taken into account through the buoyancy force. By this approach, we do not intend to say that effects of density variation are not important in those studies, but we aim at abstracting some of essential ingredients in the generation process of magnetic fields.

In the frame rotating with angular velocity $\boldsymbol{\omega}_F$, the constant-density counterparts of Eqs. (2.15) and (2.16) are [18, 19]

$$\nabla \cdot \mathbf{u} = 0, \tag{2.17}$$

$$\frac{\partial u_i}{\partial t} + \frac{\partial}{\partial x_j} u_j u_i = \left(\frac{\partial}{\partial t} + \mathbf{u} \cdot \nabla \right) u_i = -\frac{1}{\rho} \frac{\partial p}{\partial x_i} + \nu \nabla^2 u_i$$

$$+ \frac{1}{\rho} (\mathbf{j} \times \mathbf{b})_i + 2(\mathbf{u} \times \boldsymbol{\omega}_F)_i - \alpha_T (\theta - \theta_R) g_i, \tag{2.18}$$

with $\nu = \mu / \rho$ (kinematic viscosity). In the second relation of Eq. (2.18), the fourth term is the Coriolis force, and the fifth term is the buoyancy force based on the Boussinesq approximation (α_T is the thermal-expansion coefficient, θ_R is the reference temperature, and $\mathbf{g}$ is the gravitational-acceleration vector). In Eq. (2.18), p denotes the deviation from the static pressure. The temperature θ obeys

$$\frac{\partial \theta}{\partial t} + \nabla \cdot (\theta \mathbf{u}) = \lambda_\theta \nabla^2 \theta. \tag{2.19}$$

The Boussinesq approximation is originally appropriate for the situation that the temperature difference in fluid motion is not so large. Then the approximation needs careful treatment in the application to the phenomena subject to large temperature difference such as the sun. The buoyancy force originating in the density difference of constituents may also become important in geodynamo. In the outer core of the earth, its main constituent is melted iron, but silicon is also included there. Their mass difference is a promising candidate for the force driving melted iron, as well as the thermal force.

We consider Eq. (2.2) for electron gas, and retain the Lorentz and collision forces. Then we have

$$\mathbf{e}+\mathbf{v}_E\times\mathbf{b}+\frac{m_E\nu_{EI}}{e_0}(\mathbf{v}_E-\mathbf{v}_I)=0, \tag{2.20}$$

which is reduced to

$$\mathbf{e}+\mathbf{v}_E\times\mathbf{b}-\frac{m_E\nu_{EI}}{n_E e_0^{\,2}}\mathbf{j}=0, \tag{2.21}$$

under Eq. (2.14). From Eqs. (2.12) and (2.14), we have

$$\mathbf{v}_E=\mathbf{u}-\frac{1}{n_E e_0}\mathbf{j}. \tag{2.22}$$

We substitute Eq. (2.22) into Eq. (2.21), and have

$$\mathbf{j}=\sigma(\mathbf{e}+\mathbf{u}\times\mathbf{b})+\frac{\sigma}{\rho_C^{(E)}}\mathbf{j}\times\mathbf{b}, \tag{2.23}$$

where σ is the electric conductivity defined by

$$\sigma=\frac{n_E e_0^{\,2}}{m_E\nu_{EI}}. \tag{2.24}$$

The retention of the first part in Eq. (2.23) leads to the simplest Ohm's law.

In the case of constant fluid density, the use of Alfven-velocity units leads to the concise form of fundamental equations. In the units, $\mathbf{b}/\sqrt{\rho\mu_0}$ has the dimension of velocity, where μ_0 is the magnetic permeability. We make use of this fact and make the replacement

$$\frac{\mathbf{b}}{\sqrt{\rho\mu_0}}\to\mathbf{b},\quad\frac{\mathbf{j}}{\sqrt{\rho/\mu_0}}\to\mathbf{j},\quad\frac{\mathbf{e}}{\sqrt{\rho\mu_0}}\to\mathbf{e},\quad\frac{p}{\rho}\to p. \tag{2.25}$$

Under this replacement, Eq. (2.18) is reduced to

$$\frac{\partial u_i}{\partial t}+\frac{\partial}{\partial x_j}u_j u_i=\left(\frac{\partial}{\partial t}+\mathbf{u}\cdot\nabla\right)u_i=-\frac{\partial p}{\partial x_i}+\nu\nabla^2 u_i$$

$$+(\mathbf{j}\times\mathbf{b})_i+2(\mathbf{u}\times\boldsymbol{\omega}_F)_i-\alpha_T(\theta-\theta_R)g_i \tag{2.26a}$$

or

$$\frac{\partial u_i}{\partial t}+\frac{\partial}{\partial x_j}u_j u_i = -\frac{\partial}{\partial x_i}\left(p+\frac{\mathbf{b}^2}{2}\right)+\nu\nabla^2 u_i$$

$$+\frac{\partial}{\partial x_j}b_j b_i+2(\mathbf{u}\times\boldsymbol{\omega}_F)_i-\alpha_T(\theta-\theta_R)g_i. \tag{2.26b}$$

In Alfven-velocity units, the magnetic induction equation, the Ampere's law, and the Ohm's law are written as

$$\frac{\partial \mathbf{b}}{\partial t}=-\nabla\times\mathbf{e}, \tag{2.27}$$

$$\mathbf{j}=\nabla\times\mathbf{b}, \tag{2.28}$$

$$\mathbf{j}=\frac{1}{\lambda_M}(\mathbf{e}+\mathbf{u}\times\mathbf{b}), \tag{2.29}$$

respectively, where λ_M is defined by

$$\lambda_M=\frac{1}{\sigma\mu_0}. \tag{2.30}$$

We use Eqs. (2.28) and (2.29), and eliminate $\mathbf{e}$ from Eq. (2.27). As a result, we have

$$\frac{\partial \mathbf{b}}{\partial t}=\nabla\times(\mathbf{u}\times\mathbf{b})+\lambda_M\nabla^2\mathbf{b} \tag{2.31a}$$

or

$$\frac{\partial \mathbf{b}}{\partial t}+(\mathbf{u}\cdot\nabla)\mathbf{b}-(\mathbf{b}\cdot\nabla)\mathbf{u}=\lambda_M\nabla^2\mathbf{b}, \tag{2.31b}$$

from which we may see that λ_M signifies the magnetic diffusivity. Here we should recall that the disappearance of $\mathbf{e}$ effects is closely related to the quasi-neutrality assumption, Eq. (2.13), leading to Eq. (2.14).

2.2. Nondimensional parameters characterizing flows

The importance of each term in Eqs. (2.26) and (2.31) changes greatly from one phenomenon to another. The most familiar parameter is the Reynolds number R_e, which is defined by

$$R_e = \frac{\{(\mathbf{u}\cdot\nabla)\mathbf{u}\}_{\ell_R,u_R}}{\{\nu\nabla^2\mathbf{u}\}_{\ell_R,u_R}} = \frac{\ell_R u_R}{\nu}. \tag{2.32}$$

Here ℓ_R and u_R are the reference length and the reference velocity, respectively, and $\{f\}_{\xi,\eta}$ denotes the magnitude of f that is estimated using quantities ξ and η.

The nondimensional parameter related to the Coriolis force is the Taylor number

$$T_a = \left(\frac{\{\mathbf{u}\times\boldsymbol{\omega}_F\}_{u_R}}{\{\nu\nabla^2\mathbf{u}\}_{\ell_R,u_R}}\right)^2 = \frac{{\ell_R}^4{\omega_F}^2}{\nu^2}. \tag{2.33}$$

Since $\ell_R\omega_F$ is the velocity associated with frame rotation, we may see that T_a is the square of the Reynolds number R_e based on velocity $\ell_R\omega_F$ and length ℓ_R.

The magnitude of the buoyancy force due to the Boussinesq approximation is characterized by the Rayleigh number

$$R_a = \left(\frac{\{\alpha_T(\theta-\theta_R)\mathbf{g}\}_{\Delta\theta_R}}{\{\nu\nabla^2\mathbf{u}\}_{\ell_R,u_R}}\right)^2 P_r, \tag{2.34}$$

where $\Delta\theta_R$ is the reference temperature difference characterizing $\theta-\theta_R$, and P_r is the Prandtl number denoted by

$$P_r = \frac{\nu}{\lambda_\theta}. \tag{2.35}$$

The reference velocity linked with the buoyancy force is estimated as

$$\{(\mathbf{u}\cdot\nabla)\mathbf{u}\}_{\ell_R,u_R} = \{\alpha_T(\theta-\theta_R)\mathbf{g}\}_{\Delta\theta_R}, \tag{2.36}$$

which gives

$$u_R = \sqrt{\alpha_T g\Delta\theta_R\ell_R}. \tag{2.37}$$

We substitute Eq. (2.37) into Eq. (2.34), and have

$$R_a = \frac{\alpha_T g\Delta\theta_R{\ell_R}^3}{\nu\lambda_\theta}, \tag{2.38}$$

as the Rayleigh number for the Boussinesq buoyancy force. As is seen from Eqs. (2.34) and (2.36), R_a may be regarded as the square of R_e in the case of $P_r = O(1)$.

The magnetic-field counterpart of R_e is the magnetic Reynolds number

$$R_{eM} = \frac{\left\{\nabla\times(\mathbf{u}\times\mathbf{b})\right\}_{\ell_R,u_R}}{\left\{\lambda_m\nabla^2\mathbf{b}\right\}_{\ell_R,u_R}} = \frac{\ell_R u_R}{\lambda_m} = R_e P_{rM}. \tag{2.39}$$

Here P_{rM} is the magnetic Prandtl number given by

$$P_{rM} = \frac{\nu}{\lambda_M}. \tag{2.40}$$

In Eq. (2.32), large R_e signifies that the advection or inertia effect is dominant at the length scale ℓ_R and its associated velocity scale u_R, compared with the molecular diffusion effect. This fact does not mean that the latter effect is not important at large R_e, but that it may become important at the spatial scale much smaller than ℓ_R.

In order to see the physical meaning of T_a, we drop the Lorentz and buoyancy forces in Eq. (2.26), and take its curl. Then we have

$$\frac{\partial\boldsymbol{\omega}}{\partial t} = \nabla\times\left(\mathbf{u}\times\left(\boldsymbol{\omega}+2\boldsymbol{\omega}_F\right)\right)+\nu\nabla^2\boldsymbol{\omega}, \tag{2.41}$$

where $\boldsymbol{\omega}\,(=\nabla\times\mathbf{u})$ is the vorticity. In the case of large R_e, we pay special attention to the length scale ℓ_R and drop the molecular diffusion term. In the stationery state, we have

$$\nabla\times\left(\mathbf{u}\times\left(\boldsymbol{\omega}+2\boldsymbol{\omega}_F\right)\right)=0. \tag{2.42}$$

For the case of a strong Coriolis effect or $T_a >> R_e$, Eq. (2.42) is reduced to

$$\nabla\times\left(\mathbf{u}\times\boldsymbol{\omega}_F\right)=0, \tag{2.43}$$

which is equivalent to

$$\left(\boldsymbol{\omega}_F\cdot\nabla\right)\mathbf{u}=0. \tag{2.44}$$

Namely, the fluid motion does not change along the axis of frame rotation. In this sense, the motion becomes two dimensional. This finding is called the Taylor-Proudman theorem.

The Taylor-Proudman theorem becomes important in a spherical or spherical-shell region with the buoyancy force in the radial direction as a primary cause of fluid motion. The buoyancy force whose strength is characterized by the Rayleigh number R_a drives fluid from the inner to outer part of the region. With the increase in the Taylor number T_a, a fluid blob at one location is trapped around an axis along the frame-rotation vector $\boldsymbol{\omega}_F$. As a result, fluid comes up or down along this axis, while rotating; namely, it is subject to helical motion (the similar situation may be seen in the motion of a charged particle around a magnetic field line). Such fluid motion constitutes the so-called convection columns [20], as is depicted schematically in Fig. 5. A typical quantity characterizing the columns is the helicity $\mathbf{u}\cdot\boldsymbol{\omega}$. The properties of convection columns found by computer simulations will be later referred to in the light of geodynamo and solar dynamo.

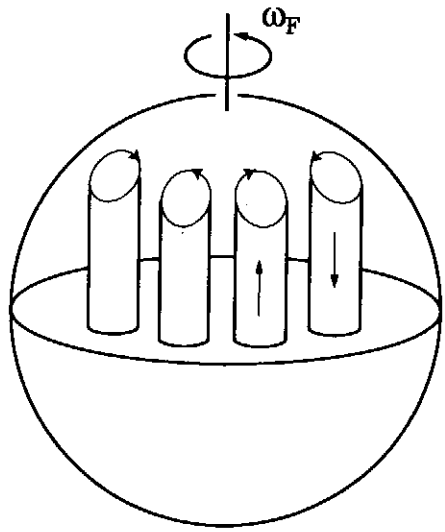

Fig. 5. Convection columns.

In the case of the earth's outer core, we have

$$\ell_R = O\left(10^6\right)\ \mathrm{m},\ \nu = O\left(10^{-6}\right)\ \mathrm{m^2\ s^{-1}},\ u_R = O\left(10^{-4}\right)\ \mathrm{m\ s^{-1}},$$

$$P_r = O\left(10^{-1}\right),\ P_{rM} = O\left(10^{-6}\right). \tag{2.45}$$

Here ν, P_r, and P_{rM} are the values for melted iron, and u_R is the value inferred from geophysical observations. We use $\omega_F = 7\times 10^{-5}\ \mathrm{rad\ s^{-1}}$, and have

$$R_e = O\left(10^8\right),\ T_a = O\left(10^{27}\right),\ R_a = O\left(10^{16}\right),\ R_{eM} = O\left(10^2\right) \tag{2.46}$$

[R_a is estimated from the discussion below Eq. (2.38), and R_{eM} is found from Eq. (2.39)]. From Eq. (2.46), the magnetic field in the outer core is much more diffusive than the momentum.

In the case of the solar convective zone, the flow velocity and the spatial scale are much larger, compared with the earth's outer core. Moreover, the convective zone is highly electrically conducting, resulting in the lower magnetic diffusivity. As a result, both R_e and R_{eM} are much larger than the values in Eq. (2.46). On the other hand, T_a in the convective zone is of $O(10^{20})$, which is smaller than the counterpart in Eq. (2.46). This fact indicates that the role of the convective columns becomes smaller in the solar convective zone. Geometrically, the solar convective zone is a thin spherical shell, and convective columns are limited to the low-latitude region. This situation also suggests a smaller role of helicity effects in the zone.

2.3. Elsasser's variables and conservation properties

For an electrically nonconducting fluid of constant density, the total amount of kinetic energy is conserved in the absence of molecular viscous effects. In the case, the turbulence part of kinetic energy obeys the equation whose mathematical and physical bases are firm. This point will become clear in later discussions. In order to see what quantities may be conserved in MHD flows, we introduce Elsasser's variables

$$\boldsymbol{\phi} = \mathbf{u} + \mathbf{b}, \quad \boldsymbol{\psi} = \mathbf{u} - \mathbf{b}, \tag{2.47}$$

which lead to

$$\mathbf{u} = \frac{\boldsymbol{\phi} + \boldsymbol{\psi}}{2}, \quad \mathbf{b} = \frac{\boldsymbol{\phi} - \boldsymbol{\psi}}{2}. \tag{2.48}$$

In Eq. (2.26b), we drop the Coriolis and Boussinesq terms, and apply Eq. (2.47) to the resulting equation. Then we have

$$\frac{\partial \boldsymbol{\phi}}{\partial t} + (\boldsymbol{\psi} \cdot \nabla)\boldsymbol{\phi} = -\nabla\left(p + \frac{\mathbf{b}^2}{2}\right) + \frac{\nu + \lambda_M}{2}\nabla^2\boldsymbol{\phi} + \frac{\nu - \lambda_M}{2}\nabla^2\boldsymbol{\psi}, \tag{2.49}$$

$$\frac{\partial \boldsymbol{\psi}}{\partial t} + (\boldsymbol{\phi} \cdot \nabla)\boldsymbol{\psi} = -\nabla\left(p + \frac{\mathbf{b}^2}{2}\right) + \frac{\nu + \lambda_M}{2}\nabla^2\boldsymbol{\psi} + \frac{\nu - \lambda_M}{2}\nabla^2\boldsymbol{\phi}. \tag{2.50}$$

In the absence of the molecular effects, Eqs. (2.49) and (2.50) give

$$\frac{\partial}{\partial t}\int_V \frac{\boldsymbol{\phi}^2}{2} dV = -\int_V \nabla \cdot \left(\frac{\boldsymbol{\phi}^2}{2} \boldsymbol{\psi} + \left(p + \frac{\mathbf{b}^2}{2} \right) \boldsymbol{\phi} \right) dV = -\int_S \mathbf{n} \cdot \left(\frac{\boldsymbol{\phi}^2}{2} \boldsymbol{\psi} + \left(p + \frac{\mathbf{b}^2}{2} \right) \boldsymbol{\phi} \right) dS, \tag{2.51}$$

$$\frac{\partial}{\partial t}\int_V \frac{\boldsymbol{\psi}^2}{2} dV = -\int_V \nabla \cdot \left(\frac{\boldsymbol{\psi}^2}{2} \boldsymbol{\phi} + \left(p + \frac{\mathbf{b}^2}{2} \right) \boldsymbol{\psi} \right) dV = -\int_S \mathbf{n} \cdot \left(\frac{\boldsymbol{\psi}^2}{2} \boldsymbol{\phi} + \left(p + \frac{\mathbf{b}^2}{2} \right) \boldsymbol{\psi} \right) dS, \tag{2.52}$$

with the aid of the Gauss integral theorem (V and S denote the whole flow region and its surrounding surface, respectively). Then the total amounts of $\boldsymbol{\phi}^2$ and $\boldsymbol{\psi}^2$ are conserved so long as there are neither their net supply nor loss across the surface.

The electrically-nonconducting counterpart of Eq. (2.51) or (2.52) is written as

$$\frac{\partial}{\partial t}\int_V \left(\frac{1}{2}\mathbf{u}^2 \right) dV = -\int_S \mathbf{n} \cdot \left(\left(\frac{1}{2}\mathbf{u}^2 + p \right) \mathbf{u} \right) dS. \tag{2.53}$$

From Eq. (2.53), we may simply confirm that the total amount of kinetic energy is conserved in the absence of molecular viscous effects.

The conservation of the total amounts of $\boldsymbol{\phi}^2$ and $\boldsymbol{\psi}^2$ is equivalent to that of $\boldsymbol{\phi}^2 \pm \boldsymbol{\psi}^2$. From Eq. (2.47), we have

$$\frac{1}{4}\left(\boldsymbol{\phi}^2 + \boldsymbol{\psi}^2 \right) = \frac{\mathbf{u}^2}{2} + \frac{\mathbf{b}^2}{2}, \tag{2.54}$$

$$\frac{1}{4}\left(\boldsymbol{\phi}^2 - \boldsymbol{\psi}^2 \right) = \mathbf{u} \cdot \mathbf{b}, \tag{2.55}$$

which are called the MHD energy and cross helicity, respectively. These two quantities are also conserved in the absence of molecular effects and their net supply or loss across a boundary. In MHD flows, however, the kinetic helicity $\mathbf{u} \cdot \boldsymbol{\omega}$ is not subject to such a conservation law, unlike the electrically nonconducting case. The foregoing discussions suggest that the MHD energy and the cross helicity are the fundamental quantities in the investigation into MHD flow.

Between the MHD energy and cross helicity, we have the relation

$$\frac{\mathbf{u}^2}{2} + \frac{\mathbf{b}^2}{2} \geq |\mathbf{u} \cdot \mathbf{b}|, \tag{2.56}$$

Here the equality holds for

$$\mathbf{u}+\mathbf{b}=0 \quad \text{or} \quad \mathbf{u}-\mathbf{b}=0, \tag{2.57a}$$

which is equivalent to

$$\phi=0 \quad \text{or} \quad \psi=0. \tag{2.57b}$$

3. Cowling's Anti-Dynamo Theorem

We introduce the spherical coordinates (r,θ,ϕ) for examining MHD phenomena in a spherical region, as in Fig. 6. We write the toroidal and poloidal components of magnetic fields, $\mathbf{b}_T$ and $\mathbf{b}_P$, as

$$\mathbf{b}_T = b_\phi \mathbf{e}_\phi, \tag{3.1}$$

$$\mathbf{b}_P = b_r \mathbf{e}_r + b_\theta \mathbf{e}_\theta, \tag{3.2}$$

where $\mathbf{e}_r$, $\mathbf{e}_\theta$, and $\mathbf{e}_\phi$ are the unit vector in each of three directions. In earth's magnetic fields, the outer core is covered with the electrically nonconducting mantle, and $\mathbf{b}_T$ is not observable. Of the poloidal component, the strongest is the dipole field whose axis is nearly along the axis of earth's rotation.

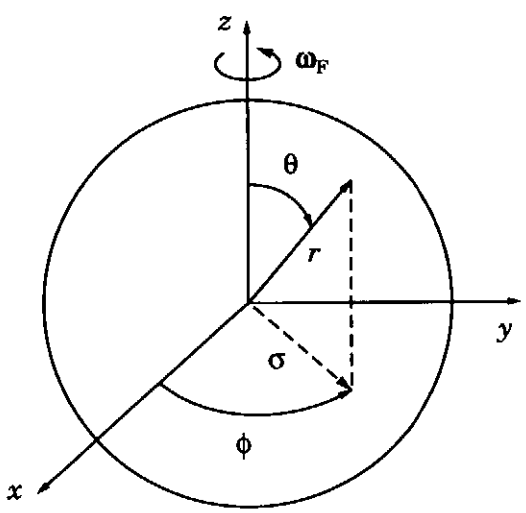

Fig. 6. Spherical and cylindrical coordinate systems.

In relation to the sustainment of axisymmetric magnetic fields, we have Cowling's anti-dynamo theorem [21, 22]. It says

"An axisymmetric flow cannot sustain an axisymmetric magnetic field in a stationary sense."

For understanding this theorem, we consider the axisymmetric poloidal field $\mathbf{b}_P$, as in Fig. 7. There C expresses the line along which $\mathbf{b}_P$ vanishes. On this line, we may rewrite the Ohm's law (2.29) as

$$\mathbf{j}_T = \frac{1}{\lambda_M}(\mathbf{e}+\mathbf{u}\times\mathbf{b}_T)_T = \frac{1}{\lambda_M}\mathbf{e}_T. \tag{3.3}$$

Here we should note that the toroidal current $\mathbf{j}_T$ is axisymmetric owing to the axisymmetry of $\mathbf{u}$ and $\mathbf{b}$. We integrate $\mathbf{j}_T$ along C and have

$$\oint_C \mathbf{j}_T\cdot\mathbf{ds} = \frac{1}{\lambda_M}\int_S(\nabla\times\mathbf{e})\cdot\mathbf{n}dS = -\frac{1}{\lambda_M}\int_S\frac{\partial\mathbf{b}}{\partial t}\cdot\mathbf{n}dS, \tag{3.4}$$

from the Stokes integral theorem, where S is an arbitrary surface spanned on C, and $\mathbf{n}$ is the unit vector normal to the surface. In a stationary state, Eq. (3.4) gives

$$\oint_C \mathbf{j}_T\cdot\mathbf{ds} = 0, \tag{3.5}$$

which signifies vanishing of $\mathbf{j}_T$ itself owing to its axisymmetry. As a result, $\mathbf{b}_P$ is not sustainable.

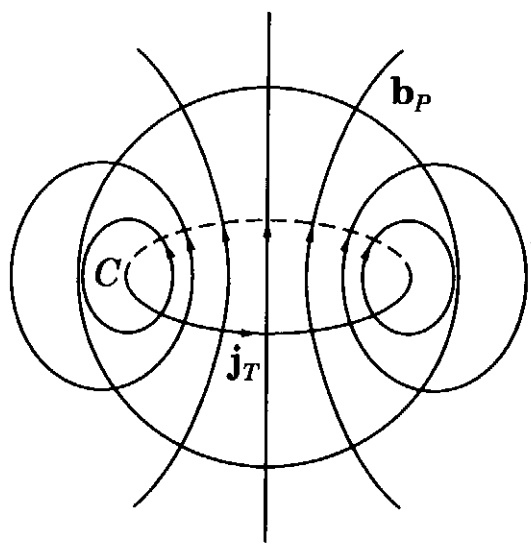

Fig. 7. Cowling's anti-dynamo theorem.

Cowling's anti-dynamo theorem indicates that a nonaxisymmetric motion is indispensable for the stationary sustainment of an axisymmetric components of $\mathbf{b}$. From the theorem, the analytical approach to the magnetic-field generation mechanism or dynamo is roughly divided into two categories. In one category, we introduce a small number of asymmetric flow components and study the process through which an

axisymmetric component of magnetic field occurs. This method is called laminar dynamo [9, 23].

The other is called mean-field theory or turbulent dynamo [9-12]. As was seen in § 2.2, Reynolds numbers encountered in astro/geophysical phenomena are very large, signifying that fluid motion is turbulent or highly asymmetric. In this method, our interest lies in the exploration of the mechanism under which symmetric fields are generated by highly asymmetric motion. The mechanism is the main theme of this review.

4. Fundamentals of Mean-Field Theory

4.1. Mean-Field Equations

In mean-field theory of dynamo, we are interested in large-scale properties of magnetic fields that are represented by earth's dipole field and solar toroidal field as the origin of sunspots. In order to abstract such properties, we apply the ensemble averaging procedure. In a spherical body such as the earth and the sun, we may regard it as equivalent to the averaging around the axis of rotation. In the averaging, the mean field is inevitably axisymmetric around the axis, and asymmetric properties are beyond the scope of this method. We shall pay special attention to axisymmetric components of field and discuss on theoretical aspects of dynamo.

We use the ensemble average $\langle\ \rangle$ and divide a quantity f into the mean F and the fluctuation around it, f', as

$$f = F + f', \quad F = \langle f \rangle, \tag{4.1}$$

where f, F, and f' denote

$$f = (\mathbf{u}, p, \boldsymbol{\omega}, \theta, \mathbf{b}, \mathbf{j}, \mathbf{e}), \tag{4.2a}$$

$$F = (\mathbf{U}, P, \boldsymbol{\Omega}, \Theta, \mathbf{B}, \mathbf{J}, \mathbf{E}), \quad f' = (\mathbf{u}', p', \boldsymbol{\omega}', \theta' \mathbf{b}', \mathbf{j}', \mathbf{e}'). \tag{4.2b}$$

We take the ensemble average of Eq. (2.26) with the Coriolis and buoyancy terms dropped, and have

$$\frac{DU_i}{Dt} = -\frac{\partial}{\partial x_i}\left(P + \left\langle \frac{\mathbf{b}'^2}{2} \right\rangle\right) + (\mathbf{J} \times \mathbf{B})_i + \frac{\partial}{\partial x_j}\left(-R_{ij}\right) + \nu \nabla^2 U_i, \tag{4.3}$$

with the solenoidal condition $\nabla \cdot \mathbf{U} = 0$. Here R_{ij} is the Reynolds stress in MHD flow and is defined by

$$R_{ij} = \langle u_i' u_j' - b_i' b_j' \rangle. \tag{4.4}$$

We may insert the neglected Coriolis and buoyancy effects into Eq. (4.3) when necessary.

The equation for the mean temperature Θ is

$$\frac{D\Theta}{Dt} = \nabla \cdot (-\mathbf{H}_\theta) + \lambda_\theta \nabla^2 \Theta, \tag{4.5}$$

from Eq. (2.19). Here $\mathbf{H}_\theta$ is the turbulent heat flux and is defined by

$$\mathbf{H}_\theta = \langle \mathbf{u}' \theta' \rangle. \tag{4.6}$$

From Eq. (2.31), the mean magnetic field $\mathbf{B}$ obeys

$$\frac{\partial \mathbf{B}}{\partial t} = \nabla \times (\mathbf{U} \times \mathbf{B} + \mathbf{E}_M) + \lambda_M \nabla^2 \mathbf{B}, \tag{4.7}$$

where $\mathbf{E}_M$ is defined by

$$\mathbf{E}_M = \langle \mathbf{u}' \times \mathbf{b}' \rangle \tag{4.8}$$

and is called the turbulent electromotive force. In this context, the mean Ohm's law is written as

$$\mathbf{J} = \frac{1}{\lambda_M} (\mathbf{E} + \mathbf{U} \times \mathbf{B} + \mathbf{E}_M). \tag{4.9}$$

In the original Ohm's law (2.29), the electric current arising from the direct interaction between $\mathbf{u}$ and $\mathbf{b}$ is normal to $\mathbf{b}$, resulting in Cowling's anti-dynamo theorem. In the presence of the turbulence effect $\mathbf{E}_M$, Eq. (3.4) is replaced with

$$\oint_C \mathbf{J}_T \cdot \mathbf{ds} = -\frac{1}{\lambda_M} \int_S \frac{\partial \mathbf{B}}{\partial t} \cdot \mathbf{n} dS + \frac{1}{\lambda_M} \oint_C \mathbf{E}_M \cdot \mathbf{ds}. \tag{4.10}$$

The occurrence of the second term in Eq. (4.10) leads to the possibility that axisymmetric $\mathbf{J}_T$ does not vanish in the stationary state with vanishing $\partial \mathbf{B} / \partial t$, escaping from Cowling's anti-dynamo theorem.

4.2. Turbulence Equations

In order to close Eqs. (4.3), (4.5), and (4.7), we need to express R_{ij}, $\mathbf{H}_\theta$, and $\mathbf{E}_M$ in terms of the mean field and the quantities characterizing MHD turbulent state. In § 2.3, we showed that the total amount of MHD energy [Eq. (2.54)] and the cross helicity [Eq. (2.55)] are conserved in the absence of molecular viscous and resistive forces. In order to explain the importance of this fact in the light of turbulence equations, we consider the case of electrically nonconducting flow. There the mean and turbulence parts of kinetic energy obey

$$\frac{\partial}{\partial t}\frac{\mathbf{U}^2}{2} = \langle u_i' u_j' \rangle \frac{\partial U_j}{\partial x_i} - \nu \left(\frac{\partial U_j}{\partial x_i} \right)^2$$

$$+ \frac{\partial}{\partial x_j} \left(-PU_i - R_{ij}U_j + \nu \frac{\partial}{\partial x_i} \left(\frac{\mathbf{U}^2}{2} \right) \right), \tag{4.11}$$

$$\frac{\partial}{\partial t} \left\langle \frac{\mathbf{u}'^2}{2} \right\rangle = -\langle u_i' u_j' \rangle \frac{\partial U_j}{\partial x_i} - \nu \left\langle \left(\frac{\partial u_j'}{\partial x_i} \right)^2 \right\rangle$$

$$+ \nabla \cdot \left(-\left\langle \frac{\mathbf{u}'^2}{2} \right\rangle \mathbf{U} - \left\langle \left(\frac{1}{2}\mathbf{u}'^2 + p' \right) \mathbf{u}' \right\rangle + \nu \nabla \left\langle \frac{\mathbf{u}'^2}{2} \right\rangle \right). \tag{4.12}$$

On the right-hand side of Eq. (4.12), each term is called the production, dissipation, and diffusion terms of turbulent energy.

In order to see the physical meaning of Eq. (4.12), we integrate it over the whole fluid region and have

$$\frac{\partial}{\partial t} \int_V \left\langle \frac{\mathbf{u}'^2}{2} \right\rangle dV = \int_V \left(-\langle u_i' u_j' \rangle \frac{\partial U_j}{\partial x_i} \right) dV - \nu \int_V \left\langle \left(\frac{\partial u_j'}{\partial x_i} \right)^2 \right\rangle dV$$

$$+ \int_S \left(-K\mathbf{U} - \left\langle \left(\frac{1}{2}\mathbf{u}'^2 + p' \right) \mathbf{u}' \right\rangle + \nu \nabla K \right) \cdot \mathbf{n} dS. \tag{4.13}$$

In the absence of mean flow, the first term on the right-hand side vanishes. The third term expresses the net supply or loss of turbulent energy across the boundary. In the absence of the latter, the turbulent state inevitably decays since the second term with the minus sign attached is negative. In other words, the first term related to $\mathbf{U}$ plays the role of sustaining the turbulent state and needs to be

$$\int_V \left(-\langle u_i' u_j' \rangle \frac{\partial U_j}{\partial x_i} \right) dV > 0. \tag{4.14}$$

The mean-flow counterpart of the first term on the right-hand side of Eq. (4.12) is the first term in Eq. (4.11) with the sign opposite to the former. This fact signifies that the energy is drained from the mean flow and is supplied to the fluctuating field. Such an energy transfer from large- to small-scale components of motion is generally called the energy cascade.

We mentioned that the MHD energy and the cross helicity, which are given by Eqs. (2.54) and (2.55), are conserved in the absence of molecular viscous and resistive effects. Then we attach special importance to their turbulent parts,

$$K = \left\langle \frac{\mathbf{u}'^2 + \mathbf{b}'^2}{2} \right\rangle, \tag{4.15}$$

$$W = \langle \mathbf{u}' \cdot \mathbf{b}' \rangle. \tag{4.16}$$

The fluctuations $\mathbf{u}'$ and $\mathbf{b}'$ obey

$$\frac{Du_i'}{Dt} + \frac{\partial}{\partial x_j}\left(u_i' u_j' - b_i' b_j' - R_{ij} \right) + \frac{\partial \vartheta'}{\partial x_i} - \nu \nabla^2 u_i'$$

$$= B_j \frac{\partial b_i'}{\partial x_j} - u_j' \frac{\partial U_i}{\partial x_j} + b_j' \frac{\partial B_i}{\partial x_j}, \tag{4.17}$$

$$\frac{Db_i'}{Dt} + \frac{\partial}{\partial x_j}\left(u_j' b_i' - u_i' b_j' - \varepsilon_{ij\ell} E_{M\ell} \right) - \lambda_M \nabla^2 b_i'$$

$$= B_j \frac{\partial u_i'}{\partial x_j} - u_j' \frac{\partial B_i}{\partial x_j} + b_j' \frac{\partial U_i}{\partial x_j}, \tag{4.18}$$

with the solenoidal conditions $\nabla \cdot \mathbf{u}' = \nabla \cdot \mathbf{b}' = 0$, where

$$\vartheta' = p + \frac{\mathbf{b}^2}{2} - \left\langle p + \frac{\mathbf{b}^2}{2} \right\rangle. \tag{4.19}$$

From Eqs. (4.17) and (4.18), we have the transport equations for K and W,

$$\frac{DZ}{Dt} = P_Z - \varepsilon_Z + \nabla \cdot \mathbf{T}_Z \quad (Z = K \text{ or } W), \tag{4.20}$$

where

$$P_K = -R_{ij}\frac{\partial U_j}{\partial x_i} - \mathbf{E}_M \cdot \mathbf{J} = -\frac{1}{2}R_{ij}S_{ij} - \mathbf{E}_M \cdot \mathbf{J}, \tag{4.21}$$

$$\varepsilon \equiv \varepsilon_K = \nu\left\langle\left(\frac{\partial u_j'}{\partial x_i}\right)^2\right\rangle + \lambda_M\left\langle\left(\frac{\partial b_j'}{\partial x_i}\right)^2\right\rangle, \tag{4.22}$$

$$\mathbf{T}_K = W\mathbf{B} + \left\langle -\left(\frac{\mathbf{u}'^2 + \mathbf{b}'^2}{2} + \vartheta'\right)\mathbf{u}' + (\mathbf{u}'\cdot\mathbf{b}')\mathbf{b}'\right\rangle + \nu\nabla\left\langle\frac{\mathbf{u}'^2}{2}\right\rangle + \lambda_M\nabla\left\langle\frac{\mathbf{b}'^2}{2}\right\rangle, \tag{4.23}$$

$$P_W = -R_{ij}\frac{\partial B_j}{\partial x_i} - \mathbf{E}_M \cdot \boldsymbol{\Omega}, \tag{4.24}$$

$$\varepsilon_W = (\nu + \lambda_M)\left\langle\frac{\partial u_j'}{\partial x_i}\frac{\partial b_j'}{\partial x_i}\right\rangle, \tag{4.25}$$

$$\mathbf{T}_W = K\mathbf{B} + \left\langle -(\mathbf{u}'\cdot\mathbf{b}')\mathbf{u}' + \left(\frac{\mathbf{u}'^2 + \mathbf{b}'^2}{2} - \vartheta'\right)\mathbf{b}'\right\rangle + \nu\langle(b_i'\cdot\nabla u_i')\rangle + \lambda_M\langle(u_i'\cdot\nabla b_i')\rangle. \tag{4.26}$$

In Eq. (4.21), we used

$$\frac{\partial U_j}{\partial x_i} = \frac{1}{2}\left(S_{ij} + \Omega_{ij}\right), \tag{4.27}$$

where

$$S_{ij} = \frac{\partial U_j}{\partial x_i} + \frac{\partial U_i}{\partial x_j}, \tag{4.28}$$

$$\Omega_{ij} = \frac{\partial U_j}{\partial x_i} - \frac{\partial U_i}{\partial x_j}. \tag{4.29}$$

In Eq. (4.20), P_Z, ε_Z, and $\nabla\cdot\mathbf{T}_Z$ are the MHD counterparts of the terms on the right-hand side of Eq. (4.12), respectively. Specifically, the MHD energy and the cross helicity are supplied from the mean to fluctuating field through P_K and P_W. These two terms will play a critical role in the discussion on the sustainment of MHD turbulent state.

In the frame rotating with angular velocity $\boldsymbol{\omega}_F$, the mean vorticity $\boldsymbol{\Omega}$ is subject to the transformation

$$\boldsymbol{\Omega} \rightarrow \boldsymbol{\Omega} + 2\boldsymbol{\omega}_F, \tag{4.30}$$

as may be seen from Eq. (2.41). In this context, we have

$$P_W \rightarrow P_W = -R_{ij}\frac{\partial B_j}{\partial x_i} - \mathbf{E}_M \cdot (\boldsymbol{\Omega} + 2\boldsymbol{\omega}_F), \tag{4.31}$$

whereas the $\boldsymbol{\omega}_F$ effect does not occur explicitly for P_K. Equation (4.31) indicates that W is sensitive to the frame rotation.

In the presence of the buoyancy force, P_K and P_W are supplemented with the thermal effects as

$$P_K: -\alpha_T \langle \theta' \mathbf{u}' \rangle \cdot \mathbf{g} = -\alpha_T \mathbf{H}_\theta \cdot \mathbf{g}, \tag{4.32}$$

$$P_W: -\alpha_T \langle \theta' \mathbf{b}' \rangle \cdot \mathbf{g}. \tag{4.33}$$

In § 6.1.3, it will be shown that the buoyancy effect contributes to the generation of turbulent energy in a thermally unstable case, that is, in the presence of the temperature gradient parallel to the gravitational acceleration vector. This point will be further referred to later.

In correspondence to Eq. (2.56), we have

$$\frac{|W|}{K} \leq 1. \tag{4.34}$$

This relation will be later found to be very useful in the estimate of the strength of magnetic fields generated by turbulent motion.

5. Theoretical Analysis of Turbulence Effects

For the estimate of R_{ij} and $\mathbf{E}_M$, we start from a kinematic approach and then proceed to a MHD approach. In what follows, we shall drop effects of Coriolis and buoyancy forces for simplicity of discussion and refer to them when necessary.

5.1. Quasi-kinematic method

Once the statistics of $\mathbf{u}'$ are given, we may evaluate $\mathbf{E}_M$ on the basis of Eq. (4.18) and examine its relationship with the generation process of $\mathbf{B}$. This approach is called kinematic dynamo. Here we follow the two-scale direct-interaction approximation

(TSDIA) method [12, 24] and perform kinematic dynamo modeling. The theoretical framework of the TSDIA is explained in Appendix.

5.1.1. Introduction of two scales and scale-parameter expansion

In order to distinguish between spatial and temporal variations of F and f' (see Fig. A1 in Appendix), we introduce a positive parameter

$$\delta_S << 1. \tag{5.1}$$

Using it, we construct two spatial and temporal variables, that is, fast and slow variables,

$$\boldsymbol{\xi}\,(=\mathbf{x}),\ \tau\,(=t);\quad \mathbf{X}\,(=\delta_S\mathbf{x}),\ T(=\delta_S t), \tag{5.2}$$

respectively. Here δ_S is not a real nondimensional parameter such as Reynolds number and is called the scale parameter hereafter. Its physical meaning is discussed in Appendix. We use two spatial and temporal scales given by Eq. (5.2), and write f [Eq. (4.1)] as

$$f = F(\mathbf{X}, T) + f'(\boldsymbol{\xi}, \tau; \mathbf{X}, T). \tag{5.3}$$

Then Eq. (4.18) may be rewritten as

$$\frac{\partial b_i'}{\partial \tau} + U_j \frac{\partial b_i'}{\partial \xi_j} + \frac{\partial}{\partial x_j}\left(u_j' b_i' - u_i' b_j'\right) - \lambda_M \nabla_\xi{}^2 b_i'$$

$$= B_j \frac{\partial u_i'}{\partial \xi_j} + \delta_S\left(-u_j' \frac{\partial B_i}{\partial X_j} + b_j' \frac{\partial U_i}{\partial X_j} - \frac{D b_i'}{DT} + B_j \frac{\partial b_i'}{\partial X_j}\right.$$

$$\left. - \frac{\partial}{\partial X_j}\left(u_j' b_i' - u_i' b_j' - \varepsilon_{ij\ell} E_{M\ell}\right)\right), \tag{5.4}$$

where

$$\nabla_\xi = \left(\frac{\partial}{\partial \xi_i}\right),\quad \nabla_X = \left(\frac{\partial}{\partial X_i}\right), \tag{5.5}$$

$$\frac{D}{DT} = \frac{\partial}{\partial T} + \mathbf{U}\cdot\nabla_X, \tag{5.6}$$

respectively, and we should that $\mathbf{E}_M$ is a function of $\mathbf{X}$ and T.

We introduce the Fourier representation in the frame moving with the velocity $\mathbf{U}$; namely, we write

$$f'(\boldsymbol{\xi}, \mathbf{X}; \tau, T) = \int f'(\mathbf{k}, \mathbf{X}; \tau, T) \exp\bigl(-i\mathbf{k} \cdot (\boldsymbol{\xi} - \mathbf{U}\tau)\bigr) d\boldsymbol{\xi}. \tag{5.7}$$

We apply Eq. (5.7) to Eq. (5.4), and have

$$\frac{\partial b_i'(\mathbf{k};\tau)}{\partial \tau} + \lambda_M k^2 b_i'(\mathbf{k};\tau)$$

$$-iN_{ij\ell}(\mathbf{k}) \iint u_j'(\mathbf{p};\tau) b_\ell'(\mathbf{q};\tau) \delta(\mathbf{k}-\mathbf{p}-\mathbf{q}) d\mathbf{p} d\mathbf{q}$$

$$= -i(\mathbf{k}\cdot\mathbf{B}) u_i'(\mathbf{k};\tau) + \delta_S \left(-u_j'(\mathbf{k};\tau) \frac{\partial B_i}{\partial X_j} + b_j'(\mathbf{k};\tau) \frac{\partial U_i}{\partial X_j} \right.$$

$$\left. - \frac{D^* b_i'(\mathbf{k};\tau)}{DT^*} + B_j \frac{\partial^* u_i'(\mathbf{k};\tau)}{\partial X_j^*} + N_{Bi} \right), \tag{5.8}$$

where

$$N_{ij\ell}(\mathbf{k}) = k_j \delta_{i\ell} - k_\ell \delta_{ij}, \tag{5.9}$$

D^* / DT^* and $\boldsymbol{\nabla}_X^*$ were defined by

$$\left(\frac{D^*}{DT^*}, \boldsymbol{\nabla}_X^* \right) = \exp(-i\mathbf{k}\cdot\mathbf{U}\tau) \left(\frac{D}{DT}, \boldsymbol{\nabla}_X \right) \exp(i\mathbf{k}\cdot\mathbf{U}\tau), \tag{5.10}$$

and $\mathbf{N}_B$ expresses the terms that are nonlinear in $\mathbf{u}'$ and $\mathbf{b}'$ and are not dependent directly on the mean field $\mathbf{U}$ and $\mathbf{B}$. We focus attention on the interaction between the mean field and fluctuations, and neglect $\mathbf{N}_B$ in what follows. Moreover, the dependence of $\mathbf{u}'$ and $\mathbf{b}'$ on $\mathbf{X}$ and T are not written explicitly.

We expand $\mathbf{b}'$ as

$$\mathbf{b}'(\mathbf{k};\tau) = \sum_{n=0}^{\infty} \delta_S{}^n \mathbf{b}_n'(\mathbf{k};\tau). \tag{5.11}$$

The first two parts are governed by

$$\frac{\partial b_{0i}'(\mathbf{k};\tau)}{\partial \tau} + \lambda_M k^2 b_{0i}'(\mathbf{k};\tau)$$

$$-iN_{ij\ell}(\mathbf{k}) \iint u_j'(\mathbf{p};\tau) b_{0\ell}'(\mathbf{q};\tau) (\mathbf{U},\mathbf{B}) \delta(\mathbf{k}-\mathbf{p}-\mathbf{q}) d\mathbf{p} d\mathbf{q}$$

$$= I_{B0i}(\mathbf{k};\tau) \equiv -i(\mathbf{k}\cdot\mathbf{B})u_i'(\mathbf{k};\tau), \tag{5.12}$$

$$\frac{\partial b_{1i}'(\mathbf{k};\tau)}{\partial\tau} + \lambda_M k^2 b_{1i}'(\mathbf{k};\tau)$$

$$-iN_{ij\ell}(\mathbf{k})\iint u_j'(\mathbf{p};\tau)b_{1\ell}'(\mathbf{q};\tau)\delta(\mathbf{k}-\mathbf{p}-\mathbf{q})d\mathbf{p}d\mathbf{q}$$

$$= I_{B1i}(\mathbf{k};\tau) \equiv -u_j'(\mathbf{k};\tau)\frac{\partial B_i}{\partial X_j} + b_{0j}'(\mathbf{k};\tau)\frac{\partial U_i}{\partial X_j} - \frac{D^* b_{0i}'(\mathbf{k};\tau)}{DT^*} + B_j\frac{\partial^* u_i'(\mathbf{k};\tau)}{\partial X_j^*}. \tag{5.13}$$

In order to solve Eqs. (5.12) and (5.13), we introduce the Green's function G_{Mij}', which obeys

$$\frac{\partial G_{Mij}'(\mathbf{k};\tau,\tau')}{\partial\tau} + \lambda_M k^2 G_{Mij}'(\mathbf{k};\tau,\tau')$$

$$-iN_{i\ell m}(\mathbf{k})\iint u_\ell'(\mathbf{p};\tau)G_{Mmj}'(\mathbf{q};\tau,\tau')\delta(\mathbf{k}-\mathbf{p}-\mathbf{q})d\mathbf{p}d\mathbf{q} = \delta_{ij}\delta(\tau-\tau'). \tag{5.14}$$

With the aid of G_{Mij}', Eq. (5.12) may be integrated as

$$b_{0i}'(\mathbf{k};\tau) = b_{00i}'(\mathbf{k};\tau) + \int_{-\infty}^{\tau} G_{Mij}'(\mathbf{k};\tau,\tau_1)I_{B0j}(\mathbf{k};\tau_1)d\tau_1. \tag{5.15}$$

Here $\mathbf{b}_{00}'$ is governed by Eq. (5.12) with the $\mathbf{B}$-related part dropped, that is,

$$\frac{\partial b_{00i}'(\mathbf{k};\tau)}{\partial\tau} + \lambda_M k^2 b_{00i}'(\mathbf{k};\tau)$$

$$-iN_{ij\ell}(\mathbf{k})\iint u_j'(\mathbf{p};\tau)b_{00\ell}'(\mathbf{q};\tau)\delta(\mathbf{k}-\mathbf{p}-\mathbf{q})d\mathbf{p}d\mathbf{q} = 0. \tag{5.16}$$

This equation contains no factors generating and sustaining the statistical anisotropy of $\mathbf{b}_{00}'$. In what follows, the statistics related to $\mathbf{b}_{00}'$ will be assumed to be isotropic, but their nonmirrorsymmetry is taken into account when necessary.

Entirely similarly, Eq. (5.13) results in

$$b_{1i}'(\mathbf{k};\tau) = \int_{-\infty}^{\tau} G_{Mij}'(\mathbf{k};\tau,\tau_1)I_{B1j}(\mathbf{k};\tau_1)d\tau_1. \tag{5.17}$$

5.1.2. Evaluation of turbulent electromotive force

Equations (5.15) and (5.17) indicate that $\mathbf{b}'$ is expressed in terms of $\mathbf{b}_{00}'$ under given $\mathbf{u}'$. Then $\mathbf{E}_M$ may be evaluated once the statistics of $\mathbf{u}'$ are known. As the

simplest turbulent state, we assume the isotropy of $\mathbf{u}'$. In this case, the covariance of $\mathbf{u}'$ may be expressed as

$$\frac{\langle u_i'(\mathbf{k};\tau)u_j'(\mathbf{k}';\tau')\rangle}{\delta(\mathbf{k}+\mathbf{k}')} = D_{ij}(\mathbf{k})Q_K(k;\tau,\tau') + \frac{i}{2}\frac{k_\ell}{k^2}\varepsilon_{ij\ell}\Gamma_K(k;\tau,\tau'), \qquad (5.18)$$

where subscript K denotes kinetic, and

$$D_{ij}(\mathbf{k}) = \delta_{ij} - \frac{k_i k_j}{k^2}. \qquad (5.19)$$

Then the turbulent kinetic energy and the turbulent kinetic helicity are expressed by

$$K_K = \left\langle \frac{\mathbf{u}'^2}{2} \right\rangle = \int Q_K(k;\tau,\tau)d\mathbf{k}, \qquad (5.20)$$

$$H_K = \langle \mathbf{u}'\cdot\boldsymbol{\omega}' \rangle = \int \Gamma_K(k;\tau,\tau)d\mathbf{k}, \qquad (5.21)$$

respectively. In relation to the second term of Eq. (5.18), we should recall Taylor columns referred to in § 2.2. The columns are characterized by nonvanishing helicity.

In the present discussion, we further introduce the correlation between $\mathbf{b}_{00}'$ and $\mathbf{u}'$, that is, the cross helicity. Its importance was discussed in § 2.3 in the light of MHD conservation properties. We write

$$\frac{\langle u_i'(\mathbf{k};\tau)b_{00j}'(\mathbf{k}';\tau')\rangle}{\delta(\mathbf{k}+\mathbf{k}')} = D_{ij}(\mathbf{k})\Lambda(k;\tau,\tau') \ , \qquad (5.22)$$

which gives

$$\langle \mathbf{u}'\cdot\mathbf{b}_{00}' \rangle = 2\int \Lambda(k;\tau,\tau)d\mathbf{k}. \qquad (5.23)$$

In purely kinematic dynamo, there is no necessity to retain Λ. In real dynamo, however, there is the close connection between magnetic field and velocity through Eq. (4.17). With this point in mind, we perform the analysis of $\mathbf{E}_M$ on the basis of Eqs. (5.18) and (5.22). The introduction of Λ will be shown to lead to a new dynamo effect that does not occur in the purely kinematic approach. It is proper to call this approach with Eq. (5.22) incorporated a quasi-kinematic dynamo, in contrast to the usual kinematic dynamo.

From Eq. (5.14), the Green's function G_{Mij}' is dependent on $\mathbf{u}'$ only that is statistically isotropic. Then we write

$$\left\langle G_{Mij}'(\mathbf{k};\tau,\tau')\right\rangle = \delta_{ij} G_M(k;\tau,\tau'). \tag{5.24}$$

We expand $\mathbf{E}_M$ as

$$E_{Mi} = \varepsilon_{ij\ell}\left(\left\langle u_j' b_{0\ell}'\right\rangle + \delta_S\left\langle u_j' b_{1\ell}'\right\rangle\right) + O\left(\delta_S{}^2\right). \tag{5.25}$$

We substitute Eqs. (5.15) and (5.17) into Eq. (5.25), and have

$$E_{Mi} = \varepsilon_{ij\ell}\left(\int \frac{\left\langle u_j'(\mathbf{k};\tau) b_{00\ell}'(\mathbf{k}';\tau)\right\rangle}{\delta(\mathbf{k}+\mathbf{k}')} d\mathbf{k}\right)$$

$$+\varepsilon_{ij\ell}\left(-iB_n \int k_n'\, d\mathbf{k} \int_{-\infty}^{\tau} \frac{\left\langle G_{M\ell m}'(\mathbf{k}';\tau,\tau_1) u_j'(\mathbf{k};\tau) u_m'(\mathbf{k}';\tau_1)\right\rangle}{\delta(\mathbf{k}+\mathbf{k}')} d\tau_1\right)$$

$$+\varepsilon_{ij\ell}\left(-\frac{\partial B_m}{\partial x_n} \int d\mathbf{k} \int_{-\infty}^{\tau} \frac{\left\langle G_{M\ell m}'(\mathbf{k}';\tau,\tau_1) u_j'(\mathbf{k};\tau) u_n'(\mathbf{k}';\tau_1)\right\rangle}{\delta(\mathbf{k}+\mathbf{k}')} d\tau_1\right)$$

$$+\varepsilon_{ij\ell}\left(\frac{\partial U_m}{\partial x_n} \int d\mathbf{k} \int_{-\infty}^{\tau} \frac{\left\langle G_{M\ell m}'(\mathbf{k}';\tau,\tau_1) u_j'(\mathbf{k};\tau) b_{00n}'(\mathbf{k}';\tau_1)\right\rangle}{\delta(\mathbf{k}+\mathbf{k}')} d\tau_1\right), \tag{5.26}$$

after the replacement concerning $\mathbf{X}$ and T,

$$\mathbf{X} \to \delta_S \mathbf{x},\ T \to \delta_S t. \tag{5.27}$$

In the context of the last two terms, we retained the first two terms in $\mathbf{I}_{B1}$ of Eq. (5.13) that are linearly dependent on $\mathbf{U}$ and $\mathbf{B}$.

In the first term of Eq. (5.26), we use

$$\int \frac{k_i k_j}{k^2} d\mathbf{k} = \frac{1}{3}\delta_{ij} \int d\mathbf{k}, \tag{5.28}$$

and have

$$-\varepsilon_{ij\ell} \int D_{j\ell}(\mathbf{k}) \Lambda(k;\tau,\tau) d\mathbf{k} = \frac{2}{3}\varepsilon_{ij\ell}\delta_{j\ell} \int \Lambda(k;\tau,\tau) d\mathbf{k} = 0. \tag{5.29}$$

To the second term, we apply the renormalization procedure (see Appendix), and have

$$\varepsilon_{ij\ell}\left(B_n \int d\mathbf{k} \int_{-\infty}^{\tau} G_{M\ell m}(\mathbf{k}';\tau,\tau_1) \frac{(-ik_n')\langle u_j'(\mathbf{k};\tau) u_m'(\mathbf{k}';\tau_1)\rangle}{\delta(\mathbf{k}+\mathbf{k}')} d\tau_1 \right)$$

$$= \left(-\frac{1}{3} \int d\mathbf{k} \int_{-\infty}^{\tau} G_M(k;\tau,\tau_1) \Gamma_K(k;\tau,\tau_1) d\tau_1 \right) B_i. \tag{5.30}$$

Here we should note that the second part of Eq. (5.18), which is related to the helicity effect, contributes to this result. The third and fourth terms may be evaluated in entirely the same way. Summarizing these results, we have

$$\mathbf{E}_M = \alpha_K \mathbf{B} - \beta_K \mathbf{J} + \gamma_K \mathbf{\Omega}. \tag{5.31}$$

Coefficients α_K, β_K, and γ_K are expressed in the form

$$\alpha_K = -\frac{1}{3} \int d\mathbf{k} \int_{-\infty}^{\tau} G_M(k;\tau,\tau_1) \Gamma_K(k;\tau,\tau_1) d\tau_1, \tag{5.32}$$

$$\beta_K = \frac{2}{3} \int d\mathbf{k} \int_{-\infty}^{\tau} G_M(k;\tau,\tau_1) Q_K(k;\tau,\tau_1) d\tau_1, \tag{5.33}$$

$$\gamma_K = \frac{2}{3} \int d\mathbf{k} \int_{-\infty}^{\tau} G_M(k;\tau,\tau_1) \Lambda(k;\tau,\tau_1) d\tau_1. \tag{5.34}$$

On dropping the third term on the left-hand side of Eq. (5.14), Eqs. (5.33) and (5.34) are reduced to the expressions obtained by the first-order smoothing approximation [9]. We should note that the approximation is applicable to the case of low magnetic Reynolds number.

Equation (5.31) shows that turbulence effects generate the electromotive force aligned with the mean magnetic field, the mean electric current density, and the mean vorticity. Their physical meanings will be later discussed in detail.

5.1.3. Evaluation of Reynolds stress

In the usual kinematic approach, our concern is focused on the evaluation of $\mathbf{E}_M$, that is, the effect of velocity fluctuation on the equation for $\mathbf{B}$. In the present approach, we are also interested in the effect arising from the correlation between velocity and magnetic field or the turbulent cross helicity. By taking the effect into account, we may examine the feedback effect of the generated magnetic field on the equation for $\mathbf{U}$. The velocity-related part of R_{ij} is simply evaluated from Eq. (5.18) and is given in the isotropic form

$$\langle u_i' u_j' \rangle = \left(\frac{2}{3} \int Q_K(k;\tau,\tau_1) d\mathbf{k} \right) \delta_{ij}. \tag{5.35}$$

We use Eqs. (5.15) and (5.17), and evaluate $\langle b_i' b_j' \rangle$. For the isotropic part of magnetic fluctuation, $\mathbf{b}_{00}'$, we write

$$\frac{\langle b_{00i}'(\mathbf{k};\tau) b_{00j}'(\mathbf{k}';\tau') \rangle}{\delta(\mathbf{k}+\mathbf{k}')} = D_{ij}(\mathbf{k}) Q_M(k;\tau,\tau'). \tag{5.36}$$

Here we may add the nonmirrorsymmetric part, which is confirmed not to contribute to the following analysis. As is similar to Eq. (5.31), we pay special attention to the contributions linearly related to $\mathbf{U}$ and $\mathbf{B}$. After the combination with Eq. (5.35), R_{ij} is written as

$$R_{ij} = \frac{2}{3} K_R \delta_{ij} - \nu_{TM} S_{ij} + \nu_{MM} M_{ij}, \tag{5.37}$$

where the mean velocity-strain tensor S_{ij} is given by Eq. (4.28), M_{ij} is its magnetic-field counterpart defined by

$$M_{ij} = \frac{\partial B_j}{\partial x_i} + \frac{\partial B_i}{\partial x_j}, \tag{5.38}$$

and the turbulent residual energy K_R is

$$K_R = \left\langle \frac{\mathbf{u}'^2 - \mathbf{b}'^2}{2} \right\rangle = \int Q_K(k;\tau,\tau) d\mathbf{k} - \int Q_M(k;\tau,\tau) d\mathbf{k}. \tag{5.39}$$

Coefficients ν_{TM} and ν_{MM} are

$$\nu_{TM} = \frac{2}{3} \int d\mathbf{k} \int_{-\infty}^{\tau} G_M(k;\tau,\tau_1) Q_M(k;\tau,\tau_1) d\tau_1, \tag{5.40}$$

$$\nu_{MM} = \frac{2}{3} \int d\mathbf{k} \int_{-\infty}^{\tau} G_M(k;\tau,\tau_1) \Lambda(k;\tau,\tau_1) d\tau_1. \tag{5.41}$$

In Eq. (5,37), the ν_{TM}-related term expresses the so-called turbulent-viscosity effect (see Appendix). On the other hand, the ν_{MM}-related term denotes the feedback effect by the generated magnetic field on the mean flow. The importance of this effect will be clarified in later discussions.

5.2. Counter-kinematic method

In § 5.1, we analyzed effects of velocity fluctuation on the **B** equation, which are represented by $\mathbf{E}_M$. In what follows, we consider effects of magnetic-field fluctuation on the **B** and **U** equations. This approach, which is called the counter-kinematic method, will be instrumental to understanding the interaction process between **U** and **B**.

5.2.1. Scale-parameter expansion

In terms of two-scale variables, Eq. (4.17) may be written as

$$\frac{\partial u_i'}{\partial \tau} + U_j \frac{\partial u_i'}{\partial \xi_j} + \frac{\partial}{\partial \xi_j}\left(u_i' u_j' - b_i' b_j'\right) + \frac{\partial \vartheta'}{\partial \xi_i} - \nu \nabla_\xi^2 u_i'$$

$$= B_j \frac{\partial b_i'}{\partial \xi_j} + \delta_S \left(-u_j' \frac{\partial U_i}{\partial X_j} + b_j' \frac{\partial B_i}{\partial X_j} - \frac{D u_i'}{DT} + B_j \frac{\partial b_i'}{\partial X_j} \right.$$

$$\left. - \frac{\partial}{\partial X_j}\left(u_j' u_i' - b_j' b_i' - R_{ji}\right) - \frac{\partial \vartheta'}{\partial X_i} \right), \tag{5.42}$$

with the solenoidal condition

$$\frac{\partial u_i'}{\partial \xi_i} = -\delta_S \frac{\partial u_i'}{\partial X_i}. \tag{5.43}$$

We apply the moving-frame Fourier representation, Eq. (5.7), to Eqs. (5.42) and (5.43), and have

$$\frac{\partial u_i'(\mathbf{k};\tau)}{\partial \tau} + \nu k^2 u_i'(\mathbf{k};\tau) - i k_i \vartheta'(\mathbf{k};\tau)$$

$$-i k_j \iint u_i'(\mathbf{p};\tau) u_j'(\mathbf{q};\tau) \delta(\mathbf{k}-\mathbf{p}-\mathbf{q}) d\mathbf{p} d\mathbf{q}$$

$$= -i(\mathbf{k}\cdot\mathbf{B}) b_i(\mathbf{k};\tau) + i k_j \iint b_i'(\mathbf{p};\tau) b_j'(\mathbf{q};\tau) \delta(\mathbf{k}-\mathbf{p}-\mathbf{q}) d\mathbf{p} d\mathbf{q}$$

$$+\delta_S \left(-u_j'(\mathbf{k};\tau) \frac{\partial U_i}{\partial X_j} + b_j'(\mathbf{k};\tau) \frac{\partial B_i}{\partial X_j} \right.$$

$$\left. - \frac{D^* u_i'(\mathbf{k};\tau)}{DT^*} - \frac{\partial^* \vartheta'(\mathbf{k};\tau)}{\partial X_i^*} + B_j \frac{\partial^* u_i'(\mathbf{k};\tau)}{\partial X_i^*} \right.$$

$$-\iint \frac{\partial^*}{\partial X_j^*}\left(u_i'(\mathbf{p};\tau)u_j'(\mathbf{q};\tau)-b_i'(\mathbf{p};\tau)b_j'(\mathbf{q};\tau)\right)\delta(\mathbf{k}-\mathbf{p}-\mathbf{q})d\mathbf{p}d\mathbf{q}\Bigg), \quad (5.44)$$

$$\mathbf{k}\cdot\mathbf{u}'(\mathbf{k};\tau)=\delta_S\left(-i\frac{\partial^* u_i'(\mathbf{k};\tau)}{\partial X_i^*}\right). \quad (5.45)$$

We expand $\mathbf{u}'$ and ϑ' as

$$\mathbf{u}'(\mathbf{k};\tau)=\sum_{n=0}^{\infty}\delta_S{}^n\mathbf{u}_n'(\mathbf{k};\tau),\quad \vartheta'(\mathbf{k};\tau)=\sum_{n=0}^{\infty}\delta_S{}^n\vartheta_n'(\mathbf{k};\tau), \quad (5.46)$$

and substitute them into Eqs. (5.44) and (5.45). The leading parts $\mathbf{u}_0'$ and ϑ_0' obey

$$\frac{\partial u_{0i}'(\mathbf{k};\tau))}{\partial\tau}+\nu k^2 u_{0i}'(\mathbf{k};\tau)-ik_i\vartheta_0'(\mathbf{k};\tau)$$

$$-ik_j\iint u_{0i}'(\mathbf{p};\tau)u_{0j}'(\mathbf{q};\tau)\delta(\mathbf{k}-\mathbf{p}-\mathbf{q})d\mathbf{p}d\mathbf{q}$$

$$=-ik_j b_i(\mathbf{k};\tau)B_j+ik_j\iint b_i'(\mathbf{p};\tau)b_j'(\mathbf{q};\tau)\delta(\mathbf{k}-\mathbf{p}-\mathbf{q})d\mathbf{p}d\mathbf{q}, \quad (5.47)$$

$$\mathbf{k}\cdot\mathbf{u}_0'(\mathbf{k};\tau)=0. \quad (5.48)$$

We use Eq. (5.48) and eliminate ϑ_0'. The resulting equation is written as

$$\frac{\partial u_{0i}'(\mathbf{k};\tau))}{\partial\tau}+\nu k^2 u_{0i}'(\mathbf{k};\tau)$$

$$-iM_{ij\ell}(\mathbf{k})u_{0j}'(\mathbf{p};\tau)u_{0\ell}'(\mathbf{q};\tau)\delta(\mathbf{k}-\mathbf{p}-\mathbf{q})d\mathbf{p}d\mathbf{q}=-i(\mathbf{k}\cdot\mathbf{B})b_i'(\mathbf{k};\tau)$$

$$+iM_{ij\ell}(\mathbf{k})\iint b_i'(\mathbf{p};\tau)b_j'(\mathbf{q};\tau)\delta(\mathbf{k}-\mathbf{p}-\mathbf{q})d\mathbf{p}d\mathbf{q}, \quad (5.49)$$

where $M_{ij\ell}(\mathbf{k})$ is defined by

$$M_{ij\ell}(\mathbf{k})=\frac{1}{2}\left(k_j D_{i\ell}(\mathbf{k})+k_\ell D_{ij}(\mathbf{k})\right). \quad (5.50)$$

In the present counter-kinematic approach, $\mathbf{b}'$ is assumed to be statistically known, and the right-hand side of Eq. (5.48) may be regarded as external forces imposed on the $\mathbf{u}_0'$ equation. It is difficult to exactly solve Eq. (5.48) owing to its nonlinearity. Then we treat those forces in the perturbational manner. We write $\mathbf{u}_0'$ as

$$\mathbf{u}_0'=\mathbf{u}_{00}'(\mathbf{k};\tau)+\mathbf{u}_{01}'(\mathbf{k};\tau)+\cdots. \quad (5.51)$$

The first two terms are govern by

$$\frac{\partial u_{00i}'(\mathbf{k};\tau))}{\partial \tau} + \nu k^2 u_{00i}'(\mathbf{k};\tau)$$

$$-iM_{ij\ell}(\mathbf{k})\iint u_{00j}'(\mathbf{p};\tau)u_{00\ell}'(\mathbf{q};\tau)\delta(\mathbf{k}-\mathbf{p}-\mathbf{q})d\mathbf{p}d\mathbf{q} = 0, \tag{5.52}$$

$$\frac{\partial u_{01i}'(\mathbf{k};\tau))}{\partial \tau} + \nu k^2 u_{01i}'(\mathbf{k};\tau)$$

$$-2iM_{ij\ell}(\mathbf{k})\iint u_{00j}'(\mathbf{p};\tau)u_{01\ell}'(\mathbf{q};\tau)\delta(\mathbf{k}-\mathbf{p}-\mathbf{q})d\mathbf{p}d\mathbf{q}$$

$$= I_{K0i} \equiv -ik_j b_i'(\mathbf{k};\tau)B_j + iM_{ij\ell}(\mathbf{k})\iint b_j'(\mathbf{p};\tau)b_\ell'(\mathbf{q};\tau)\delta(\mathbf{k}-\mathbf{p}-\mathbf{q})d\mathbf{p}d\mathbf{q}. \tag{5.53}$$

Equation (5.53) is linear in $\mathbf{u}_{01}'$ and may be integrated in terms of the Green's function G_{Kij}' obeying

$$\frac{\partial G_{Kij}'(\mathbf{k};\tau,\tau')}{\partial \tau} + \nu k^2 G_{Kij}'(\mathbf{k};\tau,\tau')$$

$$-2iM_{i\ell m}(\mathbf{k})\iint u_{00\ell}'(\mathbf{p};\tau)G_{Kmj}'(\mathbf{q};\tau,\tau')\delta(\mathbf{k}-\mathbf{p}-\mathbf{q})d\mathbf{p}d\mathbf{q} = \delta_{ij}\delta(\tau-\tau'). \tag{5.54}$$

As a result, we have

$$u_{01i}'(\mathbf{k};\tau) = \int_{-\infty}^{\tau} G_{Ki\ell}'(\mathbf{k};\tau,\tau_1)I_{K0\ell}(\mathbf{k};\tau_1)d\tau_1. \tag{5.55}$$

For obtaining the $O(\delta_S)$ part of $\mathbf{u}'$, $\mathbf{u}_1'$, we write [12, 25]

$$\mathbf{u}_1'(\mathbf{k};\tau) = \mathbf{v}_1'(\mathbf{k};\tau) - i\frac{\mathbf{k}}{k^2}\frac{\partial^* u_{0i}'(\mathbf{k};\tau)}{\partial X_i^*}, \tag{5.56}$$

leading to the solenoidal condition concerning $\mathbf{k}$,

$$\mathbf{k}\cdot\mathbf{v}_1'(\mathbf{k};\tau) = 0. \tag{5.57}$$

The solenoidal part $\mathbf{v}_1'$ obeys

$$\frac{\partial v_{1i}'(\mathbf{k};\tau)}{\partial \tau} + \nu k^2 v_{1i}'(\mathbf{k};\tau)$$

$$-2iM_{i\ell m}(\mathbf{k})\iint u_{0\ell}'(\mathbf{p};\tau)v_{1m}'(\mathbf{p};\tau)\delta(\mathbf{k}-\mathbf{p}-\mathbf{q})d\mathbf{p}d\mathbf{q}$$

$$= D_{i\ell}(\mathbf{k})b_j'(\mathbf{k};\tau)\frac{\partial B_\ell}{\partial X_j} - D_{i\ell}(\mathbf{k})u_{0j}'(\mathbf{k};\tau)\frac{\partial U_\ell}{\partial X_j} - D_{ij}(\mathbf{k})\frac{D^* u_{0j}'(\mathbf{k};\tau)}{DT^*} + N_{Ki}. \tag{5.58}$$

Here $\mathbf{N}_K$ expresses the terms nonlinear in $\mathbf{u}_0'$ and $\mathbf{b}'$ related to the last term of the $O(\delta_S)$ part in Eq. (5.44). It will be dropped in the following discussion since our interest lies in the interaction between the mean field and fluctuation.

We substitute Eq. (5.51) into the right-hand side of Eq. (5.58) and retain the contributions from $\mathbf{u}_{00}'$ for minimizing the mathematical complexity. This approximation is helpful for abstracting the effects linear in $\mathbf{B}$ and $\mathbf{U}$ and neglecting the contribution from the nonlinear term $\mathbf{N}_K$. We may integrate the resulting equation by using Eq. (5.54), and have

$$u_{1i}'(\mathbf{k};\tau) = -i\frac{k_i}{k^2}\frac{\partial^* v_{00j}'(\mathbf{k};\tau)}{\partial X_j^*}$$

$$+D_{\ell m}(\mathbf{k})\frac{\partial B_\ell}{\partial X_j}\int_{-\infty}^{\tau} G_{Kim}'(\mathbf{k};\tau,\tau_1)b_j'(\mathbf{k};\tau_1)d\tau_1$$

$$-D_{\ell m}(\mathbf{k})\frac{\partial U_\ell}{\partial X_j}\int_{-\infty}^{\tau} G_{Kim}'(\mathbf{k};\tau,\tau_1)u_{00j}'(\mathbf{k};\tau_1)d\tau_1$$

$$-\int_{-\infty}^{\tau} G_{Kij}'(\mathbf{k};\tau,\tau_1)\frac{D^* u_{00j}'(\mathbf{k};\tau_1)}{DT^*}d\tau_1. \tag{5.59}$$

5.2.2. Evaluation of turbulent electromotive force

For $\mathbf{b}'$, we also assume the same statistical property as for $\mathbf{u}'$ in the quasi-kinematic method. Namely, we write

$$\frac{\langle b_i'(\mathbf{k};\tau)b_j'(\mathbf{k}';\tau')\rangle}{\delta(\mathbf{k}+\mathbf{k}')} = D_{ij}(\mathbf{k})Q_M(k;\tau,\tau') + \frac{i}{2}\frac{k_\ell}{k^2}\varepsilon_{ij\ell}\Gamma_M(k;\tau,\tau'). \tag{5.60}$$

Equation (5.60) gives

$$K_M = \left\langle \frac{\mathbf{b}'^2}{2} \right\rangle = \int Q_M(k;\tau,\tau)d\mathbf{k}, \tag{5.61}$$

$$H_M = \langle \mathbf{b}'\cdot\mathbf{j}' \rangle = \int \Gamma_M(k;\tau,\tau)d\mathbf{k}. \tag{5.62}$$

The helicity $\mathbf{u}\cdot\boldsymbol{\omega}$ is an indicator of helical or spiral structures of fluid motion. From the Elsasser's variables in § 2.3, we may see the close correspondence between $\mathbf{u}$ and $\mathbf{b}$, resulting in the similar correspondence between $\boldsymbol{\omega}$ and $\mathbf{j}$. Then $\mathbf{b}\cdot\mathbf{j}$ expresses a helical property of magnetic-field lines. In what follows, the turbulent part of $\mathbf{b}\cdot\mathbf{j}$, H_M, will be shown to play an important role in mean-field theory of dynamo, through the combination with the turbulent kinetic helicity H_K defined by Eq. (5.21).

The leading part in Eq. (5.51), $\mathbf{u}_{00}'$, obeys Eq. (5.52), which is not explicitly dependent on the mean field generating the anisotropy of turbulent state. We assume the statistical isotropy of $\mathbf{u}_{00}'$:

$$\frac{\left\langle u_{00i}'(\mathbf{k};\tau)u_{00j}'(\mathbf{k}';\tau')\right\rangle}{\delta(\mathbf{k}+\mathbf{k}')}=D_{ij}(\mathbf{k})Q_K(k;\tau,\tau'), \tag{5.63}$$

as well as

$$\left\langle G_{Kij}'(\mathbf{k};\tau,\tau')\right\rangle=\delta_{ij}G_K(k;\tau,\tau'). \tag{5.64}$$

In Eq. (5.63), we may add the nonmirrorsymmetric part, as in Eq. (5.18), which is confirmed not to contribute to the following analysis. Moreover we keep the correlation between $\mathbf{u}_{00}'$ and $\mathbf{b}'$ in the form

$$\frac{\left\langle u_{00i}'(\mathbf{k};\tau)b_j'(\mathbf{k}';\tau')\right\rangle}{\delta(\mathbf{k}+\mathbf{k}')}=D_{ij}(\mathbf{k})\Lambda(k;\tau,\tau'). \tag{5.65}$$

The physical meanings of Eqs. (5.63) and (5.65) have already been mentioned in the quasi-kinematic method.

We expand $\mathbf{E}_M$ as

$$\begin{aligned}E_{Mi}&=\varepsilon_{ij\ell}\left(\left\langle u_{0j}'b_\ell'\right\rangle+\delta_S\left(\left\langle u_{1j}'b_\ell'\right\rangle\right)\right)+O\left(\delta_S{}^2\right)\\&=\varepsilon_{ij\ell}\left(\left\langle u_{00j}'b_\ell'\right\rangle+\left\langle u_{01j}'b_\ell'\right\rangle+\cdots\right)+\delta_S\left(\varepsilon_{ij\ell}\left\langle u_{1j}'b_\ell'\right\rangle\right)+O\left(\delta_S{}^2\right),\end{aligned} \tag{5.66}$$

by using Eq. (5.51). We substitute Eqs. (5.55) and (5.59) into Eq. (5.66), and make use of the statistics designated by Eqs. (5.60) and (5.63)-(5.65). The evaluation of $\mathbf{E}_M$ is essentially the same as for Eq. (5.31), resulting in

$$\mathbf{E}_M=\alpha_M\mathbf{B}-\beta_M\mathbf{J}+\gamma_M\boldsymbol{\Omega}, \tag{5.67}$$

where

$$\alpha_M = \frac{1}{3}\int d\mathbf{k}\int_{-\infty}^{\tau} G_K(k;\tau,\tau_1)\Gamma_M(k;\tau,\tau_1)d\tau_1, \tag{5.68}$$

$$\beta_M = \frac{1}{3}\int d\mathbf{k}\int_{-\infty}^{\tau} G_K(k;\tau,\tau_1)Q_M(k;\tau,\tau_1)d\tau_1, \tag{5.69}$$

$$\gamma_M = \frac{1}{3}\int d\mathbf{k}\int_{-\infty}^{\tau} G_K(k;\tau,\tau_1)\Lambda(k;\tau,\tau_1)d\tau_1. \tag{5.70}$$

In Eq. (5.67), the explicit dependence of $\mathbf{E}_M$ on the mean field is the same as for Eq. (5.31). A typical difference between the two expressions may be seen in Eqs. (5.32) and (5.68). These coefficients are associated with helical statistical properties of velocity and magnetic-field fluctuations, respectively, but those properties occur with opposite signs attached.

5.2.3. Evaluation of Reynolds stress

In the counter-kinematic method, the magnetic part of R_{ij} is simply written as

$$\langle -b_i' b_j' \rangle = -\left(\frac{2}{3}\int Q_M(k;\tau,\tau)d\mathbf{k}\right)\delta_{ij}, \tag{5.71}$$

from Eq. (5.60).

The velocity counterpart of Eq. (5.71) is expanded as

$$\begin{aligned}\langle u_i' u_j' \rangle &= \langle u_{0i}' u_{0j}' \rangle + \delta_S\left(\langle u_{0i}' u_{1j}' \rangle + \langle u_{1i}' u_{0j}' \rangle\right) + O\left(\delta_S{}^2\right) \\ &= \langle u_{00i}' u_{00j}' \rangle + \langle u_{00i}' u_{01j}' \rangle + \langle u_{01i}' u_{00j}' \rangle + \cdots \\ &\quad + \delta_S\left(\langle u_{00i}' u_{1j}' \rangle + \langle u_{1i}' u_{00j}' \rangle + \cdots\right) + O\left(\delta_S{}^2\right),\end{aligned} \tag{5.72}$$

where use has been made of Eq. (5.51). We substitute Eqs. (5.55) and (5.59) into Eq. (5.72), and use Eqs. (5.60) and (5.63)-(5.65). After the combination with Eq. (5.71), we have

$$R_{ij} = \frac{2}{3}K_R\delta_{ij} - \nu_{TK}S_{ij} + \nu_{MK}M_{ij}, \tag{5.73}$$

where

$$\nu_{TK} = \frac{7}{15}\int d\mathbf{k}\int_{-\infty}^{\tau} G_K(k;\tau,\tau_1)Q_K(k;\tau,\tau_1)d\tau_1, \tag{5.74}$$

$$\nu_{MK} = \frac{7}{15}\int d\mathbf{k}\int_{-\infty}^{\tau} G_K(k;\tau,\tau_1)\Lambda(k;\tau,\tau_1)d\tau_1, \tag{5.75}$$

and the leading part of the turbulent residual energy K_R is written in the same form as Eq. (5.39).

5.3. Discussions on dynamo effects from quasi-kinematic and counter-kinematic methods

5.3.1. Mathematical features of obtained expressions

From both the quasi-kinematic and counter-kinematic methods, we have the same types of expressions for the Reynolds stress R_{ij} and the turbulent electromotive force $\mathbf{E}_M$:

$$R_{ij} = \frac{2}{3}K_R\delta_{ij} - \nu_T S_{ij} + \nu_M M_{ij}, \tag{5.76}$$

$$\mathbf{E}_M = \alpha\mathbf{B} - \beta\mathbf{J} + \gamma\boldsymbol{\Omega}. \tag{5.77}$$

For R_{ij}, the quasi-kinematic method gives

$$\nu_T = \nu_{TM}\ \text{[Eq. (5.40)]},\ \nu_M = \nu_{MM}\ \text{[Eq. (5.41)]}. \tag{5.78}$$

On the other hand, the counter-kinematic method leads to

$$\nu_T = \nu_{TK}\ \text{[Eq. (5.74)]},\ \nu_M = \nu_{MK}\ \text{[Eq. (5.75)]}. \tag{5.79}$$

From the comparison among these expressions, we may see that ν_{TM} and ν_{TK} possess a common feature. They are related to the intensities of fluctuations, as is shown by the dependence on Q_M and Q_K. Such close relationship also holds between ν_{MM} and ν_{MK} since they are expressed in terms of Λ (the spectrum of the turbulent cross helicity).

For $\mathbf{E}_M$, the quasi-kinematic and counter-kinematic methods give

$$\alpha = \alpha_K\ \text{[Eq. (5.32)]},\ \beta = \beta_K\ \text{[Eq. (5.33)]},\ \gamma = \gamma_K\ \text{[Eq. (5.34)]}, \tag{5.80}$$

$$\alpha = \alpha_M\ \text{[Eq. (5.68)]},\ \beta = \beta_M\ \text{[Eq. (5.69)]},\ \gamma = \gamma_M\ \text{[Eq. (5.70)]}, \tag{5.81}$$

respectively. Concerning β and γ, we may see the properties entirely similar to ν_T and ν_M. On the other hand, α is related to the helical properties of magnetic-field and velocity fluctuations in an opposite manner, as is seen from the difference of signs in Eqs. (5.32) and (5.68).

In the investigation into real dynamos related to planetary magnetic fields, the interaction between velocity and magnetic field is very important. It is meaningful to infer such an interaction from the results by the separate treatment of velocity and magnetic-field fluctuations. In the simultaneous presence of those fluctuations, ν_T and β are inferred to be associated with their total spectrum. We symbolically write this situation as

$$Q_K + Q_M \Rightarrow \nu_T,\ \beta. \tag{5.82}$$

Concerning ν_M and γ, their relationship with the cross-helicity effect is clear, which is

$$\Lambda \Rightarrow \nu_M,\ \gamma. \tag{5.83}$$

On the other hand, we may infer

$$\Gamma_M - \Gamma_K \Rightarrow \alpha. \tag{5.84}$$

The difference $\Gamma_M - \Gamma_K$ is called the turbulent residual helicity. Its importance was first pointed out in the study of isotropic MHD turbulence by the eddy-damped quasi-normal Markovianized approximation [26].

5.3.2. Physical meanings of obtained expressions

We substitute Eqs. (5.76) and (5.77) into Eqs. (4.3), (4.7), and (4.9), and have

$$\frac{DU_i}{Dt} = -\frac{\partial}{\partial x_i}\left(P + \frac{2}{3}K_R + \left\langle\frac{\mathbf{b}'^2}{2}\right\rangle\right) + (\mathbf{J}\times\mathbf{B})_i + \frac{\partial}{\partial x_j}\left(\nu_T S_{ij} - \nu_M M_{ij}\right) + \nu\nabla^2 U_i, \tag{5.85}$$

$$\frac{\partial\mathbf{B}}{\partial t} = \nabla\times(\mathbf{E} + \mathbf{U}\times\mathbf{B} + \alpha\mathbf{B} - \beta\mathbf{J} + \gamma\boldsymbol{\Omega}) + \lambda_M\nabla^2\mathbf{B}, \tag{5.86}$$

$$\mathbf{J} = \frac{1}{\beta + \lambda_M}(\mathbf{E} + \mathbf{U}\times\mathbf{B} + \alpha\mathbf{B} + \gamma\boldsymbol{\Omega}). \tag{5.87}$$

In order to simply see the physical structures of these equations, we neglect the spatial dependence of ν_T, ν_M, α, β, and γ. Under this approximation, Eqs. (5.85) and (5.86) are reduced to

$$\frac{D\mathbf{U}}{Dt} = -\nabla\left(P + \frac{2}{3}K_R + \left\langle\frac{\mathbf{b}'^2}{2}\right\rangle\right) + \mathbf{J}\times\mathbf{B} + (\nu_T + \nu)\nabla^2\mathbf{U} - \nu_M\nabla^2\mathbf{B}, \tag{5.88}$$

$$\frac{\partial\mathbf{B}}{\partial t} = \nabla\times(\mathbf{E} + \mathbf{U}\times\mathbf{B}) + \alpha\mathbf{J} + (\beta + \lambda_M)\nabla^2\mathbf{B} - \gamma\nabla^2\mathbf{U}. \tag{5.89}$$

From Eqs. (5.87) and (5.89), we may easily confirm that β expresses the enhancement of the magnetic diffusivity by fluctuations. It is called the turbulent magnetic diffusivity in the light of the turbulent viscosity ν_T that is familiar in turbulent flow of electrically nonconducting fluids. It is also named the anomalous or turbulent resistivity.

Next, we consider the physical meaning of the α-related effect with the aid of Eq. (5.87). There the α-related term, which was first proposed by Parker [27], expresses the occurrence of $\mathbf{J}$ parallel or anti-parallel to $\mathbf{B}$, depending on the sign of α (see [9-11] for the historical development of the study of the effect). This point makes a sharp contrast with the original $\mathbf{U}\times\mathbf{B}$ term generating $\mathbf{J}$ normal to $\mathbf{B}$. This α-related mechanism is usually called the alpha effect or dynamo. In Eq. (5.84), we saw that α is expressed in terms of two types of turbulent helical properties, namely, statistical helical properties of velocity and magnetic-field fluctuations.

Of the two helical properties, the relationship of α with the turbulent kinetic helicity $\langle\mathbf{u}'\cdot\boldsymbol{\omega}'\rangle$ is explained schematically by the use of Fig. 8. In the case of small λ_M or large R_{eM}, magnetic-field lines are frozen in fluid motion, and positive $\langle\mathbf{u}'\cdot\boldsymbol{\omega}'\rangle$ tends to generate $\mathbf{J}$ anti-parallel to $\mathbf{B}$. This anti-parallelness is expressed by the negative sign in Eq. (5.32).

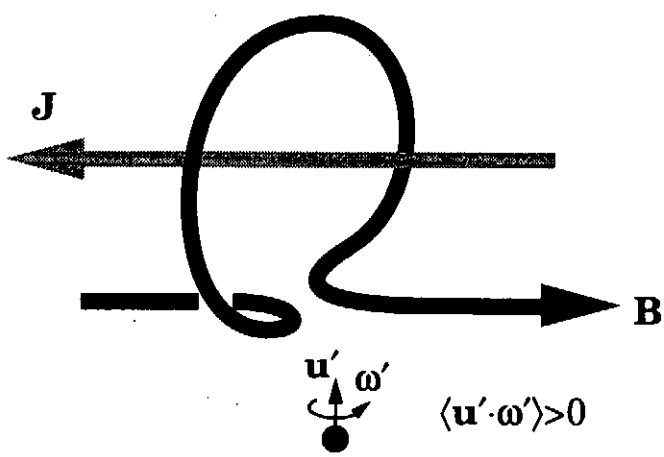

Fig. 8. Alpha dynamo.

The alpha effect due to the helical magnetic property is expressed by Eq. (5.67) with Eq. (5.68). There positive $\langle\mathbf{b}'\cdot\mathbf{j}'\rangle$ contributes to positive α. Such α generates the occurrence of $\mathbf{J}$ parallel to $\mathbf{B}$ or positive $\mathbf{B}\cdot\mathbf{J}$. This process is not so easy to explain schematically, as is done for $\langle\mathbf{u}'\cdot\boldsymbol{\omega}'\rangle$. The linkage between the signs of $\mathbf{B}\cdot\mathbf{J}$ and $\langle\mathbf{b}'\cdot\mathbf{j}'\rangle$, however, is understandable since the scale separation between $\mathbf{B}$ and $\mathbf{b}'$ is not so definite.

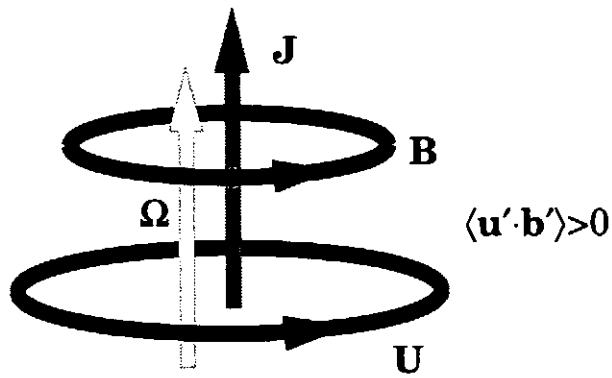

Fig. 9. Cross-helicity dynamo.

In Eq. (5.87), the γ-related term expresses the occurrence of $\mathbf{J}$ aligned with $\mathbf{\Omega}$, which is equivalent to the alignment between $\mathbf{B}$ and $\mathbf{U}$. The coefficient γ is related to the turbulent cross helicity $\langle \mathbf{u}' \cdot \mathbf{b}' \rangle$ through Eqs. (5.34) and (5.70). This alignment may be schematically depicted in Fig. 9. The linkage between $\mathbf{U} \cdot \mathbf{B}$ and $\langle \mathbf{u}' \cdot \mathbf{b}' \rangle$ resembles the situation concerning $\mathbf{B} \cdot \mathbf{J}$ and $\langle \mathbf{b}' \cdot \mathbf{j}' \rangle$. The former linkage, however, is much closer from the conservation property referred to in § 2.3. In the absence of molecular viscosity and diffusivity, the total amount of cross helicity, $\int_V \mathbf{u} \cdot \mathbf{b} dV$, is conserved. In the presence of molecular viscosity and diffusivity, the cross helicity cascades from large- to small-scale components of MHD motion, as is the sum of kinetic and magnetic energy. Such a cascade process may be regarded as a cause of the linkage between $\mathbf{U} \cdot \mathbf{B}$ and $\langle \mathbf{u}' \cdot \mathbf{b}' \rangle$.

In the frame rotating with the angular velocity $\boldsymbol{\omega}_F$, the mean vorticity $\mathbf{\Omega}$ is subject to the transformation (4.30). As a result, we have

$$\mathbf{J} = \frac{1}{\beta + \lambda_M} \left(\mathbf{E} + \mathbf{U} \times \mathbf{B} + \alpha \mathbf{B} + \gamma (\mathbf{\Omega} + 2\boldsymbol{\omega}_F) \right). \tag{5.90}$$

This indicates that the frame rotation may exert influence on the mean magnetic field in the presence of $\langle \mathbf{u}' \cdot \mathbf{b}' \rangle$. The importance of the fact will be discussed in the investigation into geodynamo. The other typical feature of the turbulent cross helicity is the explicit feedback effect on fluid motion through the Lorentz force

$$\mathbf{J} \times \mathbf{B} = \frac{1}{\beta + \lambda_M} \left(\mathbf{E} + \mathbf{U} \times \mathbf{B} + \gamma (\mathbf{\Omega} + 2\boldsymbol{\omega}_F) \right) \times \mathbf{B} \tag{5.91}$$

with no explicit alpha effect.

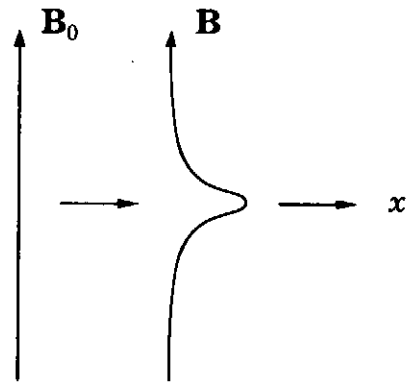

Fig. 10. Feedback effect of fluid motion by tension of magnetic field

We have the other feedback effect on fluid motion through $\langle \mathbf{u}' \cdot \mathbf{b}' \rangle$, which occurs as the last term in Eq. (5.88). It arises from the effect of mean magnetic strain that is expressed by the last term in Eq. (5.37) or (5.73). In the situation that the magnetic-field line is deformed as in Fig. 10, we may write

$$\mathbf{B}_0 = (0, B_0, 0) \rightarrow \mathbf{B} = \big(B_x(y), B_y(y), 0\big), \tag{5.92}$$

with $d^2 B_x / dy^2 < 0$. The last term in Eq. (5.88) gives

$$\nu_M > 0 \rightarrow -\nu_M \nabla^2 B_x = -\nu_M \frac{d^2 B_x}{dy^2} > 0, \tag{5.93}$$

which signifies that the magnetic field deformed in the positive x direction drives the fluid in the direction.

5.4. Magnetohydrodynamic method

In § 5. 1 and § 5. 2, we investigated into the effects of magnetic-field and velocity fluctuations on the mean magnetic-field and velocity equations in a separative manner. Through the discussions, we reached expressions (5.82)-(5.84). Of these expressions, Eqs. (5.82) and (5.84) remain as a conjecture in a fully MHD sense. In order to clarify this point, we need to treat the equations for $\mathbf{u}'$ and $\mathbf{b}'$ simultaneously. Such an analysis is very complicated. A method of alleviating the mathematical complexity is the use of Elsasser's variables introduced by Eq. (2.47). In what follows, we perform the TSDIA analysis based on these variables [12, 28, 29].

5.4.1. Elsasser's variables and two-scale description

We divide Elsasser's variables into mean and fluctuating parts, as in Eq. (4.1):

$$\boldsymbol{\phi} = \boldsymbol{\Phi} + \boldsymbol{\phi}', \quad \boldsymbol{\psi} = \boldsymbol{\Psi} + \boldsymbol{\psi}'. \tag{5.94}$$

We define

$$R_{ij}^{(E)} = \left\langle \phi_i' \psi_j' \right\rangle. \tag{5.95}$$

In terms of $R_{ij}^{(E)}$, the turbulent electromotive force $\mathbf{E}_M$ and the Reynolds stress R_{ij} are rewritten as

$$E_{Mi} = -\frac{1}{2}\varepsilon_{ij\ell} R_{j\ell}^{(E)}, \tag{5.96}$$

$$R_{ij} = \frac{1}{2}\left(R_{ij}^{(E)} + R_{ji}^{(E)}\right). \tag{5.97}$$

We may call $R_{ij}^{(E)}$ Elsasser's Reynolds stress. In the equations for the mean field $(\boldsymbol{\Phi}, \boldsymbol{\Psi})$, it plays entirely the same role as R_{ij} in the equation for $\mathbf{U}$. From Eqs. (5.96) and (5.97), however, $R_{ij}^{(E)}$ is found to be a more fundamental second-order correlation function in MHD turbulent flows.

In order to evaluate $R_{ij}^{(E)}$, we consider the equations for $\boldsymbol{\phi}'$ and $\boldsymbol{\psi}'$. There we take $\nu = \lambda_M$ and simplify the mathematical manipulation. In the case of high kinetic and magnetic Reynolds numbers, this approximation is supposed to give rise to no critical inaccuracy. From Eq. (2.49), $\boldsymbol{\phi}'$ obeys

$$\frac{\partial \phi_i'}{\partial t} + \Psi_j \frac{\partial \phi_i'}{\partial x_j} + \frac{\partial}{\partial x_j}\left(\psi_j' \phi_i' - R_{ij}^{(E)}\right) + \frac{\partial \vartheta'}{\partial x_i} - \nu \nabla^2 \phi_i' = -\psi_j' \frac{\partial \Phi_i}{\partial x_j}, \tag{5.98}$$

with the solenoidal condition

$$\nabla \cdot \boldsymbol{\phi}' = 0, \tag{5.99}$$

where ϑ' is defined by Eq. (4.19). The equation for $\boldsymbol{\psi}'$ may be obtained through the replacement

$$\boldsymbol{\phi}' \to \boldsymbol{\psi}', \quad \boldsymbol{\psi}' \to \boldsymbol{\phi}', \quad \boldsymbol{\Phi} \to \boldsymbol{\Psi}, \quad \boldsymbol{\Psi} \to \boldsymbol{\Phi}, \quad R_{ij}^{(E)} \to R_{ji}^{(E)}. \tag{5.100}$$

We apply the two-scale description to Eqs. (5.98) and (5.99), and have

$$\frac{\partial \phi_i'}{\partial \tau} + U_j \frac{\partial \phi_i'}{\partial \xi_j} + \frac{\partial}{\partial \xi_j} \psi_j' \phi_i' + \frac{\partial \vartheta'}{\partial \xi_i} - \nu \nabla_\xi{}^2 \phi_i' = B_j \frac{\partial \phi_i'}{\partial \xi_j}$$

$$+\delta_S \left(-\psi_j' \frac{\partial \Phi_i}{\partial X_j} - \frac{\partial \phi_i'}{\partial T} - \Psi_j \frac{\partial \phi_i'}{\partial X_j} - \frac{\partial}{\partial X_j} \left(\psi_j' \phi_i' - R_{ij}^{(E)} \right) - \frac{\partial \vartheta'}{\partial X_i} \right), \tag{5.101}$$

$$\frac{\partial \phi_i'}{\partial \xi_i} = -\delta_S \frac{\partial \phi_i'}{\partial X_i}. \tag{5.102}$$

Following the approach in the quasi- and counter-kinematic methods, we introduce the moving-frame Fourier representation, Eq. (5.7). Then Eqs. (5.101) and (5.102) are reduced to

$$\frac{\partial \phi_i'(\mathbf{k};\tau)}{\partial \tau} + \nu k^2 \phi_i'(\mathbf{k};\tau) - i k_i \vartheta'(\mathbf{k};\tau)$$

$$-i k_j \iint \psi_j'(\mathbf{p};\tau) \phi_i'(\mathbf{q};\tau) \delta(\mathbf{k}-\mathbf{p}-\mathbf{q}) d\mathbf{p} d\mathbf{q} = -i(\mathbf{k}\cdot\mathbf{B}) \phi_i'(\mathbf{k};\tau)$$

$$+\delta_S \left(-\psi_j'(\mathbf{k};\tau) \frac{\partial \Phi_i}{\partial X_j} - \frac{D^* \phi_i'(\mathbf{k};\tau)}{DT^*} + B_j \frac{\partial^* \phi_i'(\mathbf{k};\tau)}{\partial X_j^*} - \frac{\partial * \vartheta'(\mathbf{k};\tau)}{\partial X_i^*} \right.$$

$$\left. - \frac{\partial^*}{\partial X_j^*} \iint \psi_j'(\mathbf{p};\tau) \phi_i'(\mathbf{q};\tau) \delta(\mathbf{k}-\mathbf{p}-\mathbf{q}) d\mathbf{p} d\mathbf{q} \right), \tag{5.103}$$

$$\mathbf{k} \cdot \boldsymbol{\phi}'(\mathbf{k};\tau) = \delta \left(-\frac{\partial^* \phi_i'(\mathbf{k};\tau)}{\partial X_i^*} \right). \tag{5.104}$$

We write $\boldsymbol{\phi}'$ as

$$\boldsymbol{\phi}'(\mathbf{k};\tau) = \boldsymbol{\phi}^+(\mathbf{k};\tau) + \delta_S \left(-i \frac{\mathbf{k}}{k^2} \frac{\partial * \phi_i'(\mathbf{k};\tau)}{\partial X_i^*} \right). \tag{5.105}$$

Then $\boldsymbol{\phi}^+$ obeys the solenoidal condition concerning $\mathbf{k}$:

$$\mathbf{k} \cdot \boldsymbol{\phi}^+(\mathbf{k};\tau) = 0. \tag{5.106}$$

5.4.2. Perturbational solution

We expand $\boldsymbol{\phi}'$ and ϑ' as

$$\boldsymbol{\phi}'(\mathbf{k};\tau) = \sum_{n=0}^{\infty} \delta_S{}^n \boldsymbol{\phi}_n'(\mathbf{k};\tau), \quad \boldsymbol{\phi}^+(\mathbf{k};\tau) = \sum_{n=0}^{\infty} \delta_S{}^n \boldsymbol{\phi}_n^+(\mathbf{k};\tau), \tag{5.107}$$

$$\vartheta'(\mathbf{k};\tau) = \sum_{n=0}^{\infty} \delta_S{}^n \vartheta_n'(\mathbf{k};\tau), \tag{5.108}$$

with the similar expressions for $\boldsymbol{\psi}'$. In the $O(1)$ analysis, we have

$$\boldsymbol{\phi}_0'(\mathbf{k};\tau) = \boldsymbol{\phi}_0^+(\mathbf{k};\tau), \tag{5.109}$$

from Eq. (5.106). Then $\boldsymbol{\phi}_0'$ obeys

$$\frac{\partial \phi_{0i}'(\mathbf{k};\tau)}{\partial \tau} + \nu k^2 \phi_{0i}'(\mathbf{k};\tau) - ik_i \vartheta_0'(\mathbf{k};\tau)$$

$$-ik_j \iint \psi_{0j}'(\mathbf{p};\tau)\phi_{0i}'(\mathbf{q};\tau)\delta(\mathbf{k}-\mathbf{p}-\mathbf{q})d\mathbf{p}d\mathbf{q} = -i(\mathbf{k}\cdot\mathbf{B})\phi_{0i}'(\mathbf{k};\tau), \tag{5.110}$$

$$\mathbf{k}\cdot\boldsymbol{\phi}_0'(\mathbf{k};\tau) = 0. \tag{5.111}$$

We apply Eq. (5.111) to Eq. (5.110), and have

$$\vartheta_0'(\mathbf{k};\tau) = -\frac{k_i k_j}{k^2} \iint \psi_{0i}'(\mathbf{p};\tau)\phi_{0j}'(\mathbf{q};\tau)\delta(\mathbf{k}-\mathbf{p}-\mathbf{q})d\mathbf{p}d\mathbf{q}. \tag{5.112}$$

The substitution of Eq. (5.112) into Eq. (5.110) results in

$$\frac{\partial \phi_{0i}'(\mathbf{k};\tau)}{\partial \tau} + \nu k^2 \phi_{0i}'(\mathbf{k};\tau)$$

$$-iZ_{ij\ell}(\mathbf{k}) \iint \psi_{0j}'(\mathbf{p};\tau)\phi_{0\ell}'(\mathbf{q};\tau)\delta(\mathbf{k}-\mathbf{p}-\mathbf{q})d\mathbf{p}d\mathbf{q} = -i(\mathbf{k}\cdot\mathbf{B})\phi_{0i}'(\mathbf{k};\tau), \tag{5.113}$$

where

$$Z_{ij\ell}(\mathbf{k}) = k_j D_{i\ell}(\mathbf{k}). \tag{5.114}$$

The $\boldsymbol{\psi}_0'$ counterpart of Eq. (5.113) is given by

$$\frac{\partial \psi_{0i}'(\mathbf{k};\tau)}{\partial \tau} + \nu k^2 \psi_{0i}'(\mathbf{k};\tau)$$

$$-iZ_{ij\ell}(\mathbf{k}) \iint \phi_{0j}'(\mathbf{p};\tau)\psi_{0\ell}'(\mathbf{q};\tau)\delta(\mathbf{k}-\mathbf{p}-\mathbf{q})d\mathbf{p}d\mathbf{q} = -i(\mathbf{k}\cdot\mathbf{B})\psi_{0i}'(\mathbf{k};\tau). \tag{5.115}$$

Equations (5.114) and (5.115) are dependent linearly on $\mathbf{B}$, but they are coupled with each other, leading to the nonlinear dependence of $\boldsymbol{\phi}_0'$ and $\boldsymbol{\psi}_0'$ on $\mathbf{B}$. It is difficult to exactly solve this coupled system of equations in an analytical manner. We expand

$$\boldsymbol{\phi}_0'(\mathbf{k};\tau) = \sum_{m=0}^{\infty} \boldsymbol{\phi}_{0m}'(\mathbf{k};\tau), \tag{5.116}$$

with the similar expression for $\boldsymbol{\psi}_0'$, and solve the system by an iterative method with the right-hand sides regarded as perturbation terms. The leading term obeys

$$\frac{\partial \phi_{00i}'(\mathbf{k};\tau)}{\partial \tau} + \nu k^2 \phi_{00i}'(\mathbf{k};\tau)$$

$$-iZ_{ij\ell}(\mathbf{k}) \iint \psi_{00j}'(\mathbf{p};\tau)\phi_{00\ell}'(\mathbf{q};\tau)\delta(\mathbf{k}-\mathbf{p}-\mathbf{q})d\mathbf{p}d\mathbf{q} = 0, \tag{5.117}$$

We introduce the Green's function for Eq. (5.117) as

$$\frac{\partial G_{\phi ij}'(\mathbf{k};\tau,\tau')}{\partial \tau} + \nu k^2 G_{\phi ij}'(\mathbf{k};\tau,\tau')$$

$$-iZ_{i\ell m}(\mathbf{k}) \iint \psi_{00\ell}'(\mathbf{p};\tau) G_{\phi mj}'(\mathbf{q};\tau,\tau')\delta(\mathbf{k}-\mathbf{p}-\mathbf{q})d\mathbf{p}d\mathbf{q} = \delta_{ij}\delta(\tau-\tau'). \tag{5.118}$$

With the aid of $G_{\phi ij}'$, we have

$$\phi_{01i}'(\mathbf{k};\tau) = -i(\mathbf{k}\cdot\mathbf{B}) \int_{-\infty}^{\tau} G_{\phi ij}'(\mathbf{k};\tau,\tau_1)\phi_{00j}'(\mathbf{k};\tau_1)d\tau_1. \tag{5.119}$$

The terms $\boldsymbol{\phi}_{0n}'(n \geq 2)$ are expressed in terms of $\boldsymbol{\phi}_{0m}'(m \leq n-1)$ and $\boldsymbol{\psi}_{0m}'(m \leq n-1)$, resulting in the nonlinear dependence on $\mathbf{B}$.

The foregoing nonlinear dependence has been sought in the light of the dependence of α in Eq. (5.77) on $\mathbf{B}$. Such dependence arises from the interaction between the equations for $\mathbf{u}'$ and $\mathbf{b}'$, and attention has been paid to it from the viewpoint of determining the saturation level of induced $\mathbf{B}$. [30-32]. On the other hand, the turbulent cross helicity is an important indicator of the correlation between $\mathbf{u}'$ and $\mathbf{b}'$. By taking this fact into account, we may examine the interaction effects in an entirely different manner, as is shown by the last terms of Eqs. (5.76) and (5.77). In the present chapter, we prefer to the latter methodology and do not consider $\boldsymbol{\phi}_{0n}'(n \geq 2)$. This point will be discussed in detail through the application to planetary dynamos.

For the $O(\delta_S)$ parts in Eqs. (5.107) and (5.108), we have

$$\frac{\partial \phi_{1i}'(\mathbf{k};\tau)}{\partial \tau} + \nu k^2 \phi_{1i}'(\mathbf{k};\tau) - ik_i \vartheta_1'(\mathbf{k};\tau)$$

$$-ik_j \iint \psi_{0j}'(\mathbf{p};\tau)\phi_{1i}'(\mathbf{q};\tau)\delta(\mathbf{k}-\mathbf{p}-\mathbf{q})d\mathbf{p}d\mathbf{q}$$

$$= -i(\mathbf{k}\cdot\mathbf{B})\phi_{1i}'(\mathbf{k};\tau) - \psi_{0j}'(\mathbf{k};\tau)\frac{\partial \Phi_i}{\partial X_j} - \frac{D^*\phi_{0i}'(\mathbf{k};\tau)}{DT^*} + B_j\frac{\partial^*\phi_{0i}'(\mathbf{k};\tau)}{\partial X_j^*}$$

$$-\frac{\partial^*\vartheta_0'(\mathbf{k};\tau)}{\partial X_i^*} - ik_j\iint \psi_{1j}'(\mathbf{p};\tau)\phi_{0i}'(\mathbf{q};\tau)\delta(\mathbf{k}-\mathbf{p}-\mathbf{q})d\mathbf{p}d\mathbf{q}$$

$$-\frac{\partial^*}{\partial X_j^*}\iint \psi_{0j}'(\mathbf{p};\tau)\phi_{0i}'(\mathbf{q};\tau)\delta(\mathbf{k}-\mathbf{p}-\mathbf{q})d\mathbf{p}d\mathbf{q}, \tag{5.120}$$

$$\boldsymbol{\phi}_1'(\mathbf{k};\tau) = \boldsymbol{\phi}_1^+(\mathbf{k};\tau) - i\frac{\mathbf{k}}{k^2}\frac{\partial^*\phi_{0i}'(\mathbf{k};\tau)}{\partial X_i^*}, \tag{5.121}$$

with the similar expressions for $\boldsymbol{\psi}_1'$, where

$$\mathbf{k}\cdot\boldsymbol{\phi}_1^+(\mathbf{k};\tau) = 0. \tag{5.122}$$

As may be seen from Eqs. (5.76) and (5.77), our main interest lies in the relationship of R_{ij} and $\mathbf{E}_M$ with the mean field $\mathbf{B}$ and $\mathbf{U}$. In solving (5.120), we focus attention on the first four terms on the right-hand side and drop the last two terms. We apply Eqs. (5.121) and (5.122) to Eq. (5.120), and eliminate ϑ_1'. As a result, we have

$$\frac{\partial\phi_{1i}^+(\mathbf{k};\tau)}{\partial\tau} + \nu k^2\phi_{1i}^+(\mathbf{k};\tau)$$

$$-iZ_{ij\ell}(\mathbf{k})\iint \psi_{0j}'(\mathbf{p};\tau)\phi_{1\ell}^+(\mathbf{q};\tau)\delta(\mathbf{k}-\mathbf{p}-\mathbf{q})d\mathbf{p}d\mathbf{q}$$

$$= -D_{i\ell}(\mathbf{k})\psi_{0j}'(\mathbf{k};\tau)\frac{\partial\Phi_\ell}{\partial X_j} - \frac{D^*\phi_{0i}'(\mathbf{k};\tau)}{DT^*} + B_j\frac{\partial^*\phi_{0i}'(\mathbf{k};\tau)}{\partial X_j^*} - i(\mathbf{k}\cdot\mathbf{B})\phi_{1i}^+{}'(\mathbf{k};\tau). \tag{5.123}$$

We substitute Eq. (5.116) and its counterpart for $\boldsymbol{\psi}_0'$ into Eq. (5.123), and retain the contributions from their leading parts. We may integrate the resulting equation formally with the aid of Eq. (5.118), as

$$\phi_{1i}^+(\mathbf{k};\tau) = -\frac{\partial\Phi_\ell}{\partial X_j}D_{\ell m}(\mathbf{k})\int_{-\infty}^{\tau} G_{\phi im}'(\mathbf{k};\tau,\tau_1)\psi_{Bj}'(\mathbf{k};\tau_1)d\tau_1$$

$$-\int_{-\infty}^{\tau} G_{\phi ij}'(\mathbf{k};\tau,\tau_1)\frac{D^*\phi_{00j}'(\mathbf{k};\tau_1)}{DT^*}d\tau_1$$

$$+B_j\int_{-\infty}^{\tau} G_{\phi i\ell}'(\mathbf{k};\tau,\tau_1)\frac{\partial^* \phi_{00\ell}'(\mathbf{k};\tau_1)}{\partial X_j^*}d\tau_1$$

$$-i(\mathbf{k}\cdot\mathbf{B})\int_{-\infty}^{\tau} G_{\phi ij}'(\mathbf{k};\tau,\tau_1)\phi_{1j}^{+}{}'(\mathbf{k};\tau_1)d\tau_1. \tag{5.124}$$

Then the $O(\delta_S)$ solution is given by Eq. (5.121) combined with Eq. (5.124). Here we should note that Eq. (5.124) is still dependent on $\boldsymbol{\phi}_1^+$ though the last term. We evaluate the term in an iterative manner by using the first three terms, when necessary.

5.4.3. Evaluation of Elsasser's Reynolds stress

From Eqs. (5.119), (5.124), and their counterparts for $\boldsymbol{\psi}_{01}'$ and $\boldsymbol{\psi}_1'$, the $O(1)$ and $O(\delta_S)$ solutions may be written in terms of $\boldsymbol{\phi}_{00}'$, $\boldsymbol{\psi}_{00}'$, $G_{\phi ij}'$, and $G_{\psi ij}'$ in addition to $\mathbf{B}$ and $\mathbf{U}$. Equation (5.117) and its counterpart for $\boldsymbol{\psi}_{00}'$ are not dependent explicitly on the mean field that is a primary generator of the statistical anisotropy of $\boldsymbol{\phi}'$ and $\boldsymbol{\psi}'$. Then we assume their isotropic correlation functions, as is similar to Eqs. (5.18) and (5.60):

$$\frac{\langle Y_i(\mathbf{k};\tau)Z_j(\mathbf{k}';\tau')\rangle}{\delta(\mathbf{k}+\mathbf{k}')} = D_{ij}(\mathbf{k})Q_{YZ}(k;\tau,\tau')+\frac{i}{2}\frac{k_\ell}{k^2}\varepsilon_{ij\ell}H_{YZ}(k;\tau,\tau'), \tag{5.125}$$

$$\langle G_{Yij}'(\mathbf{k};\tau,\tau')\rangle = \delta_{ij}G_{Yij}(k;\tau,\tau'). \tag{5.126}$$

Here $\mathbf{Y}$ and $\mathbf{Z}$ represent one of $\boldsymbol{\phi}_{00}'$ and $\boldsymbol{\psi}_{00}'$. For instance, we write

$$\frac{\langle \phi_{00i}'(\mathbf{k};\tau)\psi_{00j}'(\mathbf{k}';\tau')\rangle}{\delta(\mathbf{k}+\mathbf{k}')} = D_{ij}(\mathbf{k})Q_{\phi\psi}(k;\tau,\tau')+\frac{i}{2}\frac{k_\ell}{k^2}\varepsilon_{ij\ell}H_{\phi\psi}(k;\tau,\tau'). \tag{5.127}$$

The velocity and the magnetic field corresponding to $\boldsymbol{\phi}_{00}'$ and $\boldsymbol{\psi}_{00}'$ are given by

$$\mathbf{u}_{00}' = \frac{\boldsymbol{\phi}_{00}'+\boldsymbol{\psi}_{00}'}{2},\quad \mathbf{b}_{00}' = \frac{\boldsymbol{\phi}_{00}'-\boldsymbol{\psi}_{00}'}{2}. \tag{5.128}$$

They obey Eqs. (5.16) and (5.52). We also write the correlation functions of $\mathbf{u}_{00}'$ and $\mathbf{b}_{00}'$ by using Eq. (5.125) with one of $\mathbf{u}_{00}'$ and $\mathbf{b}_{00}'$ chosen as $\mathbf{Y}$ or $\mathbf{Z}$. For instance,

$$\frac{\langle u_{00i}'(\mathbf{k};\tau)u_{00j}'(\mathbf{k}';\tau')\rangle}{\delta(\mathbf{k}+\mathbf{k}')} = D_{ij}(\mathbf{k})Q_{uu}(k;\tau,\tau')+\frac{i}{2}\frac{k_\ell}{k^2}\varepsilon_{ij\ell}H_{uu}(k;\tau,\tau') \tag{5.129}$$

corresponds to Eq. (5.18). The choice of $\mathbf{Y} = \mathbf{u}_{00}'$ and $\mathbf{Z} = \mathbf{b}_{00}'$ leads to

$$\frac{\langle u_{00i}'(\mathbf{k};\tau)b_{00j}'(\mathbf{k}';\tau')\rangle}{\delta(\mathbf{k}+\mathbf{k}')} = D_{ij}(\mathbf{k})Q_{ub}(k;\tau,\tau') + \frac{i}{2}\frac{k_\ell}{k^2}\varepsilon_{ij\ell}H_{ub}(k;\tau,\tau'), \tag{5.130}$$

which gives

$$\langle \mathbf{u}_{00}' \cdot \mathbf{b}_{00}' \rangle = 2\int Q_{ub}(k;\tau,\tau)d\mathbf{k}, \tag{5.131}$$

$$\langle \mathbf{u}_{00}' \cdot \mathbf{j}_{00}' \rangle = \int H_{ub}(k;\tau,\tau)d\mathbf{k}. \tag{5.132}$$

In the following discussions on dynamo effects, Eq. (5.132) will not play a significant role, compared with Eq. (5.131) related to the cross-helicity effect.

Among the correlation functions between $(\boldsymbol{\phi}_{00}', \boldsymbol{\psi}_{00}')$ and $(\mathbf{u}_{00}', \mathbf{b}_{00}')$, we have the relations

$$Q_{\phi\phi}(k;\tau,\tau') + Q_{\psi\psi}(k;\tau,\tau') = 2\big(Q_{uu}(k;\tau,\tau') + Q_{bb}(k;\tau,\tau')\big), \tag{5.133a}$$

$$Q_{\phi\phi}(k;\tau,\tau') - Q_{\psi\psi}(k;\tau,\tau') = 2\big(Q_{ub}(k;\tau,\tau') + Q_{bu}(k;\tau,\tau')\big), \tag{5.133b}$$

$$Q_{\phi\psi}(k;\tau,\tau') + Q_{\psi\phi}(k;\tau,\tau') = 2\big(Q_{uu}(k;\tau,\tau') - Q_{bb}(k;\tau,\tau')\big), \tag{5.133c}$$

$$Q_{\phi\psi}(k;\tau,\tau') - Q_{\psi\phi}(k;\tau,\tau') = 2\big(Q_{bu}(k;\tau,\tau') - Q_{ub}(k;\tau,\tau')\big), \tag{5.133d}$$

$$H_{\phi\phi}(k;\tau,\tau') + H_{\psi\psi}(k;\tau,\tau') = 2\big(H_{uu}(k;\tau,\tau') + H_{bb}(k;\tau,\tau')\big), \tag{5.134a}$$

$$H_{\phi\phi}(k;\tau,\tau') - H_{\psi\psi}(k;\tau,\tau') = 2\big(H_{ub}(k;\tau,\tau') + H_{bu}(k;\tau,\tau')\big), \tag{5.134b}$$

$$H_{\phi\psi}(k;\tau,\tau') + H_{\psi\phi}(k;\tau,\tau') = 2\big(H_{uu}(k;\tau,\tau') - H_{bb}(k;\tau,\tau')\big), \tag{5.134c}$$

$$H_{\phi\psi}(k;\tau,\tau') - H_{\psi\phi}(k;\tau,\tau') = 2\big(H_{bu}(k;\tau,\tau') - H_{ub}(k;\tau,\tau')\big). \tag{5.134d}$$

In the use of Elsasser's variables, Elsasser's Reynolds stress defined by Eq. (5.95) plays a central role and is expanded as

$$\begin{aligned} R_{ij}^{(E)} &= \langle \phi_{0i}' \psi_{0j}' \rangle + \delta_S\big(\langle \phi_{1i}' \psi_{0j}' \rangle + \langle \phi_{0i}' \psi_{1j}' \rangle\big) + O\big(\delta_S{}^2\big) \\ &= \langle \phi_{00i}' \psi_{00j}' \rangle + \langle \phi_{01i}' \psi_{00j}' \rangle + \langle \phi_{00i}' \psi_{01j}' \rangle + \cdots \\ &\quad + \delta_S\big(\langle \phi_{1i}' \psi_{00j}' \rangle + \langle \phi_{00i}' \psi_{1j}' \rangle + \cdots\big) + O\big(\delta_S{}^2\big). \end{aligned} \tag{5.135}$$

We substitute Eqs. (5.116) and (5.121) into Eq. (5.135), and make use of Eqs. (5.125) and (5.126). After a little lengthy mathematical manipulation, we have

$$R_{ij}^{(E)} = \frac{2}{3}K^{(E)}\delta_{ij} + \left(\frac{1}{6}\int d\mathbf{k}\int_{-\infty}^{\tau} G_{\psi}(k;\tau,\tau_1)H_{\phi\psi}(k;\tau,\tau_1)d\tau_1\right)\varepsilon_{ij\ell}B_{\ell}$$

$$+\left(\frac{1}{6}\int d\mathbf{k}\int_{-\infty}^{\tau} G_{\phi}(k;\tau,\tau_1)H_{\psi\phi}(k;\tau,\tau_1)d\tau_1\right)\varepsilon_{ij\ell}B_{\ell}$$

$$-\left(\frac{2}{3}\frac{\partial\Psi_j}{\partial x_i}+\frac{1}{15}\frac{\partial\Psi_i}{\partial x_j}\right)\int d\mathbf{k}\int_{-\infty}^{\tau} G_{\psi}(k;\tau,\tau_1)Q_{\phi\phi}(k;\tau,\tau_1)d\tau_1$$

$$-\left(\frac{2}{3}\frac{\partial\Phi_j}{\partial x_i}+\frac{1}{15}\frac{\partial\Phi_i}{\partial x_j}\right)\int d\mathbf{k}\int_{-\infty}^{\tau} G_{\phi}(k;\tau,\tau_1)Q_{\psi\psi}(k;\tau,\tau_1)d\tau_1, \qquad (5.136)$$

with

$$K^{(E)} = \frac{1}{2}\langle\boldsymbol{\phi}'\cdot\boldsymbol{\psi}'\rangle\delta_{\ell\ell} = \int Q_{\phi\psi}(k;\tau,\tau)d\mathbf{k}$$

$$-\frac{1}{2}\int d\mathbf{k}\int_{-\infty}^{\tau} G_{\psi}(k;\tau,\tau_1)\frac{DQ_{\phi\psi}(k;\tau,\tau_1)}{Dt}d\tau_1$$

$$-\frac{1}{2}\int d\mathbf{k}\int_{-\infty}^{\tau} G\phi(k;\tau,\tau_1)\frac{DQ_{\psi\phi}(k;\tau,\tau_1)}{Dt}d\tau_1$$

$$-\frac{1}{4}\left(\int k^{-2}d\mathbf{k}\int_{-\infty}^{\tau} G_{\psi}(k;\tau,\tau_1)\frac{\partial H_{\phi\psi}(k;\tau,\tau_1)}{\partial x_{\ell}}d\tau_1\right)B_{\ell}$$

$$-\frac{1}{4}\left(\int k^{-2}d\mathbf{k}\int_{-\infty}^{\tau} G_{\phi}(k;\tau,\tau_1)\frac{\partial H_{\psi\phi}(k;\tau,\tau_1)}{\partial x_{\ell}}d\tau_1\right)B_{\ell}. \qquad (5.137)$$

5.4.4. Comparison with quasi-kinematic and counter-kinematic methods

The turbulent electromotive force $\mathbf{E}_M$ and the Reynolds stress R_{ij} may be evaluated from Elsasser's Reynolds stress $R_{ij}^{(E)}$, Eq. (5.136), with the aid of Eqs. (5.96) and (5.97). In the formalism based on Elsasser's variables, $R_{ij}^{(E)}$ is expressed in terms of the correlation functions concerning $\boldsymbol{\phi}_{00}'$ and $\boldsymbol{\psi}_{00}'$. In investigating into astrophysical phenomena on the basis of these findings, it is more understandable to wrote $\mathbf{E}_M$ and R_{ij} in terms of the original variables, that is, the velocity and magnetic field corresponding to $\boldsymbol{\phi}_{00}'$ and $\boldsymbol{\psi}_{00}'$, Eq. (5.128).

In correspondence to Eq. (5.128), we introduce

$$G_+ = \frac{G_\phi + G_\psi}{2}, \quad G_- = \frac{G_\phi - G_\psi}{2}. \tag{5.138}$$

In order to see the physical meaning of these quantities, we consider the reflection of the coordinate system, $\mathbf{x} \to -\mathbf{x}$, under which we have

$$\mathbf{u} \to -\mathbf{u}, \mathbf{b} \to \mathbf{b}, \ \phi \to -\psi, \ \psi \to -\phi, \ G_{\phi ij}' \to G_{\psi ij}', \ \ G_{\psi ij}' \to G_{\phi ij}'. \tag{5.139}$$

As a result, G_+ and G_- are reflectionally symmetric and anti-symmetric, respectively.

We substitute Eq. (5.136) into Eq. (5.96), and make use of Eqs. (5.133) and (5.134). Then we have

$$\mathbf{E}_M = \alpha \mathbf{B} - \beta \mathbf{J} + \gamma \mathbf{\Omega}, \tag{5.140}$$

where

$$\alpha = \frac{1}{3}\int d\mathbf{k} \int_{-\infty}^{\tau} G_+(k, \mathbf{x}; \tau, \tau_1, t)\left(-H_{uu}(k, \mathbf{x}; \tau, \tau_1, t) + H_{bb}(k, \mathbf{x}; \tau, \tau_1, t)\right) d\tau_1$$

$$-\frac{1}{3}\int d\mathbf{k} \int_{-\infty}^{\tau} G_-(k, \mathbf{x}; \tau, \tau_1, t)\left(-H_{bu}(k, \mathbf{x}; \tau, \tau_1, t) + H_{ub}(k, \mathbf{x}; \tau, \tau_1, t)\right) d\tau_1, \tag{5.141}$$

$$\beta = \frac{1}{3}\int d\mathbf{k} \int_{-\infty}^{\tau} G_+(k, \mathbf{x}; \tau, \tau_1, t)\left(Q_{uu}(k, \mathbf{x}; \tau, \tau_1, t) + Q_{bb}(k, \mathbf{x}; \tau, \tau_1, t)\right) d\tau_1$$

$$-\frac{1}{3}\int d\mathbf{k} \int_{-\infty}^{\tau} G_-(k, \mathbf{x}; \tau, \tau_1, t)\left(Q_{ub}(k, \mathbf{x}; \tau, \tau_1, t) + Q_{bu}(k, \mathbf{x}; \tau, \tau_1, t)\right) d\tau_1, \tag{5.142}$$

$$\gamma = \frac{1}{3}\int d\mathbf{k} \int_{-\infty}^{\tau} G_+(k, \mathbf{x}; \tau, \tau_1, t)\left(Q_{ub}(k, \mathbf{x}; \tau, \tau_1, t) + Q_{bu}(k, \mathbf{x}; \tau, \tau_1, t)\right) d\tau_1$$

$$-\frac{1}{3}\int d\mathbf{k} \int_{-\infty}^{\tau} G_-(k, \mathbf{x}; \tau, \tau_1, t)\left(Q_{uu}(k, \mathbf{x}; \tau, \tau_1, t) + Q_{bb}(k, \mathbf{x}; \tau, \tau_1, t)\right) d\tau_1, \tag{5.143}$$

with the dependence on slow variables explicitly shown through $\mathbf{x}$ and t.

Entirely similarly, we may evaluate the Reynolds stress R_{ij} as

$$R_{ij} = \frac{2}{3} K_R \delta_{ij} - \nu_T S_{ij} + \nu_M M_{ij}, \tag{5.144}$$

where K_R is defined by the first relation of Eq. (5.38), and

$$\nu_T = \frac{7}{5} \beta, \tag{5.145}$$

$$\nu_M = \frac{7}{5} \gamma. \tag{5.146}$$

The ratio ν_T / β is called the turbulent magnetic Prandtl number. In the TSDIA analysis, it is larger than one, and its physical meaning will become important in § 8.2.2.

Both Eqs. (5.140) and (5.144) possess the same dependence on the mean field as their counterparts by the quasi-kinematic and counter-kinematic methods that are summarized in § 5.3.1. We are in a position to make the comparison between the coefficients by these three methods. In Eq. (5.141), the first part is related to the spectrum of the turbulent residual helicity that is defined by

$$-\mathbf{u}_{00}' \cdot \boldsymbol{\omega}_{00}' + \mathbf{b}_{00}' \cdot \mathbf{j}_{00}'. \tag{5.147}$$

This finding guarantees the conjecture by the quasi-kinematic and counter-kinematic methods, expression (5.84), and indicates the importance of the turbulent residual helicity, but not each of the kinetic and magnetic helicity. Such conclusion was also confirmed by the method based on the low/Reynolds-number expansion [33]. In the case that the MHD turbulent state may be regarded as stationary in fast time τ, we have

$$H_{bu}(k; \tau, \tau') = H_{bu}(k; \tau', \tau) = H_{ub}(k; \tau, \tau'), \tag{5.148}$$

which leads to vanishing of the second part of Eq. (5.141).

In this context, we should refer to the concept of magnetic helicity. The representative quantity characterizing helical properties of magnetic field is the helicity based on the magnetic potential $\mathbf{a}$, which is defined by

$$\mathbf{a} \cdot \mathbf{b} \quad (\mathbf{b} = \nabla \times \mathbf{a}). \tag{5.149}$$

The total amount of $\mathbf{a} \cdot \mathbf{b}$ in a whole region, $\int_V \mathbf{a} \cdot \mathbf{b} dV$, is conserved so long as there is neither net supply nor loss of magnetic helicity across the boundary. This point makes a sharp contrast with the other magnetic helicity $\mathbf{b} \cdot \mathbf{j}$ that is linked with the alpha effect. The absence of any conservation law concerning $\mathbf{b} \cdot \mathbf{j}$ is a stumbling block for

constructing a self-consistent dynamo model applicable to real-world phenomena, as will be seen later.

For the turbulent resistivity β, the first part of Eq. (5.142) indicates that the conjecture given by Eq. (5.82) is plausible; namely, β is related to the spectrum of turbulent MHD energy (the sum of turbulent kinetic and magnetic energy). The second part expresses the contribution from the turbulent cross-helicity effect in the combination of G_- (the Green's function anti-symmetric with respect to the reflection of a coordinate system). Green's functions $G_{\phi ij}{}'$ and $G_{\psi ij}{}'$ characterize the time scales of MHD turbulence that are originally pure scalars or reflectionally invariant. Then we consider that G_+ plays a bigger role, and neglect effects of G_- in the remaining parts of this review. We may make quite similar discussions on γ, as is seen from the correspondence between Eq. (5.83) and (5.143).

As one of the prominent features of the formalism based on Elsasser's variables, we may mention Eqs. (5.145) and (5.146). There we can see the clear relationship between the coefficients in $\mathbf{E}_M$ and R_{ij}. In this context, we should note that no turbulent helicity effects corresponding to the alpha effect $\alpha\mathbf{B}$ enter R_{ij} in the analysis up to $O(\delta_S)$. There what connects the equations for $\mathbf{U}$ and $\mathbf{B}$ at the level of fluctuations is the turbulent cross-helicity effect (see [34] for the discussion about the cross-helicity effect on $\mathbf{E}_M$ in the absence of mean field). In later discussions, the effect will be shown to play an important role of determining the saturation level of generated $\mathbf{B}$.

6. One-Point Dynamo Modeling with Emphasis on Self-Consistency

6.1. Necessity and significance of one-point modeling

In § 5, we examined the turbulence effects on the equations for the mean flow and magnetic field, that is, the Reynolds stress R_{ij} and the turbulent electromotive force $\mathbf{E}_M$, from a few different viewpoints. The most orthodox method of closing Eqs. (4.3) and (4.7) seems to construct the equations for the two-time spectral quantities such as $Q_{uu}(k;\tau,\tau')$ and $H_{uu}(k;\tau,\tau')$ in terms of which the coefficients in R_{ij} and $\mathbf{E}_M$ are written. The method is not feasible in the study of highly inhomogeneous MHD turbulence at all.

The foregoing circumstances are well recognized in the study of electrically nonconducting turbulent flows. In the method based on the ensemble averaging procedure, the flow components except the mean velocity are eliminated, and their effects are taken into account through the modeling of R_{ij}. Its typical model is the turbulent-

viscosity representation, Eq. (A93), in Appendix. The concept of turbulent viscosity is physically useful in describing enhanced diffusion effects on fluid motion, but there are many flow properties beyond the scope of the concept alone, and the work for adding other effects to the turbulent-viscosity representation is still in progress.

In the study of real-world flows, various types of boundary conditions, which are the origin of inhomogeneity of turbulence, become a stumbling block to the use of spectral expressions such as Eq. (A95). A great merit of the ensemble-mean method is the capability of examining complex flows at high Reynolds numbers that are far beyond the reach of the computer simulation of the primitive equations. The constraints on the method, such as the decrease in handled flow properties, should be compensated for by this merit. Then those spectral expressions need to be replaced with much more manageable one-point expressions in physical space.

The computer simulation of astrophysical and geophysical MHD flows is in progress with the advancement of a computer and a numerical scheme. The flows within the scope of the simulation, however, are still far from real-world flows in the magnitude of Reynolds and magnetic Reynolds numbers, Taylor number, etc. One of the major merits of the mean-field theory is to get a comprehensive understanding of magnetic-field generation and its feedback mechanisms, with no special constraints on the magnitude of those nondimensional parameters, although the subject of interest is limited to global MHD properties. For this purpose, we need to construct a manageable and self-consist dynamo model mimicking real-world astrophysical phenomena, with the aid of the theoretical findings. In what follows, we express the coefficients in R_{ij} and $\mathbf{E}_M$ in terms of one-point quantities in physical space. Such a method may be called turbulent MHD or dynamo modeling after the terminology in the electrically nonconducting case.

6.2. Modeling policy and procedures

One-point modeling of electrically nonconducting turbulent flows in physical space is explained theoretically in Appendix. The key task there is the choice of statistical quantities characterizing turbulent flows. It is necessary to make the number of those quantities as small as possible for reducing the mathematical burden in solving the resulting system of turbulence equations. The simplest model of the Reynolds stress R_{ij} in electrically nonconducting turbulent flows is the turbulent-viscosity (ν_T) representation, Eq. (A93) with Eq. (A108) lacking the D/DT-related parts. Equation (5.144) is essentially the same level of approximation as Eq. (A93), apart from the newly occurring magnetic-field effect. There we adopted the turbulent kinetic energy K and its dissipation rate ε as the characteristic turbulence quantities, which are defined below by

Eqs. (6.1) and (6.3) with the magnetic parts dropped, respectively. This is the choice of the least number of turbulence quantities for constructing the characteristic time scale as K/ε.

The present MHD modeling consists of the two key procedures. One is the choice of fundamental quantities characterizing MHD turbulence statistically, in terms of which the coefficients in R_{ij} and $\mathbf{E}_M$ are expressed. The other is the construction of the transport equations for those quantities. In the traditional dynamo modeling with attention focused on the alpha effect, little attention has been paid to the latter point.

As the fundamental turbulence quantities, we choose the turbulent MHD energy K, the turbulent cross helicity W, the turbulent residual helicity H, and the MHD energy dissipation rate ε, which are given by

$$K = \left\langle \frac{\mathbf{u}'^2 + \mathbf{b}'^2}{2} \right\rangle, \tag{6.1}$$

$$W = \langle \mathbf{u}' \cdot \mathbf{b}' \rangle, \tag{6.2}$$

$$H = \langle -\mathbf{u}' \cdot \boldsymbol{\omega}' + \mathbf{b}' \cdot \mathbf{j}' \rangle, \tag{6.3}$$

$$\varepsilon = \nu \left\langle \left(\frac{\partial u_j'}{\partial x_i} \right)^2 \right\rangle + \lambda_M \left\langle \left(\frac{\partial b_j'}{\partial x_i} \right)^2 \right\rangle, \tag{6.4}$$

respectively. In Eq. (5.141) for α, the first term is related to the spectrum of the turbulent residual helicity. Then the introduction of H is reasonable from the viewpoint of one-point modeling. The entirely similar situation holds for the choice of K and W in modeling β and γ.

Here we should note that the spectra of the turbulent residual helicity, MHD energy, and cross helicity occurring in Eqs. (5.141)-(5.143) correspond to the lowest-order terms in the TSDIA formalism, as may be seen from the use of Eq. (5.125). We denote those lowest-order contributions to K, W, H, and ε by K_0, W_0, H_0, and ε_0, respectively. In the present one-point modeling, we use their full counterparts, K, W, H, and ε through the replacement

$$K_0 \to K,\ W_0 \to W,\ H_0 \to H,\ \varepsilon_0 \to \varepsilon. \tag{6.5}$$

This procedure may be regarded as the physical-space renormalization in the comparison with the wavenumber-space renormalization such as Eq. (A45). In addition to K, W,

and H, ε is necessary for the construction of a characteristic time scale of MHD turbulent flow since W and H are pseudoscalars.

Under the choice of Eqs. (6.1)-(6.4), the one-point modeling of Eqs. (5.141)-(5.143) is straightforward. For instance, we write

$$H_0 = \int \left(-H_{uu}(k, \mathbf{x}; \tau, \tau, t) + H_{bb}(k, \mathbf{x}; \tau, \tau, t)\right) d\mathbf{k}, \tag{6.6}$$

$$\tau_M(k) = \int_{-\infty}^{\tau} G_+(k, \mathbf{x}; \tau, \tau_1, t) d\tau_1. \tag{6.7}$$

Equation (6.7) expresses the time scale associated with the spatial length k^{-1}. We take the energy-containing length

$$k_0^{-1} = \frac{K_0^{3/2}}{\varepsilon_0}, \tag{6.8}$$

and model

$$\tau_M(k_0) = \frac{k_0^{-1}}{\sqrt{K_0}} = \frac{K_0}{\varepsilon_0}. \tag{6.9}$$

As a result, Eq. (5.141) with only the first part retained is modeled as

$$\alpha = C_\varepsilon \frac{K}{\varepsilon} H, \tag{6.10}$$

after the renormalization, Eq. (6.5), where C_ε is a positive model constant. Entirely similarly, we have

$$\beta = C_\beta \frac{K^2}{\varepsilon} \left(= C_\beta \frac{K}{\varepsilon} K\right), \tag{6.11}$$

$$\gamma = C_\gamma \frac{K}{\varepsilon} W, \tag{6.12}$$

with positive constants C_β and C_γ.

In order to close the foregoing expressions, we need the transport equations governing K, W, H, and ε. The first two quantities are linked with the conservation laws, as was noted in § 2.3. This property results in the equations for K and W, Eq. (4.20), whose mathematical structures are firm and clear. In Eq. (4.20) with $Z = K$, what is to be modeled is the second part of Eq. (4.23). We pay attention to the first term of the part and model it as

$$\left\langle \left(\frac{\mathbf{u}'^2 + \mathbf{b}'^2}{2} + \vartheta' \right) \mathbf{u}' \right\rangle = -\frac{\nu_T}{\sigma_K} \nabla K, \tag{6.13}$$

where σ_K is a positive constant. The hydrodynamic counterpart of this modeling is referred to in § A3.2 from the viewpoint of turbulence theory.

In Eq. (4.20) with $Z = W$, we need to model Eqs. (4.25) and (4.26). In the latter, the first term of the second part denotes the transport of W by turbulence, which is modeled as

$$\langle (\mathbf{u}' \cdot \mathbf{b}') \mathbf{u}' \rangle = -\frac{\nu_T}{\sigma_W} \nabla W, \tag{6.14}$$

similar to Eq. (6.13), where σ_W is a positive constant.

Equation (4.25) is the destruction rate of W due to molecular viscous and resistive effects. As the characteristic time scale of MHD turbulence, we may consider two time scales. One is the foregoing time scale based on K and ε, and is given by K/ε. The other is its counterpart of W, that is, W/ε_W. We assume that they are close to each other. Then we have

$$\varepsilon_W = C_W \frac{K}{\varepsilon} W, \tag{6.15}$$

where C_W is a positive constant close to one.

In hydrodynamic one-point modeling, we adopt a phenomenological model equation for ε since it is related to no conservation constraint, unlike K and W. In the present MHD one-point modeling, its simplest extension to the MHD version is

$$\frac{D\varepsilon}{Dt} = C_{\varepsilon 1} \frac{\varepsilon}{K} P_K - C_{\varepsilon 1} \frac{\varepsilon^2}{K} + \nabla \cdot \left(\frac{\nu_T}{\sigma_\varepsilon} \nabla \varepsilon \right), \tag{6.16}$$

where $C_{\varepsilon 1}$, $C_{\varepsilon 2}$, and σ_ε are positive model constants.

Finally, we refer to the equation for the turbulent residual helicity H. Its equation may be written as [12]

$$\frac{DH}{Dt} = \langle u_j' u_i' + b_j' b_i' \rangle \frac{\partial \Omega_i}{\partial x_j} + \langle b_j' j_i' \rangle \frac{\partial U_i}{\partial x_j} + \langle \mathbf{u}' \times \boldsymbol{\omega}' \rangle \cdot \boldsymbol{\Omega} - \nabla \cdot \left(\langle \mathbf{u}'^2 / 2 \rangle \boldsymbol{\Omega} \right)$$

$$+\left\langle \frac{\partial u_i'}{\partial x_j} j_i' + \frac{\partial \omega_i'}{\partial x_j} b_i' - \omega_i' \frac{\partial b_i'}{\partial x_j} - u_i' \frac{\partial j_i'}{\partial x_j} \right\rangle B_j - \left\langle \omega_i' b_j' \right\rangle \frac{\partial B_i}{\partial x_j}$$

$$+\left\langle u_j' b_i' + u_i' b_j' \right\rangle \frac{\partial J_i}{\partial x_j} - \left\langle \mathbf{u}' \times \mathbf{j}' \right\rangle \cdot \mathbf{J} + \left\langle u_j' b_i' + u_i' b_j' \right\rangle \frac{\partial J_i}{\partial x_j} + R_H, \qquad (6.17)$$

where R_H denotes the remaining part that is not dependent explicitly on the mean field and is composed of the correlation functions of the third order in $\mathbf{u}'$, $\mathbf{b}'$, $\boldsymbol{\omega}'$, and $\mathbf{j}'$. This complicated form makes a sharp contrast with the case for the turbulent kinetic helicity in electrically nonconducting turbulent flows. In the latter, the total amount of kinetic helicity $\mathbf{u} \cdot \boldsymbol{\omega}$ is conserved in the absence of molecular viscous effects.

The foregoing fact is a big stumbling block for the construction of a self-consistent dynamo model that is applicable to various types of astrophysical phenomena. In the current study of mean-field theory with the alpha effect as a cornerstone, it is rather curious that little attention has been paid to this difficulty. We may mention two reasons for this situation. One is that the coefficient α is often assumed to be a given parameter and that its self-consistent determination is out of interest. The other is that attention is paid to the kinetic part of H from the kinematic viewpoint. In this case, we have its equation with the firm mathematical basis.

6.3. Summary of dynamo model

We summarize the one-point dynamo model that has been obtained with the aid of statistical methods [12, 28, 29]. We give the model by explicitly including effects of frame rotation and the buoyancy force based on the Boussinesq approximation.

6.3.1. System of model equations

The mean velocity $\mathbf{U}$, the mean magnetic field $\mathbf{B}$, and the mean temperature Θ obey

$$\frac{DU_i}{Dt} = -\frac{\partial}{\partial x_i}\left(P + \left\langle \frac{\mathbf{b}'^2}{2} \right\rangle \right) + (\mathbf{J} \times \mathbf{B})_i + \frac{\partial}{\partial x_j}\left(-R_{ij}\right) + \nu \nabla^2 U_i$$

$$+2(\mathbf{U} \times \boldsymbol{\omega}_F)_i - \alpha_T (\Theta - \Theta)_R g_i, \qquad (6.18)$$

$$\frac{\partial \mathbf{B}}{\partial t} = \nabla \times (\mathbf{U} \times \mathbf{B} + \mathbf{E}_M) + \lambda_M \nabla^2 \mathbf{B}, \qquad (6.19)$$

$$\frac{D\Theta}{Dt} = \nabla \cdot (-\mathbf{H}_\theta) + \lambda_\theta \nabla^2 \Theta, \qquad (6.20)$$

with the solenoidal condition $\nabla \cdot \mathbf{U} = \nabla \cdot \mathbf{B} = 0$. In Eq. (6.19), $\boldsymbol{\omega}_F$ is the angular velocity of frame rotation, Θ_R is the reference temperature, α_T is the coefficient of thermal expansion, and $\mathbf{g}$ is the vector of gravitational acceleration.

The Reynolds stress R_{ij}, the turbulent electromotive force $\mathbf{E}_M$, and the turbulent heat flux $\mathbf{H}_\theta$ are expressed as

$$R_{ij} \equiv \left\langle u_i' u_j' - b_i' b_j' \right\rangle = \frac{2}{3} K_R \delta_{ij} - \nu_T S_{ij} + \nu_M M_{ij}, \tag{6.21}$$

$$\mathbf{E}_M \equiv \left\langle \mathbf{u}' \times \mathbf{b}' \right\rangle = \alpha \mathbf{B} - \beta \mathbf{J} + \gamma (\boldsymbol{\Omega} + 2\boldsymbol{\omega}_F), \tag{6.22}$$

$$\mathbf{H}_\theta \equiv \left\langle \mathbf{u}' \theta' \right\rangle = -\frac{\nu_T}{\sigma_\theta} \nabla \Theta, \tag{6.23}$$

where

$$K_R = \left\langle \frac{\mathbf{u}'^2 - \mathbf{b}'^2}{2} \right\rangle, \tag{6.24}$$

$$S_{ij} = \frac{\partial U_j}{\partial x_i} + \frac{\partial U_i}{\partial x_j}, \tag{6.25}$$

$$M_{ij} = \frac{\partial B_j}{\partial x_i} + \frac{\partial B_i}{\partial x_j}. \tag{6.26}$$

In relation to Eq. (6.22), we should note the vorticity transformation rule in the rotating frame,

$$\boldsymbol{\Omega} \rightarrow \boldsymbol{\Omega} + 2\boldsymbol{\omega}_F. \tag{6.27}$$

Equation (6.23) is the so-called turbulent-diffusivity model for $\mathbf{H}_\theta$, which is at the same level approximation as Eq. (6.21) with the turbulent-viscosity representation as its primary part.

The coefficients in Eqs. (6.21)-(6.23) are given by

$$\nu_T = \frac{7}{5} \beta, \tag{6.28}$$

$$\nu_M = \frac{7}{5} \gamma, \tag{6.29}$$

$$\alpha = C_\alpha \frac{K}{\varepsilon} H, \tag{6.30}$$

$$\beta = C_\beta \frac{K^2}{\varepsilon}, \tag{6.31}$$

$$\gamma = C_\gamma \frac{K}{\varepsilon} W, \tag{6.32}$$

where

$$K = \left\langle \frac{\mathbf{u}'^2 + \mathbf{b}'^2}{2} \right\rangle, \tag{6.33}$$

$$W = \langle \mathbf{u}' \cdot \mathbf{b}' \rangle, \tag{6.34}$$

$$H = \langle -\mathbf{u}' \cdot \boldsymbol{\omega}' + \mathbf{b}' \cdot \mathbf{j}' \rangle, \tag{6.35}$$

$$\varepsilon = \nu \left\langle \left(\frac{\partial u_j'}{\partial x_i} \right)^2 \right\rangle + \lambda_M \left\langle \left(\frac{\partial b_j'}{\partial x_i} \right)^2 \right\rangle. \tag{6.36}$$

Between K and W, we have a very important relationship

$$\frac{|W|}{K} = \frac{2|\langle \mathbf{u}' \cdot \mathbf{b}' \rangle|}{\langle \mathbf{u}'^2 + \mathbf{b}'^2 \rangle} \le 1. \tag{6.37}$$

It will be later confirmed to play a critical role in the discussions on the generation processes of astro/geophysical magnetic fields.

Of Eqs. (6.33)-(6.36), the turbulent MHD energy K and the turbulent cross helicity W are governed by

$$\frac{DZ}{Dt} = P_Z - \varepsilon_Z + \nabla \cdot \mathbf{T}_Z \quad (Z = K \text{ or } W), \tag{6.38}$$

where $\varepsilon_z \equiv \varepsilon$, and

$$P_K = -R_{ij} \frac{\partial U_j}{\partial x_i} - \mathbf{E}_M \cdot \mathbf{J} - \alpha_T \mathbf{H}_\theta \cdot \mathbf{g}, \tag{6.39}$$

$$\mathbf{T}_K = W\mathbf{B} + \frac{\nu_T}{\sigma_K} \nabla K, \tag{6.40}$$

$$P_W = -R_{ij}\frac{\partial B_j}{\partial x_i} - \mathbf{E}_M \cdot (\boldsymbol{\Omega} + 2\boldsymbol{\omega}_F) - \alpha_T \frac{W}{K}\mathbf{H}_\theta \cdot \mathbf{g}, \tag{6.41}$$

$$\varepsilon_W = C_W \frac{K}{\varepsilon} W, \tag{6.42}$$

$$\mathbf{T}_W = K\mathbf{B} + \frac{\nu_T}{\sigma_W}\nabla W. \tag{6.43}$$

In Eq. (6.39), we should note that the buoyancy-force effect is included explicitly through the last term [see Eq. (4.32)]. In Eq. (6.41), the third term arises from Eq. (4.33) in the combination with a simple model

$$\mathbf{b}' = \frac{W}{K}\mathbf{u}'. \tag{6.44}$$

This model is plausible in the sense that its product with $\mathbf{u}'$ leads to an identity relation and is used only for the estimate of expression (4.33).

As the model equation for ε, we adopt

$$\frac{D\varepsilon}{Dt} = C_{\varepsilon 1}\frac{\varepsilon}{K}P_K - C_{\varepsilon 1}\frac{\varepsilon^2}{K} + \nabla\cdot\left(\frac{\nu_T}{\sigma_\varepsilon}\nabla\varepsilon\right). \tag{6.45}$$

This is a phenomenological equation, unlike Eq. (6.38), but its hydrodynamic version has been tested in various types of flows and shown to be an acceptable model, although there is still room for its improvement.

Concerning H, we have no model equation whose reliability is comparable to Eqs. (6.38) and (6.45). The sole model equation was constructed for the case of no mean velocity and was studied in the investigation into reversed-field pinches of plasmas [35, 36). Modeling the equation for H in the presence of both the mean velocity and magnetic field is a primary unresolved subject in mean-field theory of dynamo. In the following application of the present dynamo model to the study of astro/geophysical magnetic fields, we shall make discussions without resort to the details of H-transport processes.

6.3.2. Model constants

The model constants in the present dynamo model are adopted as follows;

$$R_{ij}, \mathbf{E}_M: C_\alpha \cong 0.02, C_\beta \cong 0.05, C_\gamma \cong 0.04, \tag{6.46a}$$

$\mathbf{H}_\theta$: $\sigma_\theta \cong 1$, (6.46b)

Equation for K: $\sigma_K \cong 1$, (6.46c)

Equation for W: $C_W \cong 1.1$, $\sigma_K \cong 1$, (6.46d)

Equation for ε: $C_{\varepsilon 1} \cong 1.4$, $C_{\varepsilon 2} \cong 1.9$, $\sigma_K \cong 1.3$. (6.46e)

Of these ten model constants, σ_θ, σ_K, $C_{\varepsilon 1}$, $C_{\varepsilon 2}$, and σ_ε survive in the hydrodynamic case. Then we adopt the same values as for the case.

The model constants given by Eq. (6.46a) were estimated with the aid of the computer experiment of MHD turbulent flow in a cubic region [37]. There the turbulent state is inhomogeneous in one direction and homogeneous in the other two directions. The inhomogeneity of state is sustained through the imposition of an external force.

The modeling of ε_W in the form of Eq. (6.15) or (6.42) arises from the assumption that C_W is close to one. We consider the homogeneous MHD turbulent state with vanishing $\mathbf{U}$ and $\mathbf{B}$. In this situation, Eq. (6.38) results in

$$\frac{\partial K}{\partial t} = -\varepsilon, \tag{6.47}$$

$$\frac{\partial W}{\partial t} = -C_W \frac{\varepsilon}{K} W, \tag{6.48}$$

which gives

$$\frac{\partial}{\partial t}\frac{W}{K} = -(C_W - 1)\frac{\varepsilon}{K^2} W. \tag{6.49}$$

For $C_W < 1$, initially nonvanishing $|W|/K$ continues to grow and eventually exceeds one. This result violates the constraint on $|W|/K$, Eq. (6.37). Then we need $C_W > 1$ and adopt the first of Eq. (6.46d).

7. Typical Magnetic-Field Generation Processes

In the dynamo model summarized in § 6.3, we have two typical generation mechanisms of magnetic fields; one is the alpha or turbulent residual-helicity effect, and the other is the turbulent cross-helicity effect. In what follows, we shall show that entirely different magnetic-field generation processes occur according to the relative importance of these two effects.

7.1. Dominant-helicity dynamo

7.1.1. Convection columns and helicity

In § 1, the characteristics of the geomagnetic and solar magnetic fields were explained in the light of the geometrical features of the earth's outer core (Fig. 1) and the solar convective zone (Fig. 2). The magnitude of nondimensional parameters of flows in the outer core and the convective zone was discussed in § 2.2. There the largeness of the Taylor number of the outer core was emphasized, compared with its solar counterparts, indicating the greater importance of frame-rotation effects on the geomagnetic-field generation process.

Effects of frame rotation occur typically through convection columns along the axis of rotation, as was mentioned in § 2.2. Each column is composed of the fluid motion coming up or down while rotating, leading to the occurrence of helicity. The spherical-shell region of the earth's outer core is much wider than the solar convective zone. Then the convection columns may occur more clearly in the outer core.

A computer simulation based on a system of primitive equations is a method appropriate for the study of highly three-dimensional, time-dependent global MHD flows, unlike the mean-field theory focusing on a stationary or quasi-stationary MHD state. In a number of computer simulations mimicking geodynamo [6-8, 38-42], the column-like or elongated flow structure along the rotation axis has been clearly detected. The structure consists of a few pairs of distinct convection columns. In each pair, the fluid in one column rotating in the same direction as the rotating shell sinks from the column ends towards the equatorial plane, whereas the fluid in the another rotating in the opposite direction rises from the equatorial plane towards the ends (Fig. 5). As a result, the kinematic helicity tends to be negative and positive in the northern and southern hemispheres, respectively. The column-like or elongated structure is supposed to be linked with the generation of poloidal magnetic field. Readers may consult [43, 44] for recent reviews of geodynamo.

These findings by the computer simulations signify an important role of helicity effects on MHD flows in a spherical-shell region such as the earth's outer core. In what follow, we examine the situation in which effects of helicity play a dominant role in the magnetic-field generation process. In this context, we should note that each of convection columns observed in the computer simulations is beyond the scope of the mean-field theory of dynamo. What may be dealt with explicitly by the theory is the helicity effect arising from the ensemble mean of such convective-column flows or their average around

the axis of frame rotation. We examine the helicity effect through the turbulent electromotive force $\mathbf{E}_M$ and the Reynolds stress R_{ij}.

7.1.2. Mean-field equations

We consider the mean magnetic induction equation (6.19) with Eq. (6.22) or

$$\frac{\partial \mathbf{B}}{\partial t} = \nabla \times \left(\mathbf{U} \times \mathbf{B} + \alpha \mathbf{B} - \beta \mathbf{J} + \gamma \left(\mathbf{\Omega} + 2\boldsymbol{\omega}_F \right) \right), \tag{7.1}$$

where the molecular magnetic diffusivity λ_M was neglected, compared with its turbulent counterpart β. We seek the stationary state of the magnetic field $\mathbf{B}$ that is subject to

$$\nabla \times \left(\mathbf{U} \times \mathbf{B} + \alpha \mathbf{B} - \beta \mathbf{J} + \gamma \left(\mathbf{\Omega} + 2\boldsymbol{\omega}_F \right) \right) = 0. \tag{7.2}$$

Here the turbulent-resistivity part $-\beta\mathbf{J}$ contributes to the diffusion of magnetic-field structure due to turbulent motion. In order that a distinctive global structure of $\mathbf{B}$ may continue to persist, there needs to be the effect that balances with $-\beta\mathbf{J}$ and cancels the diffusion effect arising from it. We assume the dominant-helicity state in which the alpha term $\alpha\mathbf{B}$ due to the helicity effect balances with $-\beta\mathbf{J}$; namely, we put

$$\mathbf{J} = \frac{\alpha}{\beta} \mathbf{B}, \tag{7.3}$$

where

$$\frac{\alpha}{\beta} = \frac{C_\alpha}{C_\beta} \frac{H}{K}, \tag{7.4}$$

from Eqs. (6.30) and (6.31).

Equation (7.3) represents the typical manifestation of the turbulent-helicity or alpha effect. There $\mathbf{J}$ is aligned with $\mathbf{B}$, which results in vanishing of the Lorentz force $\mathbf{J} \times \mathbf{B}$ in the mean-flow equation (6.18). From this property, the magnetic field obeying Eq. (7.3) is called the force-free field.

Of the remaining two parts in Eq. (7.2), we consider the γ-related term. A primary cause generating helicity effects is the frame rotation. Then we retain the $\boldsymbol{\omega}_F$-related part and put aside the first term or $\mathbf{U} \times \mathbf{B}$. We shall later refer to it. Then we have

$$\mathbf{J} = \frac{\alpha}{\beta} \mathbf{B} + 2 \frac{\gamma}{\beta} \boldsymbol{\omega}_F, \tag{7.5}$$

with

$$\frac{\gamma}{\beta}=\frac{C_\gamma}{C_\beta}\frac{W}{K}, \tag{7.6}$$

from Eqs. (6.31) and (6.32).

Let us see Eq. (7.3) in light of the magnetic-field growth. From Eq. (7.1), we have

$$\frac{\partial}{\partial t}\int_V \frac{\mathbf{B}^2}{2}dV=-\int_S \frac{\mathbf{B}^2}{2}\mathbf{U}\cdot\mathbf{n}dS+\int_V \mathbf{B}\cdot\big((\mathbf{B}\cdot\nabla)\mathbf{U}\big)dV$$

$$+\int_V \mathbf{B}\cdot\Big(\nabla\times\big(\alpha\mathbf{B}-\beta\mathbf{J}+\gamma(\boldsymbol{\Omega}+2\boldsymbol{\omega}_F)\big)\Big)dV, \tag{7.7}$$

where V and S denote the volume and surface of a spherical-shell region, respectively, and $\mathbf{n}$ is the outward unit vector normal to the surface. On the right-hand side, the first two terms arise from the $\mathbf{U}\times\mathbf{B}$-related part in Eq. (7.1). The first term, which was rewritten using the Stokes' integral theorem, does not contribute to the net energy increase so long as there is no net energy inflow across the boundary. The second term represents the energy increase due to the stretching of magnetic field lines by fluid motion. These facts indicates that the alignment between $\mathbf{B}$ and $\mathbf{U}$, which means vanishing of $\mathbf{U}\times\mathbf{B}$, is linked with the saturation of the magnetic-energy growth, resulting in the stationary state of $\mathbf{B}$.

Next, we consider the mean-flow equation (6.18) with Eq. (6.21). For simplicity of discussion, we assume the quasi-homogeneity of turbulent state; namely, the spatial derivatives of α, β, and γ are neglected, and their spatial variation is taken into account through the implicit dependence on location. Under Eq. (7.5), it may be rewritten as

$$\frac{D\mathbf{U}}{Dt}=-\nabla\left(P+\left\langle\frac{\mathbf{b}'^2}{2}\right\rangle+\frac{2}{3}K_R\right)-\alpha_T(\Theta-\Theta)_R\mathbf{g}$$

$$+2\left(\mathbf{U}-\frac{\gamma}{\beta}\mathbf{B}\right)\times\boldsymbol{\omega}_F+\nu_T\nabla^2\left(\mathbf{U}-\frac{\gamma}{\beta}\mathbf{B}\right), \tag{7.8}$$

where Eqs. (6.28) and (6.29) were used. In Eq. (7.8), the third term comes from the combination of the Lorentz and Coriolis forces. We mentioned above that the alignment between $\mathbf{B}$ and $\mathbf{U}$ is important for the saturation of $\mathbf{B}$. In Eq. (7.8), the alignment

$$\mathbf{U}=\frac{\gamma}{\beta}\mathbf{B}\ \text{ or }\ \mathbf{B}=\frac{\beta}{\gamma}\mathbf{U}. \tag{7.9}$$

signifies the cancellation of the momentum-diffusion effect due to turbulent motion, $\nu_T \nabla^2 \mathbf{U}$, by the magnetic feedback effect $-\nu_M \nabla^2 \mathbf{B}$. The cancellation leads to the sustainment of the mean-flow structure that is coupled with a distinct global structure of magnetic field. We should note that vanishing of $\mathbf{U} \times \mathbf{B}$ on which Eq. (7.5) is founded has been assured by Eq. (7.9).

Equation (7.9) also expresses the balance between the Lorentz and Coriolis forces. The ratio of Lorentz to Coriolis forces is called the Elsasser number. From the computer simulation of the magnetoconvection [8], the persistence of column structures is closely related to the state with the Elsasser number close to one. This state is realized by Eq. (7.9) .

Equation (7.9) stipulates the saturation level of generated $\mathbf{B}$. The alpha effect $\alpha\mathbf{B}$ is linear in $\mathbf{B}$ so long as α is not dependent explicitly on $\mathbf{B}$. As a result, Eq. (6.19) with the effect embedded cannot determine the saturation level. A method for overcoming this difficulty is the incorporation of nonlinear effects in $\mathbf{B}$ into α, as was noted in § 5.4.2 [30-32]. Equation (7.9), however, indicates that the inclusion of the turbulent cross-helicity effect results in the automatic determination of the level through the combination with the mean-flow equation.

7.1.3. Turbulence equations

In § 7.1.2, we made discussions on $\mathbf{B}$ and $\mathbf{U}$ on the basis of nonvanishing α, β, and γ. These quantities are expressed in terms of the turbulent energy K, the turbulent cross helicity W, the turbulent residual helicity H, and the energy dissipation rate ε, as in Eqs. (6.28)-(6.32). To show how these turbulence quantities are sustained consistently with $\mathbf{B}$ and $\mathbf{U}$ is indispensable for the self-consistent understanding of dynamo processes. In the past study of mean-field theory of dynamo, the sustainment of nonvanishing α and β was assumed, and little attention was paid to this aspect.

The turbulent energy K is generated by the production term in Eq. (6.38), P_K [Eq. (6.39)]. Under Eqs. (7.5) and (7.9), we have

$$R_{ij} = \mathbf{E}_M = 0, \tag{7.10}$$

which results in

$$P_K = -\alpha_T \mathbf{H}_\theta \cdot \mathbf{g}. \tag{7.11}$$

Equation (7.11) indicates that the turbulent MHD state subject to dominant helicity effects is sustained through the turbulent-energy supply by an external force such as the buoyancy force. In the case of a spherical-shell region like the earth's outer core, we have

$$\mathbf{H}_\theta = -\frac{\nu_T}{\sigma_\theta}\left(\frac{\partial \Theta}{\partial r}, 0, 0\right), \quad \mathbf{g} = (-g, 0, 0), \tag{7.12}$$

in the spherical coordinate system (r, θ, ϕ) of Fig. 6, where use has been made of Eq. (6.23). As a result, P_K is written as

$$P_K = -\alpha_T g \frac{\nu_T}{\sigma_\theta}\frac{\partial \Theta}{\partial r} > 0, \tag{7.13}$$

since $\partial\Theta / \partial r < 0$. Namely, K continues to be generated by P_K. The energy dissipation rate ε obeys Eq. (6.45). Nonvanishing ε is sustained by the first term proportional to P_K under Eq. (7.13).

Entirely similarly, the production term for W, Eq. (6.41), is given by

$$P_W = \frac{W}{K} P_K, \tag{7.14}$$

which leads to

$$W > 0 \rightarrow P_W > 0 \quad \text{and} \quad W < 0 \rightarrow P_W < 0. \tag{7.15}$$

This finding signifies that positive and negative W are generated in the region with positive and negative W, respectively, resulting in the sustainment of nonvanishing W.

In the above discussions, the buoyancy force plays a key role of sustaining the turbulent state represented by K and W. Is the dominant-helicity state possible in the absence of an external force such as the buoyancy force? In this case, we have no production mechanisms of K and W. This point will be later discussed in the context of the collimation of accretion jets that was referred to in § 1.

In the present stage of mean-field theory, the discussion comparable to those on K and W cannot be made on the turbulent residual helicity H, owing to the lack of the reliable model equation for it. The construction of the model equation is the biggest unresolved subject of mean-field theory.

7.2. Dominant/cross-helicity state

In the solar convective zone (Fig. 2), the spherical-shell region is much thinner than that of the earth's outer core. This fact suggests that convection column structures are hard to be clearly formed, compared with the outer core. With this point in mind, we shall consider the situation opposite to § 7.1, that is, the dominant/cross-helicity case.

7.2.1. Mean-field equations

As one of the prominent difference between the fluid motions in the convective zone and the outer core, we may mention the strong differential rotation in the former [45]. In the zone, the angular velocity of the rotational motion is highly dependent on location. The angular velocity decreases by about ten percent at the bottom near the equatorial plane; namely, there is the steep radial velocity gradient there. In order to properly treat this situation in an analytical manner, we adopt the inertial frame (the frame not rotating) with no translational velocity relative to the astronomical object concerned (for instance, the sun).

The mean magnetic field $\mathbf{B}$ obeys

$$\frac{\partial \mathbf{B}}{\partial t} = \nabla \times (\mathbf{U} \times \mathbf{B} + \alpha \mathbf{B} - \beta \mathbf{J} + \gamma \mathbf{\Omega}). \tag{7.16}$$

We seek its stationary state in the sense of a special solution, similar to the discussions on Eq. (7.1), as

$$\nabla \times (\mathbf{U} \times \mathbf{B} + \alpha \mathbf{B} - \beta \mathbf{J} + \gamma \mathbf{\Omega}) = 0. \tag{7.17}$$

We consider the dominant/cross-helicity state and deal with the alpha effect in a perturbational manner. We write

$$\mathbf{B} = \sum_{n=0}^{\infty} \mathbf{B}_n, \quad \mathbf{J} = \sum_{n=0}^{\infty} \mathbf{J}_n, \tag{7.18}$$

where $\mathbf{B}_n$ and $\mathbf{J}_n$ are of the nth order in α, which are symbolically written as

$$\mathbf{B}_n, \mathbf{J}_n = O(\alpha^n). \tag{7.19}$$

The first two parts obey

$$\nabla \times (\mathbf{U} \times \mathbf{B}_0 - \beta \mathbf{J}_0 + \gamma \mathbf{\Omega}) = 0, \tag{7.20}$$

$$\nabla\times(\mathbf{U}\times\mathbf{B}_1+\alpha\mathbf{B}_0-\beta\mathbf{J}_1)=0. \tag{7.21}$$

As was done in § 7.1.2, we assume the quasi-homogeneity of turbulent state and neglect the spatial derivatives of α, β, and γ. Under this approximation, a solution of equation (7.20) is

$$\mathbf{B}_0=\frac{\gamma}{\beta}\mathbf{U}, \tag{7.22}$$

$$\mathbf{J}_0=\frac{\gamma}{\beta}\mathbf{\Omega}, \tag{7.23}$$

with Eq. (7.6) for γ/β. Here we should note $\mathbf{U}\times\mathbf{B}_0=0$. Equation (7.22) shows that the toroidal field is generated from the toroidal velocity. This point will be discussed in detail in the context of solar magnetic fields.

Let us consider equation (7.21) for $\mathbf{B}_1$. We first drop the $\mathbf{U}\times\mathbf{B}_1$-related part and examine this approximation below. Then we take

$$\mathbf{J}_1=\frac{\alpha}{\beta}\mathbf{B}_0=\frac{\alpha\gamma}{\beta^2}\mathbf{U}. \tag{7.24}$$

Since the primary motion in the convection zone is the toroidal or rotational motion, we write

$$\mathbf{U}=\big(0,0,U_\phi(r,\theta)\big), \tag{7.25}$$

in the spherical coordinate system (r,θ,ϕ) (see Fig. 6). In this situation, $\mathbf{J}_1$ is toroidal. From the Ampere's law $\mathbf{J}_1=\nabla\times\mathbf{B}_1$, $\mathbf{B}_1$ is poloidal and is expresses as

$$\mathbf{B}_1=B_{1r}\mathbf{e}_r+B_{1\theta}\mathbf{e}_\theta, \tag{7.26}$$

with $\mathbf{e}_r$ and $\mathbf{e}_\theta$ as the unit vectors in the r and θ directions, respectively. Here we should recall that $\mathbf{B}_1$ is of $O(\alpha)$ in the α expansion, Eq. (7.18).

We examine the foregoing approximation of dropping the $\mathbf{U}\times\mathbf{B}_1$-related part. From equation (7.25) and (7.26), we have

$$\nabla\times(\mathbf{U}\times\mathbf{B}_1)=\left(0,0,B_{1r}\frac{\partial U_\phi}{\partial r}+B_{1\theta}\frac{1}{r}\frac{\partial U_\phi}{\partial\theta}\right), \tag{7.27}$$

where use has been made of $\nabla \cdot \mathbf{B}_1 = \nabla \cdot \mathbf{U} = 0$ and $\mathbf{U} \cdot \nabla = 0$. In the case that the primary part of $\mathbf{B}_1$ is of dipole type (see Fig. 11 bellow), it is nearly along the rotation axis in the low-latitude region or near the equatorial plane (the occurrence of the dipole component of $\mathbf{B}_1$ will be mentioned further in the later discussion on the solar field). In this situation, the radial component B_{1r} is small in the low-latitude region, indicating the smallness of $B_{1r}(\partial U_\phi / \partial r)$ there. On the other hand, the rotational velocity $\mathbf{U}$ is symmetric across the equatorial plane, and $B_{1\theta}(U_\phi / (r\partial\theta))$ also becomes small in the low-latitude region. As a result, Eq. (7.24) is an approximate solution of Eq. (7.21) in the low-latitude region. With this point in mind, we use Eq. (7.24) in later discussions.

We consider the mean-flow equation (6.18) with Eq. (6.21). We drop the Coriolis term and have

$$\frac{\partial \mathbf{U}}{\partial t} = -\nabla\left(P + \frac{1}{2}\mathbf{U}^2 + \frac{2}{3}K_R + \left\langle \frac{\mathbf{b}'^2}{2} \right\rangle \right) - \alpha_T(\Theta - \Theta_R)\mathbf{g}$$

$$+ \mathbf{U} \times \boldsymbol{\Omega} + \mathbf{J} \times \mathbf{B} + \nu_T \nabla^2 \mathbf{U} - \nu_M \nabla^2 \mathbf{B}. \tag{7.28}$$

In Eq. (7.18), we retain the leading terms, which are given by Eqs. (7.22) and (7.23). Then Eq. (7.28) may be rewritten as

$$\frac{\partial \mathbf{U}}{\partial t} = -\nabla\left(P + \frac{1}{2}\mathbf{U}^2 + \frac{2}{3}K_R + \left\langle \frac{\mathbf{b}'^2}{2} \right\rangle \right) - \alpha_T(\Theta - \Theta_R)\mathbf{g}$$

$$+ \left(1 - \left(\frac{\gamma}{\beta} \right)^2 \right) \mathbf{U} \times \boldsymbol{\Omega} + \nu_T \left(1 - \left(\frac{\gamma}{\beta} \right)^2 \right) \nabla^2 \mathbf{U}. \tag{7.29}$$

As will be shown later, we have $\gamma / \beta < 1$. Then the feedback influence on the fluid motion due to generated $\mathbf{B}$ is not strong in this case. Such a situation makes a sharp contrast with the dominant-helicity state in which the saturation level of $\mathbf{B}$ is determined through the interaction with the fluid motion.

7.2.2. Turbulence equations

In § 7.1.3, we investigated into the production term P_K [Eq. (6.39)] for understanding how nonvanishing K is sustained. We now retain the leading parts in Eq. (7.18), that is, Eqs. (7.22) and (7.23) while neglecting the alpha effect. Under this approximation, we have

$$\mathbf{E}_M = 0. \tag{7.30}$$

The combination of Eq. (6.21) with Eqs. (7.22) and (7.30) gives

$$P_K = \frac{1}{2}\nu_T\left(1-\left(\frac{\gamma}{\beta}\right)^2\right)S_{ij}{}^2 - \alpha_T \mathbf{H}_\theta \cdot \mathbf{g}. \tag{7.31}$$

In the context of the remark on Eq. (7.29), we drop the γ / β-related part and have

$$P_K = \frac{1}{2}\nu_T S_{ij}{}^2 - \alpha_T \mathbf{H}_\theta \cdot \mathbf{g}. \tag{7.32}$$

Both of these two terms are positive and contribute to the sustainment of the turbulent state from Eqs. (7.12) and (7.13).

A big difference between the P_K's in the dominant-helicity and dominant/cross-helicity dynamos lies in the first term in Eq. (7.32). In the dominant/cross-helicity case, the supply of energy is made through the mean flow and the buoyancy force, unlike the dominant-helicity case with the buoyancy force as the sole turbulent-energy source. This mechanism is essentially the same as for electrically nonconducting flows. The same situation holds for ε.

In relation to the generation of turbulent energy due to P_K, we should emphasize the differential rotation, which is specifically prominent near the bottom of the solar convective zone. The toroidal velocity given by Eq. (7.25) is written as

$$\mathbf{U} = \left(0, U_\phi(\sigma, z), 0\right) \tag{7.33}$$

in the cylindrical coordinate system (σ, ϕ, z) (see Fig. 6). Under Eq. (7.33), Eq. (7.32) is rewritten as

$$P_K = \nu_T\left(\sigma\left(\frac{\partial}{\partial\sigma}\frac{U_\phi}{\sigma}\right)\right)^2 - \alpha_T \mathbf{H}_\theta \cdot \mathbf{g}. \tag{7.34}$$

The first term clearly indicates that the differential part of rotation plays the role of energy supply from mean to fluctuating flows. This point makes a sharp contrast with the relationship of the mean magnetic field with the mean flow. In the latter, the whole rotational motion appears explicitly, as is seen from Eq. (7.22).

The production term for the turbulent cross helicity W, P_W [Eq. (6.41)], is written as

$$P_W = \frac{W}{K}\left(\frac{1}{2}\frac{C_\gamma}{C_\beta}\nu_T {S_{ij}}^2 - \alpha_T \mathbf{H}_\theta \cdot \mathbf{g}\right), \tag{7.35}$$

from Eqs. (6.31) and (6.32). Inside the parenthesis of Eq. (7.35), both parts are positive from the discussion on P_K, leading to Eq. (7.15). Namely, W is sustained through the velocity-strain and buoyancy effects. As is the same as for P_K, the occurrence of the strain effect is the feature not shared by the dominant-helicity case.

7.3. Traditional kinematic dynamos

In § 7.1 and § 7.2, we discussed two different magnetic-field generation mechanisms. One is the alpha dynamo arising from the turbulent helicity effect, and the other is the cross-helicity dynamo linked with the mean rotational motion. In the former, the cross-helicity effect becomes important in the stage of determining the saturation level of generated magnetic field. The cross-helicity effects are not treated explicitly in the traditional kinematic dynamo. In what flows, we shall scrutinize the primary differences between the present and traditional dynamos.

7.3.1. Alpha-alpha dynamo

For the comparison with the traditional kinematic dynamo, we consider Eq. (7.1) with the cross-helicity effect dropped; namely, we have

$$\frac{\partial \mathbf{B}}{\partial t} = \nabla \times (\mathbf{U} \times \mathbf{B} + \alpha \mathbf{B} - \beta \mathbf{J}). \tag{7.36}$$

For $\mathbf{U}$ and $\mathbf{B}$ axisymmetric around the axis of frame rotation, we write

$$\mathbf{U} = U_\phi \mathbf{e}_\phi + \mathbf{U}_P, \tag{7.37}$$

$$\mathbf{B} = B_\phi \mathbf{e}_\phi + \mathbf{B}_P, \tag{7.38}$$

where the poloidal components $\mathbf{U}_P$ and $\mathbf{B}_P$ are given by

$$\mathbf{U}_P = U_r \mathbf{e}_r + U_\theta \mathbf{e}_\theta, \tag{7.39}$$

$$\mathbf{B}_P = B_r \mathbf{e}_r + B_\phi \mathbf{e}_\phi = \nabla \times \left(A_\phi \mathbf{e}_\phi\right) \tag{7.40}$$

(A_ϕ is the toroidal component of the vector potential $\mathbf{A}$). From Eqs. (7.37)-(7.40), we may rewrite Eq. (7.36) as [3, 9]

$$\frac{\partial B_\phi}{\partial t} + \sigma(\mathbf{U}_P \cdot \nabla)\frac{B_\phi}{\sigma} = \alpha(\nabla \times \mathbf{B}_P)_\phi + \sigma(\mathbf{B}_P \cdot \nabla)\frac{U_\phi}{\sigma} + \beta\left(\nabla^2 - \frac{1}{\sigma^2}\right)B_\phi, \tag{7.41}$$

$$\frac{\partial A_\phi}{\partial t} + \frac{1}{\sigma}(\mathbf{U}_P \cdot \nabla)(\sigma A_\phi) = \alpha B_\phi + \beta\left(\nabla^2 - \frac{1}{\sigma^2}\right)A, \tag{7.42}$$

where the spatial variation of α and β has been dropped, as is similar to § 7.1 and § 7.2, and use has been made of the relation $\sigma = r\sin\theta$ (see Fig. 6).

Let us consider the role of each term in Eqs. (7.41) and (7.42). There the second terms on the left-hand sides represent the advection effect. The generation of magnetic fields arises from the first two terms and the first term on the right-hand sides, respectively. We focus attention on the two α-related terms. They represent the following generation cycle of magnetic field:

Poloidal field $\mathbf{B}_P$

$\rightarrow$ Toroidal current $\nabla \times \mathbf{B}_P$ by the Ampere law (7.43a)

$\rightarrow$ Toroidal field B_ϕ by the alpha effect $\alpha(\nabla \times \mathbf{B}_P)_\phi$ (7.43b)

$\rightarrow$ Toroidal current J_ϕ by the alpha effect αB_ϕ (7.43c)

$\rightarrow$ Poloidal field $\mathbf{B}_P$ by the Ampere law. (7.43d)

In the above processes, the helicity dynamo has been used twice, completing the magnetic generation cycle [9-11]. This process is called the alpha-alpha dynamo.

In the stationary state, the processes (7.43a-d) correspond to Eq. (7.4). Therefore the saturation level of $\mathbf{B}$ cannot be determined within the framework of Eq. (7.41) and (7.42), as was stressed in § 7.1.2. To overcome this difficulty, the inclusion of nonlinear effects on the α has been studied in the kinematic approach [30-32].

7.3.2. Alpha-omega dynamo

In Eq. (7.41), we have one more term that leads to the generation of the toroidal magnetic field B_ϕ. It is the second term on the right-hand side, which is linked with the spatial nonuniformity of the angular velocity U_ϕ / σ or the differential rotation. In § 7.2.2, its importance was stressed in the light of the sustainment mechanism of turbulent

MHD state [recall Eq. (7.34)]. In the context of Eq. (7.41), the differential rotation signifies

Generation of the toroidal field B_ϕ by the distortion of the poloidal field $\mathbf{B}_P$. (7.44)

The physical meaning of the process (7.44) may be explained as follows. As a typical case, we consider a magnetic-field tube parallel to the rotation or z axis. The quantity $(\mathbf{B}_P \cdot \nabla)U_\phi / \sigma$ signifies the change of the angular velocity U_ϕ / σ along the poloidal component of the tube. At high Reynolds numbers, magnetic fields are nearly frozen in a fluid and move with it. For positive $(\mathbf{B}_P \cdot \nabla)U_\phi / \sigma$, the upper part of the poloidal magnetic tube moves faster in the toroidal direction than its lower counterpart. The resulting deformation of the tube leads to the occurrence of the toroidal component of magnetic field. This process is called the omega dynamo. In the case that the tube is stretched, its cross section decreases and the strength of magnetic tension increases. The over-stretched tube overcomes the stretching by the fluid motion and, in turn, shrinks (recall the motion of a spring). As a result, the omega dynamo indicates oscillatory behaviors in time. The cycle consisting of the processes (7.43c, d) and (7.44) is named the alpha-omega dynamo.

In the foregoing two different types of generation circles, which works preferentially is dependent on the relative magnitude of the first to second terms on the right-hand side of Eq. (7.41). We denote the reference values of α, the length, and the angular velocity of the mean fluid motion by α_R, L_R, and Ω_R, respectively. The relative magnitude is given by

$$D_{\alpha\omega} = \frac{\alpha_R}{L_R \Omega_R}. \tag{7.45}$$

In solar magnetic fields, the differential rotation is prominent specifically near the bottom of the convective zone, as was noted in § 7.2.2. In their past study, much more attention was paid to the alpha-omega dynamo in close relation to the solar polarity reversal [5, 46].

8. Application to Astro/Geophysical and Fusion Dynamos

8.1. Solar magnetic fields

In § 1, we summarized some representative observational properties associated with sunspots [3, 4]. In this section, we shall consider how those properties may be

interpreted with the aid of the findings by the mean-field dynamo model obtained in § 7, specifically, the model based on the dominant/cross-helicity concept [47, 48].

8.1.1. Sunspot's magnetic field

Sunspots represent the cross sections of an intense toroidal magnetic-field tube when it rises up owing to buoyancy forces and break through the photosphere that is the thin layer adjacent to the outer boundary of the convective zone. In the light of Eq. (7.22), the mean toroidal magnetic field B_ϕ is related to the mean toroidal velocity U_ϕ as

$$B_\phi = \frac{C_\gamma}{C_\beta}\frac{W}{K}U_\phi, \tag{8.1}$$

where use has been made of Eq. (7.6).

One of the prominent solar polarity properties is that the polarity of a pair of sunspots is opposite in the northern and southern hemispheres (see Fig. 3). This property signifies that the direction of the toroidal magnetic field in the convective zone is opposite in the two hemispheres. We may seek its cause in the turbulent cross helicity W in Eq. (8.1). The quantity changes its sign under the reflection of a coordinate system, namely, it is a pseudo-scalar.

In rotating spherical objects such as the sun and the earth, the axis of rotation is the sole factor distinguishing between the northern and southern hemispheres in a dynamical sense. Scalars are statistically symmetric with respect to the equatorial plane, but pseudo-scalars become statistically antisymmetric. Then we have

$$W(r, \pi - \theta) = -W(r, \theta), \tag{8.2}$$

in the spherical coordinate (Fig. 6), where the dependence on ϕ was dropped since the MHD state is assumed to be axisymmetric. The same situation holds for the turbulent residual helicity H as

$$H(r, \pi - \theta) = -H(r, \theta). \tag{8.3}$$

From Eqs. (8.1) and (8.2), the toroidal field B_ϕ is anti-symmetric with respect to the equatorial plane, resulting in the sunspot's polarity depicted in Fig. 3.

Let us examine Eq. (8.1) from a quantitative viewpoint. A typical velocity associated with the solar rotational motion is the equatorial speed, which is about $2000\ \mathrm{m\ s^{-1}}$. Then we adopt

$$U_\phi \cong 1000 \text{ m s}^{-1}, \quad \frac{C_\gamma}{C_\beta} \cong 1 \tag{8.4}$$

[see Eq. (6.46a) for the latter]. Equations (8.1) and (8.4) give

$$B_\phi = 10^3 \frac{W}{K} \left(\text{m s}^{-1}\right). \tag{8.5}$$

The magnetic field in original Gauss units, B_ϕ^*, is related to B_ϕ as

$$B_\phi^* = 0.4 \times 10^{-12} \sqrt{n} B_\phi \ \ (G), \tag{8.6}$$

from Eq. (2.25), where $n\,(m^{-3})$ is the number density of hydrogen [3]. We combine Eq. (8.5) with Eq. (8.6), and have

$$B_\phi^* = 0.4 \times 10^{-9} \frac{W}{K} \sqrt{n} \ \ (G). \tag{8.7}$$

Concerning the magnitude of W / K, we have the strong constraint, Eq. (6.37). In the convective zone, the fluid is highly electrically conducting owing to the high temperature, resulting in large magnetic Reynolds number in addition to large Reynolds number. This situation suggests that the correlation between velocity and magnetic field is not low. Then we assume

$$\frac{|W|}{K} = O\left(10^{-1}\right), \tag{8.8}$$

which results in

$$B_\phi^* = O\left(10^{-11}\right)\sqrt{n} \ \ (G). \tag{8.9}$$

As a typical magnetic field of large sunspots, we choose $B_\phi^* = O(10^3)\,G$, which gives

$$n = O(10^{28}) \text{ m}^{-3}. \tag{8.10}$$

From observations [3], n is estimated as

$$n = O\left(10^{32}\right) \text{m}^{-3} \text{ in the core,} \tag{8.11a}$$

$$n = O\left(10^{23}\right) \text{m}^{-3} \text{ in the photosphere.} \tag{8.11b}$$

Equation (8.10) falls between these two values. Then Eqs. (8.1) and (8.8) are consistent with the occurrence of the toroidal field of $O(10^3)\,G$ in sunspots.

8.1.2. Relationship of sunspot's polarity with polar field

As is shown in Fig. 3, the polarity of the leading sunspot is coincident with the polarity of the polar field (the magnetic field in the pole region). In order to see this relationship, we consider Eq. (7.17) in the pole region. There we divide $\mathbf{\Omega}$ into the uniform rotation part $\boldsymbol{\omega}_F$ and the deviation from it, $\mathbf{\Omega}_D$, as

$$\mathbf{\Omega} = 2\boldsymbol{\omega}_F + \mathbf{\Omega}_D \tag{8.12}$$

(subscript D denotes differential-rotation part). In the pole region, $\mathbf{\Omega}_D$ is small, compared with its counterpart near the equatorial plane, and the rotational velocity $\mathbf{U}$ is also low. Then Eq. (7.17) is approximated by

$$\nabla\times(\alpha\mathbf{B} - \beta\mathbf{J} + 2\gamma\boldsymbol{\omega}_F) = 0. \tag{8.13}$$

It is satisfied by

$$\mathbf{B} = -\frac{2\gamma}{\alpha}\boldsymbol{\omega}_F \tag{8.14}$$

since this $\mathbf{B}$ leads to vanishing of $\mathbf{J}$ (the spatial derivatives of α and γ are neglected). Equation (8.14) shows that the polar field is aligned with the rotation axis. Such alignment was really observed in the computer simulation [49].

We examine the polarity rule with the aid of Eq. (8.14). With the left side of Fig. 3 in mind, we consider

$$\text{Northern hemisphere: } W > 0,\ H > 0; \tag{8.15a}$$

$$\text{Southern hemisphere: } W < 0,\ H < 0, \tag{8.15b}$$

which is equivalent to

$$\text{Northern hemisphere: } \gamma > 0,\ \alpha > 0; \tag{8.16a}$$

$$\text{Southern hemisphere: } \gamma < 0,\ \alpha < 0, \tag{8.16b}$$

from Eqs. (6.30) and (6.32). The assumption about the sign of H is based on the computer experiment mimicking the solar convection zone. It suggests that $-\mathbf{u}\cdot\boldsymbol{\omega}$ and

$\mathbf{b}\cdot\mathbf{j}$ tend to be positive in the northern hemisphere [50]; namely, the local residual helicity $-\mathbf{u}\cdot\boldsymbol{\omega}+\mathbf{b}\cdot\mathbf{j}$ tends to be positive there.

From Eq. (8.1), the positive toroidal magnetic field B_ϕ is induced in the northern hemisphere under the condition (8.15). Rising-up of the loops of the field under the buoyancy effect leads to the sunspot's polarity at the left-side of Fig. 3. In the pole region, Eq. (8.14) shows that the negative poloidal field or the field anti-parallel to the rotation axis is induced. This polarity is coincident with the leading-sunspot polarity.

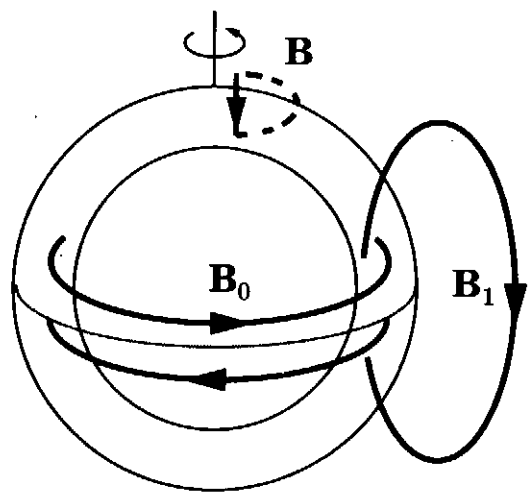

Fig. 11. Configuration of generated magnetic fields.

From Eq. (7.24), $\mathbf{J}_1$ is symmetric across the equatorial plane since $\alpha\gamma > 0$. The resulting field $\mathbf{B}_1$ is anti-symmetric; namely it is of dipole type with the axis parallel to the axis of rotation [recall the reference to the dipole field below Eq. (7.27)]. The polar field is anti-parallel to the rotation axis. The configuration of these fields is schematically summarized in Fig. 11.

The right side of Fig. 3 corresponds to

$$\text{Northern hemisphere: } W < 0,\ H > 0; \tag{8.17a}$$

$$\text{Southern hemisphere: } W > 0,\ H < 0. \tag{8.17b}$$

Namely, the transition of the left-side to right-side polarity occurs through the change of the sign of W, but not H. This conclusion is reasonable from the fact that the sign of the residual helicity $-\mathbf{u}\cdot\boldsymbol{\omega}+\mathbf{b}\cdot\mathbf{j}$ is invariant under the reversal of the sign of $\mathbf{b}$, that is, $\mathbf{b}\to-\mathbf{b}$.

8.1.3. Lorentz force and meridional flow

One of the representative flows observed at the solar surface is the meridional flow or circulation [3, 51-53]. The flow of 20~30 m s^{-1} is nearly stationary and is towards the poles. It is considered to be parts of large convection cells.

In § 8.1.1 and § 8.1.2, attention was focused on effects of turbulence on the mean magnetic field. One of the merits of introducing cross-helicity effects is that feedback effects of induced magnetic fields on fluid motion may be treated efficiently. They occur twofold; one is the effect through the Reynolds stress R_{ij}, and another is the Lorentz force $\mathbf{J}\times\mathbf{B}$.

We examine the poleward meridional flow from the viewpoint of the Lorentz force exerted to the fluid motion. We approximate $\mathbf{B}$ and $\mathbf{J}$ by $\mathbf{B}_0$ [Eq. (7.22)] and $\mathbf{J}_0$ [Eq. (7.23)]. We retain the solid-rotation part in Eq. (8.12), and have

$$\mathbf{J}_0\times\mathbf{B}_0=\left(\frac{\gamma}{\beta}\right)^2 r{\omega_F}^2\left(-2\sin^2\theta,-\sin 2\theta,0\right), \tag{8.18}$$

in the spherical coordinate system, which consists of the r and θ components. Of these components, what is interesting in relation to the meridional flow is the latter, that is,

$$\left(\mathbf{J}_0\times\mathbf{B}_0\right)_\theta=-\left(\frac{\gamma}{\beta}\right)^2 r{\omega_F}^2\sin 2\theta, \tag{8.19}$$

Irrespective of the sign of W in γ, Eq. (8.19) is negative (positive) in the northern (southern) hemisphere. This force contributes to the driving of fluid towards the poles in both the hemispheres.

The dependence of the velocity of observed meridional flow is approximately proportional to [51]

$$C\sin\theta-\sin 2\theta, \tag{8.20}$$

with

$$C\cong 0.2. \tag{8.21}$$

Namely, the velocity is nearly proportional to $\sin 2\theta$. It is noteworthy that such θ dependence is coincident with its Lorentz-force counterpart, Eq. (8.19). This fact indicates that the force is a candidate for the cause of the meridional flow.

8.1.4. Mean-field-theory interpretation of polarity reversal

We use Eqs. (7.22)-(7.24) and seek a cause of the polarity reversal from the viewpoint of mean-field theory. We examine an initial stage in which the magnetic field $\mathbf{B}$ is weak, with a small seed of positive (negative) turbulent cross helicity W in the northern (southern) hemisphere [condition (8.15)]. In this stage, the alpha effect $\alpha\mathbf{B}$ is considered smaller than the cross-helicity effect $\gamma\mathbf{\Omega}$, owing to weak $\mathbf{B}$. Such a situation is described by Eqs. (7.22) and (7.23) in a quasi-stationary sense. The alpha effect, in turn, induces the toroidal current $\mathbf{J}_1$ through Eq. (7.24), resulting in the occurrence of the poloidal field $\mathbf{B}_1$ from the Ampere law (see Fig. 11).

In the foregoing generation process of the mean magnetic field, we pay attention to the change of the cross helicity. The cross helicity of the mean field given by Eqs. (7.22) and (7.23) is $\mathbf{U}\cdot\mathbf{B}_0$. In Fig. 11, the poloidal field $\mathbf{B}_1$ is combined with the alpha effect to generate the poloidal current $\mathbf{J}_2$. This current is aligned with $\mathbf{B}_1$ under the condition (8.15). The occurrence of such $\mathbf{J}_2$ leads to the toroidal field $\mathbf{B}_2$ under the Ampere law, and the direction is the same as $\mathbf{B}_0$. As a result, the cross helicity of the mean field increases as

$$\mathbf{U}\cdot\mathbf{B}_0 \rightarrow \mathbf{U}\cdot\mathbf{B}_0 + \mathbf{U}\cdot\mathbf{B}_2, \tag{8.22}$$

in the northern hemisphere.

It was noted in § 2.3 that the total amount of cross helicity is conserved in the absence of molecular viscosity and magnetic diffusivity so long as there is no supply of cross helicity by external effects. Nonvanishing molecular viscosity and magnetic diffusivity give rise to the decrease in the total amount. In the solar convective zone, the buoyancy term in Eq. (7.32) contributes to the external supply of cross helicity, enabling the existence of the quasi-stationary state of the total amount of cross helicity. In the northern hemisphere, the increase in the cross helicity of the mean field given by Eq. (8.22) needs to be balanced with the decrease in the cross helicity of the turbulent part. In other words, the occurrence of $\mathbf{B}_2$ gives rise to the destruction of W, which also means the destruction of $\mathbf{B}_0$ since the latter is generated from $\mathbf{U}$ through the intermediary of the W. The weakening of $\mathbf{B}_0$ leads to the decrease in the cross helicity of the mean field, which, in turn, brings the increase in W connecting $\mathbf{B}_0$ and $\mathbf{U}$. These features of the cross helicity suggest a periodic variation of the solar mean field. Its more detailed investigation into the polarity reversal may be done with the aid of the production term of W, Eq. (6.41) [48].

8.2. Geomagnetic fields

8.2.1. Computer simulation of geodynamo

In § 7.1.1, we mentioned the accomplishments by computer simulations mimicking the geodynamo. The most prominent feature there is the occurrence of the elongated flow structure along the rotation axis. Its details, however, differ from one computer simulation from another. Such a difference is considered to arise from the relative strength of the buoyancy to Coriolis effects, that is, the relative magnitude of R_a (Rayleigh number) to T_a (Taylor number). In the earth's outer core, R_a and T_a are $O(10^{16})$ and $O(10^{27})$, respectively [see Eq. (2.46)].

The elongated flow structure in the simulation by Glatzmaier and Roberts [6] with $R_a = O(10^7)$ and $T_a = O(10^{11})$ is more irregular, compared with that by Kageyama and Sato [7] with $R_a = O(10^4)$ and $T_a = O(10^6)$. This finding suggests that larger T_a results in more irregular elongated structures. In these two simulations, it is concluded that the generation process of magnetic fields is closer to the alpha-omega dynamo of § 7.3.2. The simulation by Olson et al. [8] with $R_a = O(10^2)$ and $T_a = O(10^8)$ is closer to the earth-like condition in the relative magnitude of T_a to R_a. There the magnetic-field generation process resembles the alpha-alpha dynamo of § 7.3.1.

In the earth's outer core, P_{rM} (magnetic Prandtl number) is $O(10^{-6})$. This means that the magnetic field is much more dissipative, compared with the momentum. Nevertheless the geomagnetic energy is inferred to be $O(10^4) \sim O(10^6)$ times the kinetic energy, as was noted in § 1. In the current simulations, the energy of the generated magnetic field is $O(10) \sim O(10^3)$ times larger than the energy of fluid motion in the rotating frame. This result is consistent with the above inference. In the simulations, however, P_{rM} is usually chosen to be larger than one; namely, the fluid motion is more dissipative. The simulation by Olson et al. adopting $P_{rM} = 1$ is closer to the outer-core situation, but it is still much larger than its real value.

With this reservation concerning the nondimensional parameters, the computer-simulation findings about the geodynamo may be summarized as follows.

(i) A prominent feature of MHD flows in a spherical-shell region is the occurrence of the column-like or elongated structure owing to the frame-rotation or Coriolis-force effect. Increasing T_a with fixed R_a, however, leads to larger deformation or higher irregularity of the structure.

(ii) The flow inside the column is linked with the generation of the poloidal component of magnetic field, specifically, the dipole one.

(iii) The energy of induced magnetic fields is much larger than the kinetic energy of the flow driven by the buoyancy force.

(iv) The toroidal magnetic field is stronger than the poloidal magnetic field.

The mean-field theory is founded on the ensemble averaging or the averaging around the rotation axis. Then it cannot detect the elongated flow structure consisting of a few pairs of convection columns. It should be stressed that the concern of the theory as to the geodynamo is the resultant fluid motion, the resultant turbulent helicity, etc. after the averaging of flow [54].

8.2.2. Saturation of generated magnetic field

In § 7.1, we discussed the MHD state subject to dominant effects of helicity. In the state, the mean magnetic field $\mathbf{B}$ obeys Eq. (7.3) that is linear in $\mathbf{B}$. The saturation level of $\mathbf{B}$ is determined by Eq. (7.9) through the interaction with the mean flow $\mathbf{U}$. In the mean-field theory based on the ensemble averaging, the fluid motion consists of the axisymmetric poloidal and toroidal components, $\mathbf{U}_P$ and $\mathbf{U}_T$, which are written as

$$\mathbf{U}_P = U_r(r,\theta)\mathbf{e}_r + U_\theta(r,\theta)\mathbf{e}_\theta, \tag{8.23}$$

$$\mathbf{U}_T = U_\phi(r,\theta)\mathbf{e}_\phi, \tag{8.24}$$

respectively, in the spherical coordinate system (r,θ,ϕ). Here $\mathbf{U}_P$ comes from the ensemble average of the flow in the column structure. Equation (7.9) indicates that $\mathbf{B}_P$ is determined by this $\mathbf{U}_P$, as is consistent with the item (ii) in § 8.2.1. Specifically, $\mathbf{U}_P$ is reflectionally symmetric with respect to the equatorial plane. Then $\mathbf{B}_P$ is reflectionally anti-symmetric since W in γ is a pseudo-scalar, signifying that $\mathbf{B}_P$ contains the dipole component.

From Eq. (7.9), the ratio of the magnetic energy T_M to the flow energy T_K is

$$\frac{T_M}{T_K} = \frac{\mathbf{B}^2/2}{\mathbf{U}^2/2} = \left(\frac{\beta}{\gamma}\right)^2 = \left(\frac{C_\beta}{C_\gamma}\right)^2\left(\frac{W}{K}\right)^2. \tag{8.25}$$

It is written as

$$\frac{T_M}{T_K} \cong \left(\frac{W}{K}\right)^2 \geq 1, \tag{8.26}$$

with the aid of Eqs. (6.37) and (6.46a). The energy of the induced magnetic field is larger than the energy of the fluid motion that is the generator of the former.

In order to estimate the magnitude of T_M / T_K, we consider the toroidal and poloidal components of the magnetic field, $\mathbf{B}_T$ and $\mathbf{B}_P$. The flow velocity in the outer core is inferred to be $O(10^{-4})$ m s^{-1} through the indirect observations, for instance, the westward immigration of magnetic fields. It corresponds to $\mathbf{U}_T$, and $\mathbf{U}_P$ is inferred to be by one order smaller than $\mathbf{U}_T$. Then we assume

$$|\mathbf{U}_T| = 10^{-4} \text{ m s}^{-1}, \ |\mathbf{U}_P| = 10^{-5} \text{ m s}^{-1}. \tag{8.27}$$

The primary part of the poloidal field is the dipole component, whose magnitude at the surface is $O(1)$ G. We may write the poloidal field in original Gauss units, $\mathbf{B}_P^*$, as

$$|\mathbf{B}_P^*| = |\sqrt{\rho\mu_0}||\mathbf{B}_P| = O(1) \text{ G}, \tag{8.28}$$

from Eq. (2.25). We use the physical parameters [1]

$$\rho = 0.8 \times 10^4 \text{ Kg m}^{-3} \text{ (iron)}, \tag{8.29a}$$

$$\mu_0 = 1.3 \times 10^{-6} \text{ henry m}^{-1} \text{ (vacuum)}. \tag{8.29b}$$

Under Eq. (8.29), Eq. (8.28) gives

$$|\mathbf{B}_p| = 10^{-3} \text{ m s}^{-1}. \tag{8.30}$$

From the latter of Eq. (8.27), this suggests

$$\frac{|W|}{K} = O\left(10^{-2}\right) \tag{8.31}$$

in the outer core. On the other hand, the former gives

$$|\mathbf{B}_T| = \frac{C_\gamma}{C_\beta} \frac{W}{K} |\mathbf{U}_T| = O(10) \text{ G}, \tag{8.32}$$

which is consistent with the observational inference about the toroidal field [recall the item (iv) in § 8.2.1].

In relation to Eq. (8.31), we should recall Eq. (8.8) for the solar convective zone. The zone mainly consists of hydrogen gases that are highly ionized owing to high temperature. On other hand, the outer core consists of melted iron, and the magnetic Prandtl number P_{rM} is much lower than one. This fact indicates that the correlation between the magnetic field and the velocity, which may be characterized by W, is lower than its solar counterpart. Considering the difference between these two regions, Eq. (8.31) is reasonable, and Eq. (8.26) results in

$$\frac{T_M}{T_K} = O(10^4), \tag{8.33}$$

in correspondence to the item (iii) in § 8.2.1.

From the viewpoint of the molecular magnetic Prandtl number P_{rM}, the conclusion such as Eq. (8.33) is rather curious since $P_{rM} << 1$. In a turbulent MHD state, however, the turbulent magnetic Prandtl number

$$P_{rMT} = \frac{\nu_T}{\beta} \tag{8.34}$$

is more important. From Eq. (6.28), we have

$$P_{rMT} = \frac{7}{5}, \tag{8.35}$$

in sharp contrast with $P_{rM} << 1$. This reversal of magnitude between P_{rM} and P_{rM} may be considered to be a cause of $T_M >> T_K$.

8.2.3. Frame-rotation effect on magnetic field

In the item (i) of § 8.2.1, it was stated that effects of frame rotation occur twofold; one leads to the formation of convection columns, and another gives rise to their deformation or irregularity. In the present mean-field theory, the former signifies the importance of the resultant helicity, whereas the latter may be interpreted as the disturbance to the Coriolis force. The explicit effect of frame rotation on the magnetic field in the dominant-helicity state occurs through the third term of the right-hand side of Eq. (7.5). It gives rise to the nonvanishing Lorentz force

$$\mathbf{J} \times \mathbf{B} = -2\frac{\gamma}{\beta}\mathbf{B} \times \boldsymbol{\omega}_F, \tag{8.36}$$

resulting in parts of the third term on the right-hand side of Eq. (7.8).

As the magnetic field $\mathbf{B}$ approaches the saturation level given by Eq. (7.9), both the original frame-rotation effect and the turbulent diffusion effect decrease in Eq. (7.8), owing to the feedback effect by the generated magnetic field. The weakening of the frame-rotation effect at the level of mean motion is considered to be linked with that of a clear column-like structure before averaging. In short, the Coriolis force combined with the Lorentz force may play a role different from the Coriolis effect in the absence of magnetic field. This may be considered to be a cause of the T_a effect that was noted in the item (i) of § 8.2.1. The picture presented here for the velocity and magnetic-field interaction processes is summarized in Fig. 12.

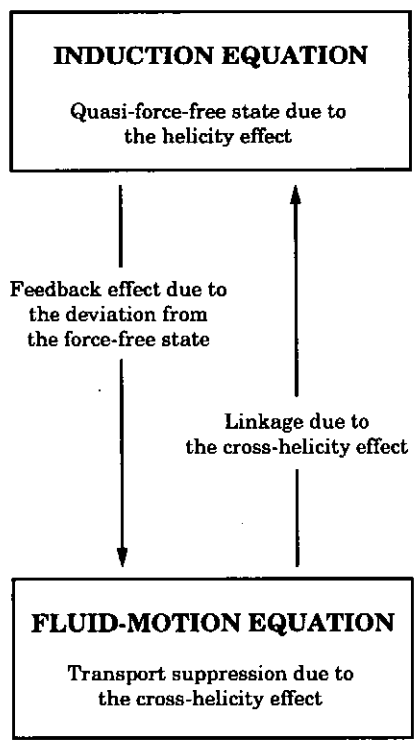

Fig. 12. Magnetic-field generation and feedback effect on fluid motion.

8.3. Collimation of accretion jets

8.3.1. Computer simulation and mean-field theory

In § 1, we remarked that high-speed jets are ubiquitously observed around high-mass astronomical objects such as galactic nuclei, protostars, binary x-ray sources, etc. [13-15] (see also Fig. 13). These jets are often flows of electrically conducting gases, and one of the prominent features of the jets is their high collimation. As the representative interests of accretion jets, we may mention their generation and collimation mechanisms.

A computer simulation based on a system of primitive MHD equations is a powerful tool for the investigation into flows around an accretion disk. The generation mechanism of accretion jets has been explored by the computer simulations [55-57]. There magnetic field lines are twisted by accreting, rotating gases, and the reconnection of these lines is the cause of the force driving the jets in the two directions normal to the disk. At present, the simulation of the occurrence of jets is limited to their initial stage since the simulation of their stationary behavior needs a big computational domain and a large amount of computational time. The similar difficulty is encountered in the simulation of jet collimation.

With these situations of a computer simulation in mind, it is meaningful to examine accretion jets, specifically, the collimation mechanism of jets from the viewpoint of the mean-field theory [58]. In the mean-field model developed above, no effect of fluid compressibility is taken into account. In the electrically nonconducting case, fluid compressibility has influence on the suppression of turbulence, resulting in the decrease in the growth of jet width. Therefore it is necessary to seek the relationship of jet collimation with both of compressibility and magnetic-field effects. Moreover, relativistic effects become critical for the jets related to active galactic nuclei whose speed approaches light speed. In what follows, we shall confine ourselves to the magnetic effect and seek the collimation mechanism.

8.3.2. Driving force of bipolar jets

To understand the later analysis of jet collimation, we simply refer to the toroidal-field generation process due to the cross-helicity effect in disk geometry. We adopt the cylindrical coordinate system (σ, θ, ϕ) (Fig. 6). Accretion disks obey the so-called Keplerian motion, whose angular velocity is proportional to $\sigma^{-1/2}$ and is highly differential. Then we adopt the inertial frame, as in § 7.2.1. The mean magnetic field $\mathbf{B}$ is governed by Eq. (7.17), that is,

$$\nabla \times (\mathbf{U} \times \mathbf{B} + \alpha \mathbf{B} - \beta \mathbf{J} + \gamma \boldsymbol{\Omega}) = 0. \tag{8.37}$$

An accretion disk is thin in the vertical or z direction, compared with its horizontal extent. Owing to the absence of the vertical flow comparable to the horizontal motion, there is little room for the occurrence of strong helicity effects. Then we neglect the helicity effect in Eq. (8.37) and have

$$\mathbf{B} = \frac{\gamma}{\beta} \mathbf{U}, \tag{8.38}$$

which is the same as Eq. (7.22). Equation (8.38) shows that the rotational motion generates the toroidal field B_ϕ in the presence of nonvanishing β and γ. The sign of γ proportional to W is opposite in the upper and lower halves of the disk since W is a pseudoscalar. In the case of positive W in the upper half, the toroidal field is shown in Fig. 13.

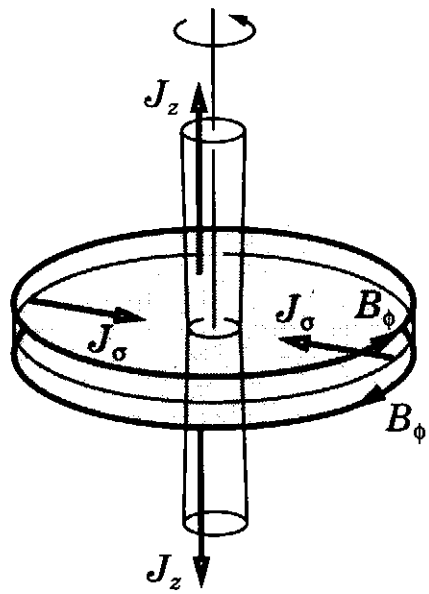

Fig. 13. Magnetic-field configuration in an accretion disk.

The other important feature in relation to Eq. (8.38) is the occurrence of the radial electric current towards the center of the disk, J_σ. Parts of J_σ become the current along the rotation axis, J_z. This J_z generates the toroidal field under the Ampere law, which gives rise to a strong magnetic pressure near the central part in the disk and contributes to driving of jets [59, 60].

The foregoing discussions are based on nonvanishing K and W. We need to consider their sustainment mechanism. In Eq. (6.38), they are generated by P_K [Eq. (6.39)] and P_W [Eq. (6.41)], in both of which the buoyancy effects are dropped. In the stationary state, we have Eq. (7.30), that is, vanishing $\mathbf{E}_M$. Then we have

$$P_K = \frac{1}{2}\nu_T\left(1-\left(\frac{\gamma}{\beta}\right)^2\right)S_{ij}{}^2 \cong \nu_T\left(\sigma\left(\frac{\partial}{\partial\sigma}\frac{U_\phi}{\sigma}\right)\right)^2, \tag{8.39}$$

$$P_W = \frac{W}{K}P_K, \tag{8.40}$$

from Eqs. (7.31), (7.34), and (7.35). In the second relation of Eq. (8.39), the γ/β-related part was neglected owing to the reason explained below. The Keplerian rotation leads to positive P_K and sustains K. As result, W is also sustained under Eq. (8.40).

In this context, we refer to $|W|/K$ in galactic magnetic fields. Galaxies are rotating with constant velocity in their great portion, except the central part. The magnitude of magnetic fields observed in each galaxy is nearly proportional to its rotational speed. The application of Eq. (8.38) to this relation gives the estimate [61]

$$\frac{|W|}{K} = O\left(10^{-1}\right), \tag{8.41}$$

which is similar to its solar counterpart, Eq. (8.8) . The second relation in Eq. (8.39) is guaranteed under Eq. (8.41).

The motion of gases is turbulent inside the disk. Then jets carry away nonvanishing K and W from the disk region, in addition to the angular momentum associated with the Keplerian rotation. As a result, the jet region continues to be in a MHD turbulent state even if K and W are not produced through P_K and P_W inside the jet. This point will become important in the later discussion on the jet collimation.

8.3.3. Collimation mechanism due to magnetic effect

We focus attention on the intermediate region far from the top of the jet and the root adjacent to the disk, and consider its stationary MHD state. Vanishing of $\partial\mathbf{B}/\partial t$ is guaranteed by

$$\mathbf{J} = \frac{\alpha}{\beta}\mathbf{B} + \frac{\gamma}{\beta}\mathbf{\Omega} + \frac{1}{\beta}\mathbf{U}\times\mathbf{B}, \tag{8.42}$$

as is confirmed from Eq. (8.37). The occurrence of bipolar jets is considered to be related to the release of the angular momentum possessed by the gases accreting onto a central high-mass body. Then jets are composed of the longitudinal and rotational motion, resulting in the helicity at the mean-flow level. This situation resembles the motion inside each convection column discussed in geodynamo, and indicates the importance of helicity effects in the study of jet collimation.

From Eq. (8.42), the mean Lorentz force is

$$\mathbf{J}\times\mathbf{B} = -\frac{\gamma}{\beta}\mathbf{U}\times\mathbf{\Omega} + \frac{1}{\beta}(\mathbf{U}\times\mathbf{B})\times\mathbf{B}. \tag{8.43}$$

We now assume

$$\mathbf{U}\times\mathbf{B}=0, \tag{8.44}$$

which reduces Eq. (8.43) to

$$\mathbf{J}\times\mathbf{B}=-\frac{\gamma}{\beta}\mathbf{U}\times\mathbf{\Omega}. \tag{8.45}$$

Equation (8.44) will be found to be consistent with the later discussion.

The mean rotational motion of jets is characterized by the mean vorticity $\mathbf{\Omega}$. In order to examine its behavior, we consider the mean-flow equation (6.18) with both the Coriolis and buoyancy effects dropped, which is given by

$$\frac{\partial\mathbf{U}}{\partial t}=-\nabla\left(P+\frac{1}{2}\mathbf{U}^2+\frac{2}{3}K_R+\left\langle\frac{\mathbf{b}'^2}{2}\right\rangle\right)$$

$$+\mathbf{U}\times\mathbf{\Omega}+\mathbf{J}\times\mathbf{B}+\nu_T\nabla^2\mathbf{U}-\nu_M\nabla^2\mathbf{B} \tag{8.46}$$

(the spatial variation of ν_T and ν_M is neglected from the assumption of local homogeneity). We substitute Eq. (8.45) into Eq. (8.46), and take the curl of the resulting equation. Then we have

$$\frac{\partial\mathbf{\Omega}}{\partial t}=\nabla\times\left(\left(\mathbf{U}-\frac{\gamma}{\beta}\mathbf{B}\right)\times\mathbf{\Omega}+\nu_T\nabla^2\left(\mathbf{U}-\frac{\gamma}{\beta}\mathbf{B}\right)\right), \tag{8.47}$$

where use has been made of Eqs. (6.28) and (6.29).

The stationary state of Eq. (8.47), that is,

$$\frac{\partial\mathbf{\Omega}}{\partial t}=0 \tag{8.48}$$

is guaranteed by

$$\mathbf{B}=\frac{\beta}{\gamma}\mathbf{U}. \tag{8.49}$$

The growth of jet width arises from the diffusion of $\mathbf{\Omega}$, which originally arises from the term

$$\nabla\times\left(\nu_T\nabla^2\mathbf{U}\right)=\nu_T\nabla^2\mathbf{\Omega} \tag{8.50}$$

in Eq. (8.47). Under Eq. (8.49), this $\boldsymbol{\Omega}$ diffusion effect disappears through the feedback effect of the generated magnetic field. Equation (8.49) also guarantees Eq. (8.44) previously assumed, reducing Eq. (8.42) to

$$\mathbf{J} = \frac{1}{1-(\gamma/\beta)^2}\frac{\alpha}{\beta}\mathbf{B}, \tag{8.51}$$

since $\boldsymbol{\Omega} = (\gamma/\beta)\mathbf{J}$ from Eq. (8.49).

Under Eq. (8.41), Eq. (8.51) is written as

$$\mathbf{J} = \frac{\alpha}{\beta}\mathbf{B}. \tag{8.52}$$

This relation is a typical manifestation of the helicity or alpha effect, as is entirely similar to the geodynamo. Equation (8.51) is linear in $\mathbf{B}$ and cannot determine the magnitude of $\mathbf{B}$. The coupling with the fluid motion through the cross-helicity effect relates $\mathbf{B}$ to $\mathbf{U}$, as in Eq. (8.49), leading to the determination of its saturation level. This situation is also the same as for the geodynamo.

Under Eq. (8.49) guaranteeing the stationary state of $\boldsymbol{\Omega}$, Eq. (8.46) results in

$$\nabla\left(P + \frac{1}{2}\mathbf{U}^2 + \frac{2}{3}K_R + \left\langle\frac{\mathbf{b}'^2}{2}\right\rangle\right) = 0, \tag{8.53}$$

and the mean pressure P is determined by the Bernoulli's theorem

$$P + \frac{1}{2}\mathbf{U}^2 + \frac{1}{2}K + \frac{1}{6}K_R = \text{const}, \tag{8.54}$$

where use has been made of $\left\langle\mathbf{b}'^2\right\rangle = K - K_R$.

8.3.4. Sustainment of turbulent state

In § 8.3.3, we investigated into the MHD state that is free from the diffusion effect, although the state is turbulent. The MHD turbulent state characterized by nonvanishing K and W is the most important ingredient in the present jet-collimation mechanism, as is seen from the dependence of β and γ on these two quantities. The elucidation of the mechanism of sustaining K and W is critical for understanding the jet collimation from the viewpoint of mean-field theory. As was emphasized in § 6.2, we do not still have the model equation for the turbulent residual helicity H whose mathematical and physical

bases are as firm as the equations for K and W. In order to avoid the uncertainty arising from this situation, we shall make the following discussion with the full use of the equations for K and W.

From Eqs. (8.49) and (8.51), we have

$$R_{ij} = \frac{2}{3} K_R, \tag{8.55}$$

$$\mathbf{E}_M = 0. \tag{8.56}$$

In the absence of buoyancy effects, Eqs. (6.39) and (6.41) result in

$$P_K = P_W = 0, \tag{8.57}$$

and the most typical production mechanisms of K and W are lost in the jet-collimation process developed in § 8.3.3. This situation seems to contradict the foregoing discussions and should be addressed consistently.

Gases in a disk accrete onto a central high-mass body, while differentially rotating, and they are in turbulent state, as was noted in § 8.3.2. Some of those gases are ejected as bipolar jets, which signifies the transfer of the turbulent energy K from the disk to the jet region. This transfer is the source of K in the jet.

In order to see this situation in mathematical terms, we use Eqs. (6.42), (8.55), and (8.56), and rewrite Eq. (6.38) as

$$\nabla(K\mathbf{U} - W\mathbf{B}) = -\varepsilon, \tag{8.58}$$

$$\nabla(W\mathbf{U} - K\mathbf{B}) = -C_W \frac{K}{\varepsilon} W, \tag{8.59}$$

where the transport effects due to the fluctuations only, $\mathbf{T}_K$ and $\mathbf{T}_W$, were discarded, compared with the mean-field/dependent parts $W\mathbf{B}$ and $K\mathbf{B}$ ($|\mathbf{B}|$ and $|\mathbf{U}|$ are usually much larger than $|\mathbf{b}'|$ and $|\mathbf{u}'|$). We substitute Eq. (8.49) into Eqs. (8.58) and (8.59), and have

$$\left(\frac{C_\beta}{C_\gamma} - 1\right)(\mathbf{U}\cdot\nabla)K = \varepsilon, \tag{8.60}$$

$$(\mathbf{U}\cdot\nabla)\left(\left(\frac{C_\beta}{C_\gamma}\left(\frac{K}{W}\right)^2 - 1\right)W\right) = C_W \frac{K}{\varepsilon} W, \tag{8.61}$$

where use has been made of Eqs. (6.31) and (6.32). In this context, we should note

$$\frac{C_\beta}{C_\gamma} > 1, \tag{8.62}$$

$$\frac{C_\beta}{C_\gamma}\left(\frac{K}{W}\right)^2 > 1, \tag{8.63}$$

from Eqs. (6.37) and (6.46a).

In accretion-disk jets, mean MHD turbulent flows are statistically axisymmetric around the rotation or z axis (Fig. 13). Considering that U_z is the main component of mean flow, we rewrite (8.60) as

$$\left(\frac{C_\beta}{C_\gamma} - 1\right) U_z \frac{\partial K}{\partial z} = \varepsilon. \tag{8.64}$$

The disk is in a turbulent state with nonvanishing K. Equation (8.64) indicates that this K is advected and transported to the jet region, balancing with the energy dissipation ε.

In Eq. (8.61), we discard the spatial variation of the nondimensional quantity $(C_\beta / C_\gamma)(K / W)^2 - 1$. Then the mathematical structure of the resulting equation is similar to Eq. (8.64), and W is advected and transported from the disk to jet region.

Finally, we refer to the sustainment of the turbulent residual helicity H that is related to α as Eq. (6.30). In the present stage of the progress in mean-field theory, we have no reliable model equation for it, as has already been noted. This situation arises from the fact that no conservation property holds for the residual helicity $-\mathbf{u}\cdot\boldsymbol{\omega} + \mathbf{b}\cdot\mathbf{j}$ in ideal MHD flow. We seek a cause of nonvanishing H from the residual helicity of mean field

$$H_m = -\mathbf{U}\cdot\boldsymbol{\Omega} + \mathbf{B}\cdot\mathbf{J}. \tag{8.65}$$

It may be rewritten as

$$H_m = \left(\frac{C_\beta}{C_\gamma}\left(\frac{K}{W}\right)^2 - 1\right)\mathbf{U}\cdot\boldsymbol{\Omega} \cong \frac{C_\beta}{C_\gamma}\left(\frac{K}{W}\right)^2 \mathbf{U}\cdot\boldsymbol{\Omega}, \tag{8.66}$$

from Eqs. (6.31), (6.32), (8.49), and (8.52). One of the prominent characteristics of accretion-disk jets is that gases flow while rotating. This fact signifies nonvanishing of $\mathbf{U}\cdot\boldsymbol{\Omega}$ or H_m. As a result, it is highly probable that nonvanishing H is also sustained in the presence of nonvanishing H_m.

8.3.5. Physical interpretation of jet collimation

In § 8.3.3, we showed that the turbulent diffusion of the momentum and magnetic field may be suppressed under the combined cross-helicity and helicity effects. The suppression of turbulent diffusion is a cause of jet collimation. The saturation level of $\mathbf{B}$ is given by Eq. (8.49). Here we should note that the primary component of $\mathbf{B}$ is of the dipole type since W or γ is antisymmetric with respect to the midplane of the disk. From Eqs. (6.37) and (8.49), we have

$$\frac{\mathbf{B}^2}{2} > \frac{\mathbf{U}^2}{2}. \tag{8.67}$$

Namely, the magnetic energy is larger than the kinetic energy. Specifically, the magnetic field may become very large under (8.41). One of the prominent features of magnetic field is the force of tension, under which magnetic field lines resist against their bending due to fluid motion. It is highly probable that the jet possessing such an intense magnetic field inside may strongly resist against their bending.

8.4. Reversed-field pinches of plasmas

The representative approach to plasma confinement by magnetic fields is tokamaks in torus geometry (Fig. 14). In the approach, the toroidal magnetic field $\mathbf{B}_T$ generated by external coils wrapped with a torus is much stronger than the poloidal one $\mathbf{B}_P$ coming from a toroidal plasma current. Compared with the motion of plasmas along this strong toroidal field, the motion normal to it is highly suppressed owing to the tension of the toroidal field. The relationship between $\mathbf{B}_T$ and $\mathbf{B}_P$ in tokamaks is characterized by

$$q_S = \frac{a}{R}\frac{|\mathbf{B}_T|}{|\mathbf{B}_P|} > 1, \tag{8.68}$$

where R and a are the major and minor radii, respectively. The quantity q_S is called the safety factor [16]. From this constraint, the minor radius a cannot be made much smaller than R.

In the context of q_S, a confinement approach that is in a directly opposite position to tokamaks is reversed-field pinches of plasmas (RFP's) [62-64]. In the approach, the poloidal magnetic field is nearly comparable to the toroidal field. The RFP state is characterized by

$$q_S << 1, \tag{8.69}$$

and a can be chosen to be much smaller than R. In the theoretical investigation into RFP's, the torus is often approximated by a circular cylinder.

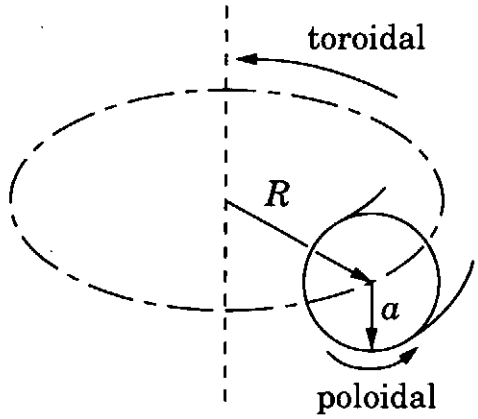

Fig. 14. Toroidal geometry in controlled fusion.

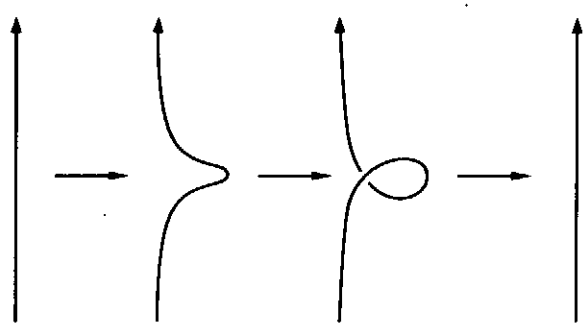

Fig. 15. Reversal of toroidal magnetic field.

The most prominent feature of RFP's is the reversal of the toroidal magnetic field at the outer edge of plasma. This phenomenon may be explained intuitively as follows. In the initial setting-up phase, the poloidal field generated by a strong toroidal plasma current interacts with the toroidal magnetic field, and a large deformation of the latter is induced by kink and sausage instability. Such deformation leads to the formation of the loop of a magnetic-field line because of its tension, as in Fig. 15, and the reconnection of the field line results in the reversal of the toroidal magnetic field at the plasma edge. In the situation, the continuation of plasma currents is equivalent to that of the reversed toroidal magnetic field. As a result, the alignment between the imposed current and the generated reversed magnetic field is a key ingredient of RFP's. Mathematically, this property is closely associated with Eq. (7.3). The process of magnetic-field reversal was examined in detail by the computer simulation of the MHD equations [65, 66].

8.4.1. Derivation of force-free field by mean-field theory

In RFP's, there is no macroscopic plasma flow. Then we have no mechanism of generating and sustaining the turbulent cross helicity, as is seen from Eq. (6.41) with the frame-rotation term dropped. We neglect the effect and write

$$\mathbf{E}_M = \alpha\mathbf{B} - \beta\mathbf{J}, \tag{8.70}$$

from which the equation for the mean magnetic field $\mathbf{B}$ obeys

$$\frac{\partial \mathbf{B}}{\partial t} = \nabla \times (\alpha\mathbf{B} - \beta\mathbf{J}). \tag{8.71}$$

The solution

$$\mathbf{J} = \kappa_m \mathbf{B} \tag{8.72}$$

guarantees the stationary state of $\mathbf{B}$, where

$$\kappa_m = \frac{\alpha}{\beta} \tag{8.73}$$

This close relationship between the mean-field theory and RFP's was first pointed out by Gimblett and Watkins [67].

We seek the solution of Eq. (8.72) in cylindrical geometry and examine its relationship with RFP's. To this end, we employ the cylindrical coordinates (σ, ϕ, z), where the ϕ and z directions represent the poloidal and toroidal directions, respectively. We assume the constancy of α and take the curl of Eq. (8.72). Then we have

$$\nabla^2\mathbf{B} + {\kappa_m}^2\mathbf{B} = 0. \tag{8.74}$$

Under the condition of the axisymmetry and z independence of $\mathbf{B}$, we are led to

$$\frac{d^2B_z}{dr^2} + \frac{1}{r}\frac{dB_z}{dr} + {\kappa_m}^2 B_z = 0, \tag{8.75}$$

$$B_\phi = -\frac{1}{\kappa_m}\frac{dB_z}{dr}, \tag{8.76}$$

from Eqs. (8.72) and (8.74). The solution of Eq. (8.75) and (8.76) is given by

$$B_z = B_0 J_0(\kappa_m r), \tag{8.77a}$$

$$B_\phi = B_0 J_1(\kappa_m r), \tag{8.77b}$$

where $B_0 = J_0(0)$, and J_n is the first-kind Bessel function of the nth order.

The Bessel function $J_n(s)$ possesses an infinite number of zero points, s_m's, at which $J_n(s_m) = 0$. The first zero point s_1 is about 2.4. This fact indicates that the toroidal magnetic field reverses its sign at the edge of plasma under the condition

$$|\kappa_m a| > 2.4. \tag{8.78}$$

This situation is depicted schematically in Fig. 16. The solution of the Bessel-function type, Eq. (8.77), may capture well the feature of the global magnetic fields in RFP's and has been a guiding principle in studying RFP's experimentally and theoretically.

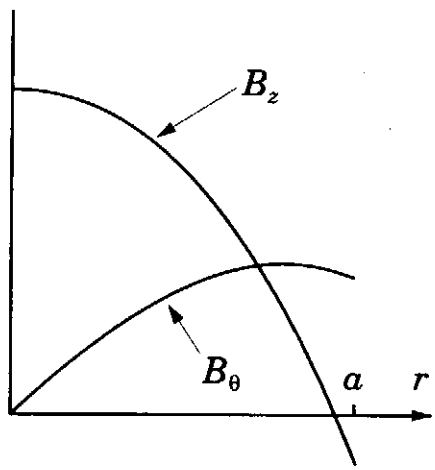

Fig. 16. Magnetic-field profile in RFP's.

Equation. (8.77) with constant κ_m suffers from some shortfalls near the edge of plasma. For instance, it cannot satisfy the condition of vanishing **J** there. Within the framework of mean-field theory, α and β are not constant, but they are determined by the equations for K, H, and ε. A model equation for H was proposed as [35, 36]

$$\frac{\partial H}{\partial t} = -C_{H1}\frac{\varepsilon^2}{K^3}\mathbf{B}\cdot\mathbf{E}_M - C_{H2}\frac{\varepsilon}{K}H + \nabla\cdot\left(\frac{\beta}{\sigma_H}\nabla H\right), \tag{8.79}$$

where C_{H1}, C_{H2}, and σ_H are positive constants. The mean-field theory with Eq. (8.79) added was confirmed to reproduce the primary features of RFP's under spatially varying κ_m.

8.4.2. Derivation of force-free field by variational method

The force-free field, Eq. (8.70), was originally derived by Taylor [68] from an entirely different viewpoint. There RFP's were regarded as a state relaxing from an initial unstable state subject a proper constraint. From the fact that the total amount of magnetic helicity, $\int_V \mathbf{a}\cdot\mathbf{b}dV$, is conserved in the absence of molecular effects, Taylor considered that the final state in the relaxation process may be described by the condition

$$\text{minimum } \int_V \frac{1}{2}\mathbf{b}^2 dV \text{ under constant } \int_V \mathbf{a}\cdot\mathbf{b}dV. \tag{8.80}$$

Here V denotes the region occupied by plasma, and $\mathbf{a}$ is the vector potential and is related to $\mathbf{b}$ as $\mathbf{b}=\nabla\times\mathbf{a}$. In the comparison between these two integrals, the former contains higher-wavenumber components, owing to the relation $\mathbf{b}=\nabla\times\mathbf{a}$. As a result, the former is considered to be affected more strongly by small-scale destruction effects.

We write the condition (8.80) in the variational form

$$\delta\left(\int_V\left(\frac{\mathbf{b}^2}{2}-\frac{\kappa_m}{2}\mathbf{a}\cdot\mathbf{b}\right)dV\right)=0, \tag{8.81}$$

with $\mathbf{a}$ fixed at the surface of V, where $\kappa_m/2$ is a constant Lagrange multiplier. By partial integration, Eq. (8.81) is reduced to

$$\int_V(\nabla\times\mathbf{b}-\kappa_m\mathbf{b})\cdot\delta\mathbf{a}dV=0, \tag{8.82}$$

resulting in the same type of expression as Eq. (8.72). We should note that the constancy of κ_m is a key factor in this derivation.

8.5. Plasma rotation in Tokamaks

A big breakthrough of tokamaks was attained through the so-called high-confinement (H) modes [69]. The transition of plasma state from low-confinement (L) to H modes may be characterized by a steep radial electric field and a poloidal plasma rotation, just inside the separatrix [70-74]. Their occurrence resulting in the formation of transport barriers of thermal energy may be regarded as a kind of structure formation in plasmas [75]. Understanding of this mechanism is expected to pave the way for the further improvement of plasma confinement and is a central subject in the study of magnetically confined plasmas.

In a sharp contrast with the foregoing edge transport barriers, the discharges with transport barriers in a core region, which are called the internal or core transport barriers, have recently attracted much attention [76-79]. Such discharges are characterized by the negative magnetic shear s_M, that is,

$$s_M = (\sigma / q_S) \frac{dq_S}{dr} < 0 \tag{8.83}$$

[q_S is the safety factor defined by Eq. (8.68), and r is the minor radial coordinate]. The transport barrier in a core region is accompanied by a steep gradient of poloidal flow, as in an edge region of H modes. Here the discharge characterized by negative s_M is simply called reversed-shear (RS) modes. The inhomogeneous plasma rotation, which is observed in the region with minimum q_S, is considered to play a critical role for those modes. The internal transport barriers are very similar to the H-mode counterparts in the sense that both are accompanied by the steep spatial variation of a radial electric field and a poloidal flow.

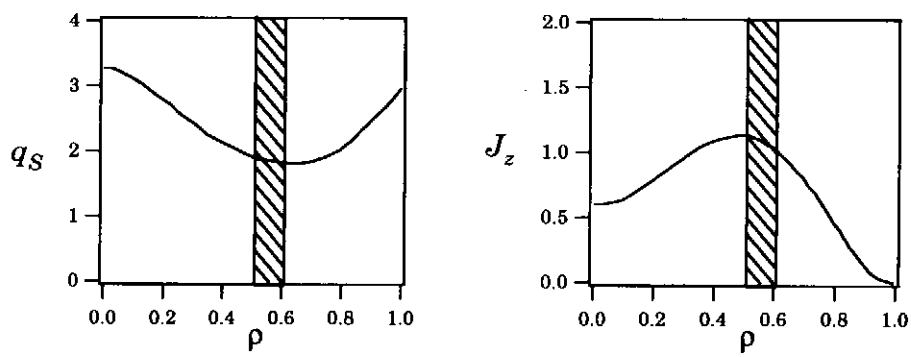

Fig. 17. Safety factor and current density in RS mode.

One of the prominent characteristics in RS modes is the existence of minimum q_S, as in Fig. 17, where $\rho = r / a$ (a is the minor radius). This q_S profile comes from the concave profile of the electric current density J_z that is also shown in Fig. 17 [80]. The transport barrier accompanied by the poloidal rotation of plasma is formed near the minimum-q_S point. We examine the relationship of concave J_z with the occurrence of plasma rotation, with the aid of the mean-field theory [81]. It should be recalled, however, that many interesting phenomena associated with electric-field effects on tokamaks are beyond the scope of the one-fluid MHD system on which the mean-field theory is founded.

We assume the axisymmetry of all statistical quantities and neglect the dependence on the toroidal or z direction. In the mean-flow equation (6.18), we drop the Coriolis and buoyancy terms. The resulting equation and its counterpart for the mean vorticity $\mathbf{\Omega}$ are given by Eqs. (8.46) and (8.47), respectively. In the latter equation, $\mathbf{\Omega}$ is small at the onset stage of the plasma rotation. We drop the first term on its right-hand side. The poloidal rotation is characterized by the z component of the mean vorticity, which obeys

$$\frac{\partial \Omega_z}{\partial t} = \nu_T \nabla^2 \Omega_z - \nu_M \nabla^2 J_z, \tag{8.84}$$

where the spatial dependence of ν_T and ν_M was neglected for simplicity of discussion.

In the absence of the second ν_M-related term in Eq. (8.84), Ω_z is subject to the resistive effect only, and there is no room for its autonomous generation. We now seek the Ω_z generation process due to the ν_M-related effect. For this purpose, we pick up its contribution and write

$$\frac{\partial \Omega_z}{\partial t} = -\frac{5C_\gamma}{7}\frac{K}{\varepsilon} W \nabla^2 J_z + R_{\Omega 1}, \tag{8.85}$$

where use has been made of Eqs. (6.29) and (6.32), and $R_{\Omega 1}$ denotes the remaining contribution. Of three turbulence quantities K, ε, and W, the last quantity is a pseudo-scalar that changes its sign under the reflection of the coordinate system, $\mathbf{x} \to -\mathbf{x}$. This fact indicates that W plays a critical role in the Ω_z generation since the sign of rotational motion is dependent on the choice of a coordinate system.

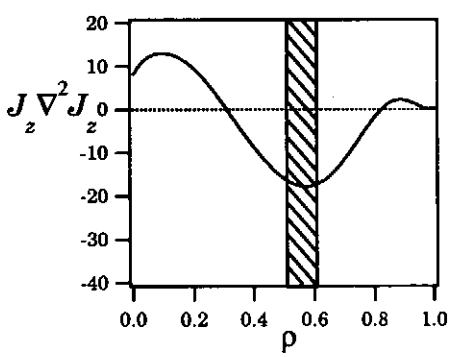

Fig. 18. Magnitude of $J_z \nabla^2 J_z$ corresponding to Fig. 17.

The quantity W is generated by P_W [Eq. (6.41)]. At the onset of Ω_z, the second term in Eq. (6.22) is primary, resulting in

$$\mathbf{E}_M \cong -\beta \mathbf{J}. \tag{8.86}$$

We combine Eq. (8.86) with P_W and have

$$P_W \cong \beta J_z \Omega_z. \tag{8.87}$$

In obtaining Eq. (8.87), we retained only the $\boldsymbol{\Omega}$-dependent part of Eq. (6.41) since our interest lies in the generation process of $\boldsymbol{\Omega}$. The contribution of Eq. (8.87) to the generation rate of W, $\partial W / \partial t$, is

$$\frac{\partial W}{\partial t} = \beta J_z \Omega_z + R_W = C_\beta \frac{K^2}{\varepsilon} J_z \Omega_z + R_W, \tag{8.88}$$

in correspondence to Eq. (8.85), where Eq. (6.31) was used.

We eliminate W from Eqs. (8.85) and (8.88), and connect Ω_z directly with J_z. Here we focus attention on the temporal growth of W, and neglect the temporal change of J_z, K, and ε. Then we have

$$\frac{\partial^2 \Omega_z}{\partial t^2} - \left(-\frac{5 C_\beta C_\gamma}{7} \frac{K^3}{\varepsilon^2} J_z \nabla^2 J_z \right) \Omega_z = R_{\Omega 2}, \tag{8.89}$$

where $R_{\Omega 2}$ expresses all the remaining contributions and is not discussed here. Equation (8.89) indicates that Ω_z may grow under the condition

$$\chi_\Omega{}^2 \cong -\frac{5 C_\beta C_\gamma}{7} \frac{K^3}{\varepsilon^2} J_z \nabla^2 J_z > 0, \tag{8.90}$$

where χ_Ω represents its temporal growth rate.

We examine Eq. (8.90) in the light of the concave profile of J_z. The latter profile is shown in Fig. 17 [80], and corresponding $J_z \nabla^2 J_z$ is shown in Fig. 18. There large negative $J_z \nabla^2 J_z$ occurs near the location of minimum q_S or at $\rho \cong 0.6$. Equations (8.89) and (8.90) suggest that the poloidal rotation starts to be driven there. This finding is consistent with the fact that a poloidal flow in RS modes is observed near the minimum-q_S point or the transport barrier.

9. Summary

In this review, we investigated into the mean-field theory of dynamo with special emphasis on the following three points. The first point is understanding of effects of fluctuations on mean or global field. The second is the construction of a self-consistent

dynamo model that is applicable to real-world phenomena. The third is the clarification of fundamental aspects of some planetary magnetic fields.

In relation to the first point, we showed that the dynamo effect generating the global magnetic field aligned with the global rotational motion occurs as long as the correction between velocity and magnetic-field fluctuations is taken into account. In the second point, we showed that the use of conservation properties is important for the construction of turbulence equations with firm mathematical and physical bases. In the third, the combination of the traditional helicity (alpha) effect with the cross-helicity effect make possible the determination of the saturation level of generated magnetic field, without a nonlinear effect on the alpha effect.

The representative unresolved problem in the mean-field theory is the construction of a model equation for the turbulent residual helicity that is necessary for the determination of the alpha effect. The residual helicity is connected to no conservation property, unlike the energy and the cross helicity. As a result, the study of the equation of the turbulent residual helicity remains in a very premature stage. In the past study of dynamo, little attention was paid to this point. Its construction is indispensable for the further development of the mean-field theory.

REFERENCES

[1] Melchior P 1986 *The Physics of the Earth's Core* (Oxford, Pergamon)

[2] Merrill, R T, McElhinny M W and McFaden P L 1996 *The Magnetic Field of the Earth* (San Diego: Academic)

[3] Priest E 1982 *Solar Magnetohydrodynamics* (Dordrecht: Reidel)

[4] Wilson P W *Solar and Stellar Activity Cycles* (Cambridge: Cambridge University Press)

[5] Stix M 1981 Solar Phys. **74** 79

[6] Glatzmaier G A and Roberts P H 1995 Phys. Earth Planet. Inter. **91** 63

[7] Kageyama A and Sato T 1995 Phys. Plasmas **2** 1421

[8] Olson P, Christensen U and Glatzmaier G A 1999 J. Geophys. Res. **104** 10383

[9] Moffatt M K 1978 *Magnetic Field Generation in Electrically Conducting Fluids* (Cambridge: Cambridge University Press)

[10] Krause F and Rädler K-H 1980 *Mean-Field Magnetohydrodynamics and Dynamo Theory* (Oxford: Pergamon)

[11] Roberts P H 1990 *Astrophysical Fluid Dynamics* ed J-P Zahn and Zinn-Justin (Amsterdam: Elsevier) p 229

[12] Yoshizawa A 1998 *Hydrodynamic and Magnetohydrodynamic Turbulent Flows:*

Modelling and Statistical Theory (Dordrecht: Kluwer)
[13] Begelman M C, Blandford, R D and Rees M J 1984 Rev. Mod. Phys. **58** 255
[14] Ferrari, A 1998 Annu. Rev. Astron. Astrophys. **36** 539
[15] Kato S, Fukue and Mineshige S 1998 *Black-Hole Accretion Disks* (Kyoto: Kyoto University Press)
[16] Miyamoto K 1976 *Plasma Physics for Nuclear Fusion* (Cambridge: The MIT Press)
[17] Roberts P H *An Introduction to Magnetohydrodynamics* (London: Longmans)
[18] Pedlosky J 1979 *Geophysical Fluid Dynamics* (New York: Springer)
[19] Phillips O M 1966 *The Dynamics of the Upper Ocean* (Cambridge, Cambridge University Press)
[20] Busse F 1970 J. Fluid Mech. **44** 441
[21] Cowling T G 1934 Mon. Not. Astr. Roy. Soc. **94** 39
[22] Hoyng P 1993 in *The Sun: A Laboratory for Astrophysics*, ed J T Schmelz and J C Brown (Dordrecht: Kluwer)
[23] Braginsky S I 1991 Geophys. Astrophys. Fluid Dyn. **60** 89
[24] Yoshizawa A 1984 Phys. Fluids **27** 1377
[25] Hamba F 1987 J. Phys. Soc. Jpn. **56** 2721
[26] Pouquet A, Frisch U and Léorat J 1976 J. Fluid Mech. **77** 321
[27] Parker E N 1955 Astrophys J. 122 293
[28] Yoshizawa A 1985 Phys. Fluids **28** 3313
[29] Yoshizawa A 1990 Phys. Fluids B **2** 1589
[30] Gruzinov A V and Diamond P H 1994 Phys. Rev. Lett. **72** 1651
[31] Gruzinov A V and Diamond P H 1996 Phys. Plasmas **3** 1853
[32] Field G B, Blackman E G and Chou H 1999 Astrophys. J. **513** 638
[33] Chen H and Montgomery D 1987 Plasma Phys. Control. Fusion. **29** 205
[34] Blackman E G 2000 Astrophys. J. **529** 138
[35] Yoshizawa A and Hamba F 1988 Phys. Fluids **31** 2276
[36] Hamba F 1990 Phys. Fluids B **2** 3064
[37] Hamba F 1990 Phys. Fluids A **4** 441
[38] Glatzmaier G A and Roberts P H 1995 Nature **377** 203
[39] Kageyama A and Sato T 1993 Phys. Fluids B **5** 2793
[40] Kitauchi H and Kida S 1998 Phys. Fluids **10** 457
[41] Sarson G R, Jones C A and Longbottom A W 1998 Geophys. Astrophys. Fluid Dyn. **88** 225
[42] Kitayama J S, Matsushima M and Honkura Y 1999 Phys. Earth Planet. Inter. **111** 141
[43] Busse F H G 2000 Ann. Rev. Fluid Mech. **32** 383

[44] Zhang K and Schubert G 2000 Ann. Rev. Fluid Mech. **32** 409
[45] Schou J et al 1998 Astrophys. J. **505** 390
[46] Yoshimura H 1983 Astrophys. J. Suppl. **52** 36
[47] Yoshizawa A 1993 Publ. Astron. Soc. Jpn. **45** 129
[48] Yoshizawa A, Kato H and Yokoi N 2000 Astrophys. J **537** 1039
[49] Gilman P A 1983 Astrophys. J. Suppl. **53** 243
[50] Glatzmaier G A 1985 Astrophys. J. **291** 300
[51] Hathaway D H et al 1996 Sciences **272** 130
[52] Giles P M, Duvall Jr T L, Scherrer P H and Bogart R S 1997 Nature **390** 52
[53] Basu S, Antia H M and Tripathy S C 1999 Astrophys. J. **512** 458
[54] Yoshizawa A, Yokoi N and Kato H 1999 Phys. Plasmas **6** 4586
[55] Uchida Y and Shibata K 1985 Publ. Astron. Soc. Jpn. **37** 515
[56] Stone J M and Norman M L 1994 Astrophys. J. **433** 746
[57] Matsumoto R et al 1996 Astrophys. J. **461** 115
[58] Yoshizawa A, Yokoi N and Kato H 2000 Phys. Plasmas **7** 2646
[59] Yoshizawa A and Yokoi N 1993 Astrophys. J. **407** 540
[60] Nishino S and Yokoi N 1998 Publ. Astron. Soc. Jpn. **50** 653
[61] Yokoi N 1996 Astron. Astrophys. **311** 731
[62] Bodin H A B and Newton A A 1980 Nucl. Fusion **20** 1255
[63] Bodin H A B 1987 Plasma Phys. Control. Fusion **29** 1297
[64] Miyamoto K 1988 Plasma Phys. Control. Fusion **30** 1493
[65] Schnack D D, Caramana C J and Nebel R A 1985 Phys. Fluids **28** 321
[66] Kusano K and Sato T 1986 Nucl. Fusion **26** 1051
[67] Gimblett C G and Watkins M K 1975 *Proc. Seventh European Conf. on Controlled Fusion and Plasma Physics* Vol I (Lausanne: Ecole de Polytechnique Fédéral de Lausanne) p 63
[68] Taylor J B 1974 Phys. Rev. Lett. **33** 1139
[69] Wagner F et al 1982 Phys. Rev. Lett. **49** 1408
[70] Itoh S-I and Itoh K 1988 Phys. Rev. Lett. **60** 2276
[71] Shaing K C and Crume Jr E C 1989 Phys. Rev. Lett. **63** 2369
[72] Itoh K and Itoh S. -I. 1996 Plasma Phys. Control. Fusion **38** 1
[73] Burrell K H 1997 Phys. Plasmas **4** 1499
[74] Ida K 1998 Plasma Phys. Control. Fusion **40** 1429
[75] Itoh K, Itoh S-I and Fukuyama A 1999 *Transport and Structural Formation in Plasmas* (Bristol: Institute of Physics)
[76] Koide Y et al 1994 Phys. Rev. Lett. **72** 3662
[77] Levinton F M et al 1995 Phys. Rev. Lett. **75** 4417
[78] Strait E J 1995 Phys. Rev. Lett. **75** 4421

[79] Synakowski E J 1998 Phys. Control. Fusion **40** 581
[80] Fujita F 1997 J Plasma Fusion Res. **73** 549
[81] Yoshizawa A, Yokoi N, Itoh S-I and Itoh K 1999 Phys. Plasmas **6** 3194

Appendix: Statistical Theory and Modeling of Electrically Nonconducting Turbulence

In the study of statistical theories of homogeneous isotropic turbulence, attention has been focused on smaller-scale properties of turbulence associated with inertial and dissipation ranges [A1-A3]. In turbulence modeling, a characteristic time scale of energy-containing eddies is one of the important factors, as is seen from Eq. (6.9). The behavior of those eddies are linked with the turbulent-energy production mechanism, and its examination is beyond the scope of isotropic turbulence theories. Then there is a wide gap between them and the turbulence modeling whose MHD version is the main theme of mean-field theory.

Here we explain a theoretical framework of inhomogeneous turbulence, specifically, a two-scale direct-interaction approximation (TSDIA) [12, 24] and give a theoretical method for deriving turbulence models necessary for the analysis of real-world flows. This explanation is helpful to understanding of the relationship between mean-field dynamo theory and turbulence theories.

A1. Perturbational method

A1.1. Introduction of two-scale variables

In the decomposition of a flow quantity f by Eq. (4.1), the spatial or temporal variations of the mean F and the fluctuation f' are depicted schematically in Fig. A1. In general, the variation of F is much slower, compared with f'. A method useful for describing such different properties is the introduction of multiple scales.

We use a positive small parameter δ_S [Eq. (5.1)] and introduce two spatial and temporal variables (ξ, τ) and $(\mathbf{X}, T)$ [Eq. (5.2)]. For the change of the original coordinate

$$\mathbf{x} \to \mathbf{x} + \mathbf{r}, \tag{A1}$$

we have

$$\xi \to \xi + \mathbf{r}, \quad \mathbf{X} \to \mathbf{X} + \delta_S \mathbf{r}, \tag{A2}$$

which indicates that the change of $\mathbf{X}$ is small under Eq. (5.1). We write f as Eq. (5.3). From Eq. (A2), we have

$$F(\mathbf{X},T) \to F(\mathbf{X},T) + \delta_S r_i \frac{\partial F(\mathbf{X},T)}{\partial X_i} + O\left((\delta_S r)^2\right), \tag{A3a}$$

$$f'(\xi,\tau;\mathbf{X},T) \to f'(\xi,\tau;\mathbf{X},T) + r_i \frac{\partial}{\partial \xi_i} f'(\xi,\tau;\mathbf{X},T) + O(\delta_S r), \tag{A3b}$$

which guarantee that the variation of F is much slower than that of f'. Hereafter $(\mathbf{X},T)$ and (ξ,τ) are called slow and fast variables, respectively. We should note the dependence of f' on $(\mathbf{X},T)$. By adopting $\mathbf{u}'$ as f', we may understand it since $\mathbf{u}'$ is connected with $\mathbf{U}$ through Eq. (4.17) with magnetic parts dropped.

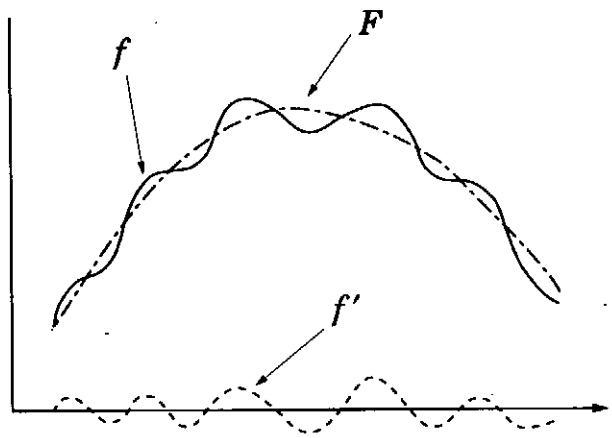

Fig. A1. Variations of mean and fluctuation.

We apply Eqs. (5.2) and (5.3) to the solenoidal condition $\nabla \cdot \mathbf{u}' = 0$ and Eq. (4.17) for the electrically nonconducting case. We have

$$\frac{\partial u_i'}{\partial \xi_i} + \delta_S \frac{\partial u_i'}{\partial X_i} = 0, \tag{A4}$$

$$\frac{\partial u_i'}{\partial \tau} + U_j \frac{\partial u_i'}{\partial \xi_j} + \frac{\partial}{\partial \xi_j} u_j' u_i' + \frac{\partial p'}{\partial \xi_i} - \nu \nabla_\xi^2 u_i'$$

$$= \delta_S \left(-u_j' \frac{\partial U_i}{\partial X_j} - \frac{Du_i'}{DT} - \frac{\partial p'}{\partial X_i} - \frac{\partial}{\partial X_j}\left(u_j' u_i' - R_{ij}\right) + 2\nu \frac{\partial u_i'}{\partial X_j \partial \xi_j} \right)$$

$$+ \delta_S^2 \left(\nu \nabla_X^2 u_i' \right), \tag{A5}$$

where ∇_ξ, ∇_X, and D/DT are defined by Eqs. (5.5) and (5.6).

A1.2. Fourier representation of fast-varying modes

In the investigation into homogeneous turbulence with no mean flow, we write $\mathbf{u}'$ in the Fourier representation with the amplitude $\mathbf{u}'(\mathbf{k})$. The second term on the left-hand side of Eq. (A5) shows that $\mathbf{u}'$ is swept away by the slowly-varying mean flow $\mathbf{U}$. In order to properly express this situation, we introduce the Fourier representation in the frame moving with the velocity $\mathbf{U}$, Eq. (5.7).

We apply Eq. (5.7) to Eqs. (A4) and (A5), and have

$$\mathbf{k}\cdot\mathbf{u}'(\mathbf{k};\tau)=\delta_S\left(-i\nabla_X^*\cdot\mathbf{u}'(\mathbf{k};\tau)\right), \tag{A6}$$

$$\frac{\partial u_i'(\mathbf{k};\tau)}{\partial\tau}+\nu k^2 u_i'(\mathbf{k};\tau)-ik_i p'(\mathbf{k};\tau)$$

$$-ik_j\iint u_i'(\mathbf{p};\tau)u_j'(\mathbf{q};\tau)\delta(\mathbf{k}-\mathbf{p}-\mathbf{q})d\mathbf{p}d\mathbf{q}$$

$$=\delta_S\left(-u_j'(\mathbf{k};\tau)\frac{\partial U_i}{\partial X_j}-\frac{D^*u_i'(\mathbf{k};\tau)}{DT^*}-\frac{\partial p'(\mathbf{k};\tau)}{\partial X_i^*}\right.$$

$$\left.-\iint\frac{\partial^*}{\partial X_j^*}\left(u_i'(\mathbf{p};\tau)u_i'(\mathbf{q};\tau)\right)\delta(\mathbf{k}-\mathbf{p}-\mathbf{q})d\mathbf{p}d\mathbf{q}+\delta(\mathbf{k})\frac{\partial R_{ij}}{\partial X_j}\right), \tag{A7}$$

where D^*/DT^* and ∇_X^* are defined by Eq. (5.10). Here and hereafter, the dependency of f' on slow variables $\mathbf{X}$ and T is not written explicitly, except when necessary. The new differential operators given by Eq. (5.10) arise from the use of the Fourier representation in the moving frame. On the right-hand side of Eq. (A7), the R_{ij}- and ν-related terms are neglected, owing to their minor importance in later analyses.

In Eq. (A6), we should note that $\mathbf{u}'(\mathbf{k};\tau)$ does not obey the usual solenoidal condition concerning $\mathbf{k}$, that is, $\mathbf{k}\cdot\mathbf{u}'(\mathbf{k};\tau)=0$. This situation originates from that the Fourier representation of $\mathbf{u}'$ was made for the fast-varying components of motion only. In order to properly deal with Eq. (A6), we introduce the transformation [A4]

$$\mathbf{u}'(\mathbf{k};\tau)=\mathbf{v}'(\mathbf{k};\tau)+\delta_S\left(-i\frac{\mathbf{k}}{k^2}\nabla_X^*\cdot\mathbf{u}'(\mathbf{k};\tau)\right). \tag{A8}$$

As a result, $\mathbf{v}'(\mathbf{k};\tau)$ is subject to the solenoidal condition concerning $\mathbf{k}$, that is,

$$\mathbf{k}\cdot\mathbf{v}'(\mathbf{k};\tau)=0, \tag{A9}$$

and various mathematical tools developed in the study of homogeneous turbulence are available for inhomogeneous turbulence.

A1.3. Scale-parameter expansion

Once the δ_S-related terms in Eqs. (A6) and (A7) are dropped, we have the same system of equations as for homogeneous turbulence, except the implicit influence of slowly-varying properties of $\mathbf{U}$ through $\mathbf{X}$ and T. This mathematical situation suggests that inhomogeneous turbulence may be investigated by the perturbational method based on δ_S.

We expand

$$\mathbf{u}'(\mathbf{k};\tau) = \sum_{n=0}^{\infty} \delta_S{}^n \mathbf{u}_n'(\mathbf{k};\tau), \quad \mathbf{v}'(\mathbf{k};\tau) = \sum_{n=0}^{\infty} \delta_S{}^n \mathbf{v}_n'(\mathbf{k};\tau), \tag{A10}$$

$$p'(\mathbf{k};\tau) = \sum_{n=0}^{\infty} \delta_S{}^n p_n'(\mathbf{k};\tau). \tag{A11}$$

We substitute Eqs. (A10) and (A11) into Eqs. (A7)-(A9), and have

$$\mathbf{u}_n'(\mathbf{k};\tau) = \mathbf{v}_n'(\mathbf{k};\tau) - i\frac{\mathbf{k}}{k^2}\nabla_X^* \cdot \mathbf{u}_{n-1}'(\mathbf{k};\tau), \tag{A12}$$

$$\frac{\partial u_{ni}'(\mathbf{k};\tau)}{\partial \tau} + \nu k^2 u_{ni}'(\mathbf{k};\tau) - ik_i p_n'(\mathbf{k};\tau)$$

$$-ik_j \iint \left(u_{ni}'(\mathbf{p};\tau)u_{0j}'(\mathbf{q};\tau) + u_{0i}'(\mathbf{p};\tau)u_{nj}'(\mathbf{q};\tau)\right)\delta(\mathbf{k}-\mathbf{p}-\mathbf{q})d\mathbf{p}d\mathbf{q}$$

$$= -u_{n-1j}'(\mathbf{k};\tau)\frac{\partial U_i}{\partial X_j} - \frac{D^* u_{n-1i}'(\mathbf{k};\tau)}{DT^*} - \frac{\partial^* p_{n-1}'(\mathbf{k};\tau)}{\partial X_i^*}$$

$$-\sum_{m=0}^{n-1} \iint \frac{\partial^*}{\partial X_j^*}\left(u_{mi}'(\mathbf{p};\tau)u_{n-m-1i}'(\mathbf{q};\tau)\right)\delta(\mathbf{k}-\mathbf{p}-\mathbf{q})d\mathbf{p}d\mathbf{q}, \tag{A13}$$

where $\mathbf{v}_n'(\mathbf{k};\tau)$ obeys the usual solenoidal condition

$$\mathbf{k}\cdot\mathbf{v}_n'(\mathbf{k};\tau) = 0. \tag{A14}$$

Lowest-order equations

As has already been noted, the lowest-order equations are of the same form as for homogeneous turbulence. Then we have

$$\frac{\partial u_{0i}'(\mathbf{k};\tau)}{\partial \tau} + \nu k^2 u_{0i}'(\mathbf{k};\tau)$$

$$-iM_{ij\ell}(\mathbf{k})\iint u_{0j}'(\mathbf{p};\tau)u_{0\ell}'(\mathbf{q};\tau)\delta(\mathbf{k}-\mathbf{p}-\mathbf{q})d\mathbf{p}d\mathbf{q} = 0, \tag{A15}$$

$$p_0'(\mathbf{k};\tau) = -\frac{k_i k_j}{k^2}\iint u_{0j}'(\mathbf{p};\tau)u_{0j}'(\mathbf{q};\tau)\delta(\mathbf{k}-\mathbf{p}-\mathbf{q})d\mathbf{p}d\mathbf{q}, \tag{A16}$$

where we should note

$$\mathbf{u}_0'(\mathbf{k};\tau) = \mathbf{v}_0'(\mathbf{k};\tau). \tag{A17}$$

First-order equations

Explicit effects of mean flow occur in the first-order equations. From Eqs. (A12)-(A14), these equations are written as

$$\mathbf{u}_1'(\mathbf{k};\tau) = \mathbf{v}_1'(\mathbf{k};\tau) - i\frac{\mathbf{k}}{k^2}\nabla_X^* \cdot \mathbf{u}_0'(\mathbf{k};\tau), \tag{A18}$$

$$\frac{\partial u_{1i}'(\mathbf{k};\tau)}{\partial \tau} + \nu k^2 u_{1i}'(\mathbf{k};\tau) - ik_i p_1'(\mathbf{k};\tau)$$

$$= -u_{0j}'(\mathbf{k};\tau)\frac{\partial U_i}{\partial X_j} - \frac{D^* u_{0i}'(\mathbf{k};\tau)}{DT^*} - \frac{\partial^* p_0'(\mathbf{k};\tau)}{\partial X_i^*}$$

$$-\iint \frac{\partial^*}{\partial X_j^*}\left(u_{0i}'(\mathbf{p};\tau)u_{0i}'(\mathbf{q};\tau)\right)\delta(\mathbf{k}-\mathbf{p}-\mathbf{q})d\mathbf{p}d\mathbf{q}, \tag{A19}$$

with

$$\mathbf{k}\cdot\mathbf{v}_1'(\mathbf{k};\tau) = 0. \tag{A20}$$

We substitute Eq. (A18) into Eq. (A19), and apply Eq. (A20). Then we have

$$p_1'(\mathbf{k};\tau) = -2i\frac{k_j}{k^2}\frac{\partial U_j}{\partial X_i}u_{0i}'(\mathbf{k};\tau)$$

$$-2\frac{k_i k_j}{k^2}\iint u_{0i}'(\mathbf{p};\tau)u_{1j}'(\mathbf{q};\tau)\delta(\mathbf{k}-\mathbf{p}-\mathbf{q})d\mathbf{p}d\mathbf{q}$$

$$-2i\frac{1}{k^2}M_{\ell ij}(\mathbf{k})\iint \frac{\partial^*}{\partial X_\ell^*}\left(u_{0i}'(\mathbf{p};\tau)u_{0j}'(\mathbf{q};\tau)\right)\delta(\mathbf{k}-\mathbf{p}-\mathbf{q})d\mathbf{p}d\mathbf{q}. \tag{A21}$$

We use Eqs. (A16), (A18) and (A21), and eliminate p_1' from Eq. (A19), obtaining

$$\frac{\partial v_{1i}'(\mathbf{k};\tau)}{\partial \tau} + \nu k^2 v_{1i}'(\mathbf{k};\tau)$$

$$-2iM_{ij\ell}(\mathbf{k})\iint u_{0j}'(\mathbf{p};\tau)v_{1\ell}'(\mathbf{q};\tau)\delta(\mathbf{k}-\mathbf{p}-\mathbf{q})d\mathbf{p}d\mathbf{q}$$

$$= I_{1i}(\mathbf{k};\tau) \equiv -D_{i\ell}(\mathbf{k})u_{0j}'(\mathbf{k};\tau)\frac{\partial U_\ell}{\partial X_j} - D_{ij}(\mathbf{k})\frac{D^* u_{0j}'(\mathbf{k};\tau)}{DT^*}$$

$$+2M_{ij\ell}(\mathbf{k})\iint \frac{q_\ell}{q^2}u_{0j}'(\mathbf{p};\tau)\nabla_X^* \cdot \mathbf{u}_0'(\mathbf{q};\tau)\delta(\mathbf{k}-\mathbf{p}-\mathbf{q})d\mathbf{p}d\mathbf{q}$$

$$-D_{in}(\mathbf{k})M_{j\ell mn}(\mathbf{k})\iint \frac{\partial^*}{\partial X_m^*}\left(u_{0j}'(\mathbf{p};\tau)u_{0\ell}'(\mathbf{q};\tau)\right)\delta(\mathbf{k}-\mathbf{p}-\mathbf{q})d\mathbf{p}d\mathbf{q}, \quad \text{(A22)}$$

where

$$M_{ij\ell m}(\mathbf{k}) = \frac{1}{2}\delta_{i\ell}\delta_{jm} + \frac{1}{2}\delta_{im}\delta_{j\ell} - \frac{k_i k_j}{k^2}\delta_{\ell m}. \quad \text{(A23)}$$

A2. Introduction of Green's function

The lowest-order equation (A15) is not dependent explicitly on $\mathbf{U}$, but it is a nonlinear equation. The first-order equation (A22) depends on both $\mathbf{U}$ and $\mathbf{u}_0'$ in a complicated manner, but it is a linear equation. The latter equation may be integrated formally with the aid of a Green's function.

A.2.1. Green's function in inhomogeneous turbulence

We rewrite Eq. (A22) as

$$\frac{\partial v_{1i}'(\mathbf{k};\tau)}{\partial \tau} + \nu k^2 v_{1i}'(\mathbf{k};\tau)$$

$$-2iM_{ij\ell}(\mathbf{k})\iint u_{0j}'(\mathbf{p};\tau)v_{1\ell}'(\mathbf{q};\tau)\delta(\mathbf{k}-\mathbf{p}-\mathbf{q})d\mathbf{p}d\mathbf{q}$$

$$= \int \delta(\mathbf{k}-\mathbf{k}_1)d\mathbf{k}_1 \int_{-\infty}^{\tau} I_{1j}(\mathbf{k}_1;\tau_1)\delta(\tau-\tau_1)d\tau_1. \quad \text{(A24)}$$

In correspondence to the left-hand side of Eq. (A24), we introduce the Green's function $G_{ij}'(\mathbf{k},\mathbf{k}';\tau,\tau')$ obeying

$$\frac{\partial G_{ij}'(\mathbf{k},\mathbf{k}';\tau,\tau')}{\partial\tau}+\nu k^2 G_{ij}'(\mathbf{k},\mathbf{k}';\tau,\tau')$$

$$-2iM_{i\ell m}(\mathbf{k}))\iint u_{0\ell}'(\mathbf{p},\tau)G_{mj}'(\mathbf{q},\mathbf{k}';\tau,\tau')\delta(\mathbf{k}-\mathbf{p}-\mathbf{q})d\mathbf{p}d\mathbf{q}$$

$$=D_{ij}(\mathbf{k}')\delta(\mathbf{k}-\mathbf{k}')\delta(\tau-\tau'). \tag{A25}$$

We use G_{ij}' and integrate Eq. (A24) as

$$v_{1i}'(\mathbf{k};\tau)=\int d\mathbf{k}_1\int_{-\infty}^{\tau}G_{ij}'(\mathbf{k},\mathbf{k}_1;\tau,\tau_1)I_{1j}(\mathbf{k}_1;\tau_1)d\tau_1. \tag{A26}$$

Here we chose $-\infty$ as the lower limit of integral. This is due to the premise that our interest lies in a stationary state of turbulence independent of initial conditions. Considering the dependence of the right-hand side of Eq. (A25) on $\delta(\mathbf{k}-\mathbf{k}')$, we put

$$G_{ij}'(\mathbf{k},\mathbf{k}';\tau,\tau')=G_{ij}'(\mathbf{k}';\tau,\tau')\delta(\mathbf{k}-\mathbf{k}'). \tag{A27}$$

We substitute Eq. (A27) into Eq. (A25), and perform the integration with respect to $\mathbf{k}'$. Then we have

$$\frac{\partial G_{ij}'(\mathbf{k};\tau,\tau')}{\partial\tau}+\nu k^2 G_{ij}'(\mathbf{k};\tau,\tau')$$

$$-2iM_{i\ell m}(\mathbf{k})\iint u_{0\ell}'(\mathbf{p};\tau)G_{mj}'(\mathbf{q};\tau,\tau')\delta(\mathbf{k}-\mathbf{p}-\mathbf{q})d\mathbf{p}d\mathbf{q}$$

$$=D_{ij}(\mathbf{k})\delta(\tau-\tau'). \tag{A28}$$

In this context, Eq. (A26) is reduced to

$$v_{1i}'(\mathbf{k};\tau)=\int_{-\infty}^{\tau}G_{ij}'(\mathbf{k};\tau,\tau_1)I_{1j}(\mathbf{k};\tau_1)d\tau_1. \tag{A29}$$

From Eqs. (A18) and (A19), the first-order solution $\mathbf{u}_1'$ is given by

$$u_{1i}'(\mathbf{k};\tau)=\int_{-\infty}^{\tau}G_{ij}'(\mathbf{k};\tau,\tau_1)I_{1j}(\mathbf{k};\tau_1)d\tau_1-i\frac{k_i}{k^2}\nabla_X^*\cdot\mathbf{u}_0'(\mathbf{k};\tau). \tag{A30}$$

The second-order solution $\mathbf{u}_2'$ may be calculated in an entirely similar manner [12, 24, A5]. The manipulation, however, is very complicated owing to the occurrence of many terms. For alleviating the complexity, we focus attention on the effects linear in $\mathbf{u}_0'$. After this simplification, we have

$$\mathbf{u}_2'(\mathbf{k};\tau)=\mathbf{v}_2'(\mathbf{k};\tau)-i\frac{\mathbf{k}}{k^2}\nabla_X^*\cdot\mathbf{v}_1'(\mathbf{k};\tau)-\frac{\mathbf{k}k_i}{k^4}\frac{\partial^*}{\partial X_i^*}\nabla_X^*\cdot\mathbf{u}_0'(\mathbf{k};\tau). \tag{A31}$$

Here $\mathbf{v}_2'$ is given by

$$v_{2i}'(\mathbf{k};\tau) = \int_{-\infty}^{\tau} G_{ij}'(\mathbf{k};\tau,\tau_1) I_{2j}(\mathbf{k};\tau_1) d\tau_1 \ , \tag{A32}$$

with $\mathbf{I}_2$ defined by

$$I_{2i}(\mathbf{k};\tau) = i\frac{k_m}{k^2} D_{ij}(\mathbf{k}) \frac{\partial^2 U_m}{\partial X_j \partial X_n} u_{0n}'(\mathbf{k};\tau) - D_{im}(\mathbf{k}) \frac{\partial U_m}{\partial X_j} v_{1j}'(\mathbf{k};\tau)$$

$$+ i\frac{k_j}{k^2} D_{im}(\mathbf{k}) \frac{\partial U_j}{\partial X_n} \frac{\partial^* u_{0n}'(\mathbf{k};\tau)}{\partial X_m^*} + i\frac{k_m}{k^2} D_{ij}(\mathbf{k}) \frac{\partial U_j}{\partial x_m} \nabla_X^* \cdot \mathbf{u}_0'(\mathbf{k};\tau)$$

$$- \frac{D^* v_{1i}'(\mathbf{k};\tau)}{DT^*} + \frac{1}{k^2} D_{ij}(\mathbf{k}) \frac{\partial}{\partial \tau} \frac{\partial^*}{\partial X_j^*} \nabla_X^* \cdot \mathbf{u}_0'(\mathbf{k};\tau). \tag{A33}$$

A2.2. Green's function in homogeneous turbulence and isotropic turbulence theory

In § A2.1, the Green's function G_{ij}' was introduced in relation to the perturbational solution of a system of equations for inhomogeneous turbulence. There the lowest-order solution $\mathbf{u}_0'$ was treated as known. For calculating various statistical quantities with the aid of the perturbational solution, it is indispensable to know statistical properties of $\mathbf{u}_0'$. No explicit effects of $\mathbf{U}$ enter Eq. (A15) for $\mathbf{u}_0'$, and such effects arise through the implicit dependence on slow variables $\mathbf{X}$ and T. Then the statistical properties of $\mathbf{u}_0'$ may be examined by homogeneous turbulence theories.

A2.2.1. Direct-interaction approximation

The prototype of homogeneous turbulence theories is the direct-interaction approximation (DIA) by Kraichnan [A1, A2, A6, A7]. Its understanding is helpful to understanding not only other homogeneous turbulence theories, but also the mathematical procedures for evaluating the Reynolds stress etc. in inhomogeneous turbulence.

In order to solve Eq. (A15) in a perturbational manner, we regard the third term on the left-hand side as a perturbation, and formally integrate

$$u_{0i}'(\mathbf{k},\tau) = w_i(\mathbf{k},\tau) + iM_{mj\ell}(\mathbf{k}) \iint \delta(\mathbf{k}-\mathbf{p}-\mathbf{q}) d\mathbf{p} d\mathbf{q}$$

$$\times \int_{-\infty}^{\tau} \hat{G}_{im}(\mathbf{k};\tau,\tau_1) u_{0j}'(\mathbf{p};\tau_1) u_{0\ell}'(\mathbf{q};\tau_1) d\tau_1. \tag{A34}$$

Here the first term $\mathbf{w}$, which is assumed to be a random flow obeying a Gaussian distribution, denotes $\mathbf{u}_0{}'$ at $t=-\infty$. The second term expresses the effect arising from the nonlinear interaction thereafter. Moreover $\hat{G}_{ij}$ obeys

$$\frac{\partial \hat{G}_{ij}(\mathbf{k};\tau,\tau')}{\partial \tau}+\nu k^2\hat{G}_{ij}(\mathbf{k};\tau,\tau')=D_{ij}(\mathbf{k})\delta(\tau-\tau'), \tag{A35}$$

and is given by

$$\hat{G}_{ij}(\mathbf{k};\tau,\tau')=D_{ij}(\mathbf{k})S(\tau-\tau')\exp\left(-\nu k^2(\tau-\tau')\right), \tag{A36}$$

where $S(\tau)$ is the unit step function defined by $S(\tau)=0\,(\tau<0)$ and $1\,(\tau>0)$. Equation (A35) is reduced from Eq. (A25) with the nonlinear term dropped, and corresponds to the Green's or response equation in the low-Reynolds-number limit. We should note that $\hat{G}_{ij}$ is a deterministic quantity.

Similar to Eq.(A34), we rewrite Eq. (A25) as

$$G_{ij}{}'(\mathbf{k};\tau,\tau')=\hat{G}_{ij}(\mathbf{k};\tau,\tau')+2iM_{n\ell m}(\mathbf{k})\iint\delta(\mathbf{k}-\mathbf{p}-\mathbf{q})d\mathbf{p}d\mathbf{q}$$

$$\times\int_{\tau'}^{\tau}\hat{G}_{in}(\mathbf{k};\tau,\tau_1)u_{0\ell}{}'(\mathbf{p};\tau_1)G_{mj}{}'(\mathbf{q};\tau_1,\tau')d\tau_1. \tag{A37}$$

Here the lower limit of integral, τ', means that a disturbance is added at τ', as in Eq. (A25), and its effect occurs for $\tau>\tau'$.

We solve Eqs. (A35) and (A37) in an iterative manner with each first term as the leading part. As a result, we have

$$u_{0i}{}'(\mathbf{k};\tau)=w_i(\mathbf{k};\tau)+iM_{mj\ell}(\mathbf{k})\iint\delta(\mathbf{k}-\mathbf{p}-\mathbf{q})d\mathbf{p}d\mathbf{q}$$

$$\times\int_{-\infty}^{\tau}\hat{G}_{im}(\mathbf{k};\tau,\tau_1)w_j(\mathbf{p};\tau_1)w_\ell(\mathbf{q};\tau_1)d\tau_1+\cdots\cdots, \tag{A38}$$

$$G_{ij}{}'(\mathbf{k};\tau,\tau')=\hat{G}_{ij}(\mathbf{k};\tau,\tau')+2iM_{n\ell m}(\mathbf{k})\iint\delta(\mathbf{k}-\mathbf{p}-\mathbf{q})d\mathbf{p}d\mathbf{q}$$

$$\times\int_{\tau'}^{\tau}\hat{G}_{in}(\mathbf{k};\tau,\tau_1)w_\ell(\mathbf{p};\tau_1)\hat{G}_{mj}(\mathbf{q};\tau_1,\tau')d\tau_1+\cdots\cdots. \tag{A39}$$

In the DIA, the two-time covariance

$$Q_{ij}(\mathbf{k};\tau,\tau')=\frac{\left\langle u_{0i}{}'(\mathbf{k};\tau)u_{0j}{}'(\mathbf{k}';\tau')\right\rangle}{\delta(\mathbf{k}+\mathbf{k}')} \tag{A40}$$

and the mean of the Green's function

$$G_{ij}(\mathbf{k};\tau,\tau') = \left\langle G_{ij}'(\mathbf{k};\tau,\tau') \right\rangle \tag{A41}$$

are chosen as the fundamental statistical quantities of turbulence. We construct the equations governing these two quantities.

From Eq. (A15), Eq. (A40) obeys

$$LQ_{ij}(\mathbf{k};\tau,\tau') \equiv \left(\frac{\partial}{\partial\tau} + \nu k^2\right) Q_{ij}(\mathbf{k};\tau,\tau'),$$

$$= iM_{i\ell m}(\mathbf{k}) \iint \frac{\left\langle u_{0\ell}'(\mathbf{p};\tau) u_{0m}'(\mathbf{q};\tau) u_{0j}'(\mathbf{k}';\tau') \right\rangle}{\delta(\mathbf{k}+\mathbf{k}')} \delta(\mathbf{k}-\mathbf{p}-\mathbf{q}) d\mathbf{p} d\mathbf{q}. \tag{A42}$$

We substitute the perturbational solution (A38) and (A39) into the right-hand side of Eq. (A42), and make use of the Gaussianity of $\mathbf{w}$. Then the right-hand side is expressed in terms of the second-order correlation concerning $\mathbf{w}$, that is,

$$\hat{Q}_{ij}(\mathbf{k};\tau,\tau') = \frac{\left\langle \omega_i(\mathbf{k};\tau)\omega_j(\mathbf{k}';\tau') \right\rangle}{\delta(\mathbf{k}+\mathbf{k}')}. \tag{A43}$$

Here we retain the contributions of the lowest order in $\hat{Q}_{ij}$, and have

$$\begin{aligned} LQ_{ij}(\mathbf{k};\tau,\tau') &= 2\iint M_{iab}(\mathbf{k}) M_{ecd}(\mathbf{k}) \delta(\mathbf{k}-\mathbf{p}-\mathbf{q}) d\mathbf{p} d\mathbf{q} \\ &\times \int_{-\infty}^{\tau'} \hat{G}_{je}(\mathbf{k}';\tau',\tau_1) \hat{Q}_{ac}(\mathbf{p};\tau,\tau_1) \hat{Q}_{bd}(\mathbf{q};\tau,\tau_1) d\tau_1 \\ &- 4\iint M_{iab}(\mathbf{k}) M_{dce}(\mathbf{q}) \delta(\mathbf{k}-\mathbf{p}-\mathbf{q}) d\mathbf{p} d\mathbf{q} \\ &\times \int_{-\infty}^{\tau} \hat{G}_{bd}(\mathbf{q};\tau,\tau_1) \hat{Q}_{ac}(\mathbf{p};\tau,\tau_1) \hat{Q}_{ej}(-\mathbf{k};\tau_1,\tau') d\tau_1. \end{aligned} \tag{A44}$$

We apply the renormalization

$$\hat{Q}_{ij}(\mathbf{k};\tau,\tau') \to Q_{ij}(\mathbf{k};\tau,\tau'), \quad \hat{G}_{ij}(\mathbf{k};\tau,\tau') \to G_{ij}(\mathbf{k};\tau,\tau') \tag{A45}$$

to Eq. (A44), and have

$$\begin{aligned} LQ_{ij}(\mathbf{k};\tau,\tau') &= 2\iint M_{iab}(\mathbf{k}) M_{ecd}(\mathbf{k}) \delta(\mathbf{k}-\mathbf{p}-\mathbf{q}) d\mathbf{p} d\mathbf{q} \\ &\times \int_{-\infty}^{\tau'} G_{je}(\mathbf{k}';\tau',\tau_1) Q_{ac}(\mathbf{p};\tau,\tau_1) Q_{bd}(\mathbf{q};\tau,\tau_1) d\tau_1 \end{aligned}$$

$$-4\iint M_{iab}(\mathbf{k})M_{dce}(\mathbf{q})\delta(\mathbf{k}-\mathbf{p}-\mathbf{q})d\mathbf{p}d\mathbf{q}$$

$$\times\int_{-\infty}^{\tau} G_{bd}(\mathbf{q};\tau,\tau_1)Q_{ac}(\mathbf{p};\tau,\tau_1)Q_{ej}(-\mathbf{k};\tau_1,\tau')d\tau_1. \tag{A46}$$

If the latter half is not made in Eq. (A45), the resulting equation for $\tau=\tau'$ is coincident with the so-called quasi-normal approximation [A8]. In the formalism, the past events are overestimated, resulting in the occurrence of the negative energy spectrum.

We apply entirely the same procedure to G_{ij}, and have

$$LG_{ij}(\mathbf{k};\tau,\tau') = D_{ij}(\mathbf{k})\delta(\tau-\tau') - 4\iint M_{iab}(\mathbf{k})M_{dce}(\mathbf{q})\delta(\mathbf{k}-\mathbf{p}-\mathbf{q})d\mathbf{p}d\mathbf{q}$$

$$\times\int_{\tau'}^{\tau} G_{bd}(\mathbf{q};\tau,\tau_1)G_{ej}(-\mathbf{k};\tau_1,\tau')Q_{ac}(\mathbf{p};\tau,\tau_1)d\tau_1. \tag{A47}$$

This is combined with Eq. (A46) to constitute the DIA system of equations. The derivation of the DIA system may be more systematically with the aid of a diagrammatic representation [12, A2, A9].

A2.2.2. Difficulty about Green's function

In order to see the relationship of the foregoing DIA system with the Kolmogorov -5/3 power spectrum, we assume the isotropy of turbulence and write

$$Q_{ij}(\mathbf{k};\tau,\tau') = D_{ij}(\mathbf{k})Q(k;\tau,\tau'), \tag{A48}$$

$$G_{ij}(\mathbf{k};\tau,\tau') = D_{ij}(\mathbf{k})G(k;\tau,\tau'), \tag{A49}$$

from Eq. (5.18) with the helicity part dropped.

We substitute Eqs. (A48) and (A49) into Eqs. (A46) and (A47), and have

$$LQ(k;\tau,\tau') = k^2\iint\Big(N_{Q1}(k,p,q)\int_{-\infty}^{\tau'} G(k;\tau',\tau_1)Q(p;\tau,\tau_1)Q(q;\tau,\tau_1)d\tau_1$$

$$-N_{Q2}(k,p,q)\int_{-\infty}^{\tau} dt_1 G(q;\tau,\tau_1)Q(p;\tau,\tau_1)Q(k;\tau_1,\tau')\Big)\delta(\mathbf{k}-\mathbf{p}-\mathbf{q})d\mathbf{p}d\mathbf{q}, \tag{A50}$$

$$LG(k;\tau,\tau') = \delta(\tau-\tau') - k^2\iint N_G(k,p,q)\delta(\mathbf{k}-\mathbf{p}-\mathbf{q})d\mathbf{p}d\mathbf{q}$$

$$\times\int_{\tau'}^{\tau} G(q;\tau,\tau_1)G(k;\tau_1,\tau')Q(p;\tau,\tau_1)d\tau_1. \tag{A51}$$

For geometrical factors, we have the relations

$$N_{Q1}(k,p,q) = M_{eab}(\mathbf{k})M_{ecd}(\mathbf{k})D_{ac}(\mathbf{p})D_{bd}(\mathbf{q})$$

$$= N(k,p,q) \equiv \frac{q}{k}\left(xz + y^3\right), \tag{A52}$$

$$N_{Q2}(k,p,q) = N_G(k,p,q)$$

$$= 2M_{dab}(\mathbf{k})M_{bcd}(\mathbf{q})D_{ac}(\mathbf{p}) = N(k,p,q), \tag{A53}$$

where x, y, and z are the cosines of the angles opposite to sides k, p, and q that constitute a triangle. Specifically, the one-time covariance $Q(k;\tau,\tau)$ obeys

$$\left(\frac{\partial}{\partial\tau} + 2\nu k^2\right)Q(k;\tau,\tau) = 2k^2 \iint N(k,p,q)\Big(\int_{-\infty}^{\tau} d\tau_1 G(k;\tau,\tau_1)Q(p;\tau,\tau_1)Q(q;\tau,\tau_1)$$

$$-\int_{-\infty}^{\tau} d\tau_1 G(q;\tau,\tau_1)Q(p;\tau,\tau_1)Q(k;\tau_1,\tau)\Big)\delta(\mathbf{k}-\mathbf{p}-\mathbf{q})d\mathbf{p}d\mathbf{q}. \tag{A54}$$

For $Q(k;\tau,\tau')$ and $G(k;\tau,\tau')$, we assume the simplest stationary expressions

$$Q(k;\tau,\tau') = \sigma(k)\exp\left(-\omega(k)|\tau-\tau'|\right), \tag{A55}$$

$$G(k;\tau,\tau') = S(\tau-\tau')\exp\left(-\omega(k)(\tau-\tau')\right), \tag{A56}$$

where $\sigma(k)$ is related to the energy spectrum $E(k)$ as

$$E(k) = 4\pi k^2\sigma(k). \tag{A57}$$

The Kolmogorov -5/3 power law corresponds to

$$\sigma(k) = \frac{K_O}{4\pi}\varepsilon^{2/3}k^{-11/3}, \tag{A58}$$

with the inverse of the characteristic time,

$$\omega(k) = \frac{1}{C_\tau}\varepsilon^{1/3}k^{2/3}, \tag{A59}$$

where the energy dissipation rate ε is given by Eq. (4.22) with the magnetic part dropped, and K_O and C_τ are numerical coefficient (specifically, the former is called the Kolmogorov constant).

We substitute Eqs. (A55) and (A56) into Eq. (A54), and have

$$2\nu k^2\sigma(k) = 2k^2 \iint N(k,p,q)\frac{\sigma(p)(\sigma(q)-\sigma(k))}{\omega(k)+\omega(p)+\omega(q)}\delta(\mathbf{k}-\mathbf{p}-\mathbf{q})d\mathbf{p}d\mathbf{q}. \quad \text{(A60)}$$

We choose the wavevector $\mathbf{r}$ obeying

$$k_E << r << k_D, \quad \text{(A61)}$$

where k_E and k_D are the wavenumbers characterizing the energy-containing and -dissipation ranges, respectively. We integrate Eq. (A60) with respect to the wavevector $\mathbf{k}$, as

$$2\nu\int_{k>r} r^2\sigma(k)d\mathbf{k} = 2\int_{k>r} k^2 d\mathbf{k}$$

$$\times\iint N(k,p,q)\frac{\sigma(p)(\sigma(q)-\sigma(k))}{\omega(k)+\omega(p)+\omega(q)}\delta(\mathbf{k}-\mathbf{p}-\mathbf{q})d\mathbf{p}d\mathbf{q}. \quad \text{(A62)}$$

We use

$$\varepsilon = 2\nu\int k^2E(k)dk = 2\nu\int_{k>r} k^2\sigma(k)d\mathbf{k}, \quad \text{(A63)}$$

where we should note that little energy is dissipated in the inertial range. We combined Eqs. (A58) and (A59) with Eqs. (A62) and (A63), obtaining

$$K_O{}^2C_\tau = 5.2. \quad \text{(A64)}$$

The simple expressions such as Eqs. (A55) and (A56) cannot satisfy the response equation (A51) exactly. Then we seek its weak solution; namely, we integrate Eq. (A51) as

$$\int_{\tau'+0}^{\infty}\Big(LG(k;\tau,\tau') + k^2\iint N_G(k,p,q)\delta(\mathbf{k}-\mathbf{p}-\mathbf{q})d\mathbf{p}d\mathbf{q}$$

$$\times\int_{\tau'}^{\tau} G(q;\tau,\tau_1)G(k;\tau_1,\tau')Q(p;\tau,\tau_1)d\tau_1\Big)d\tau = 0. \quad \text{(A65)}$$

Then we have

$$\omega(k) = \nu k^2 + k^2\iint N(k,p,q)\frac{\sigma(p)}{\omega(p)+\omega(q)}\delta(\mathbf{k}-\mathbf{p}-\mathbf{q})d\mathbf{p}d\mathbf{q}, \quad \text{(A66)}$$

from Eqs. (A55) and (A56).

On substituting Eqs. (A58) and (A59) into Eq. (A66), we encounter the difficulty that the resulting integral does not converge in the lower limit of $\mathbf{p} \to 0$. Such divergence

of integral is called the infrared divergence [A10-A12]. Its cause is quite similar to the effect of $\mathbf{U}$ on $\mathbf{u}'$ in Eq. (5.7) with $\mathbf{u}'$ adopted as f'. As may be seen from the second term on the left-hand side of Eq. (A5), the small eddies expressed by $\mathbf{u}'$ are swept away by the large-scale motion $\mathbf{U}$. The time scale due to this sweeping-away effect, τ_S, is

$$\tau_S \propto (\mathbf{k}\cdot\mathbf{U})^{-1}. \tag{A67}$$

It is entirely different from the lifetime of eddies whose size is $2\pi/k$, that is, $\omega(k)^{-1}$ given by Eq. (A59).

In the context of inhomogeneous turbulence, the explicit sweeping-away effect may be removed through the moving-frame Fourier representation, Eq. (5.7). In the investigation of homogeneous turbulence, however, the sweeping-away effect still survives in the two-time equations (A50) and (A51), resulting in the above difficulty. The construction of a formalism free from the difficulty has long been a central theme in the study of homogeneous turbulence. At present, the infrared divergence was successfully removed with the aid of the Lagrangian description of turbulence field [A7, A13].

In the following explanation of inhomogeneous-turbulence theory, we make use of Eqs. (A55) and (A56). This is solely for the estimate of anisotropy induced by mean-velocity gradients. We should stress that the Lagrangian formalism is necessary for the analysis of homogeneous-turbulence statistics themselves. With this point in mind, we adopt

$$K_O \cong 1.5 \tag{A68}$$

as a typical observational value, which leads to

$$C_\tau = 2.3, \tag{A69}$$

from Eq. (A64).

A3. Statistical evaluation of Reynolds stress

A3.1. Wavenumber-space representation

Under the two-scale description based on Eqs. (5.2) and (5.3), the Reynolds stress

$$R_{ij} = \left\langle u_i'(\mathbf{x}) u_j'(\mathbf{x}) \right\rangle \tag{A70}$$

is expressed in the form

$$R_{ij} = \langle u_i'(\xi, \mathbf{X}; \tau, T) u_j'(\xi, \mathbf{X}; \tau, T) \rangle. \tag{A71}$$

We assume the homogeneity concerning ξ, and define

$$R_{ij}(\mathbf{k}, \mathbf{X}; \tau, T) = \frac{\langle u_i'(\mathbf{k}, \mathbf{X}; \tau, T) u_j'(\mathbf{k}', \mathbf{X}; \tau, T) \rangle}{\delta(\mathbf{k} + \mathbf{k}')}. \tag{A72}$$

Using Eq. (A72), we may write

$$R_{ij} = \int R_{ij}(\mathbf{k}, \mathbf{X}; \tau, T) d\mathbf{k}. \tag{A73}$$

We substitute the scale-parameter expansion (A10) into Eq. (A72), and retain the terms up to $O(\delta_S)$. Then we have

$$R_{ij}(\mathbf{k}; \tau) = \frac{\langle u_{0i}'(\mathbf{k}; \tau) u_{0j}'(\mathbf{k}'; \tau) \rangle}{\delta(\mathbf{k} + \mathbf{k}')}$$

$$+\delta_S \left(\frac{\langle u_{1i}'(\mathbf{k}; \tau) u_{0j}'(\mathbf{k}'; \tau) \rangle}{\delta(\mathbf{k} + \mathbf{k}')} + \frac{\langle u_{0i}'(\mathbf{k}; \tau) u_{1j}'(\mathbf{k}'; \tau) \rangle}{\delta(\mathbf{k} + \mathbf{k}')} \right). \tag{A74}$$

The $O(1)$ term has already been given by Eqs. (A40) and (A48), and are written as

$$\frac{\langle u_{0i}'(\mathbf{k}; \tau) u_{0j}'(\mathbf{k}'; \tau) \rangle}{\delta(\mathbf{k} + \mathbf{k}')} = D_{ij}(\mathbf{k}) Q(k; \tau, \tau). \tag{A75}$$

In relation to the first part of the $O(\delta_S)$ term, we define

$$R_{ij}^{(1)} = -\frac{\partial U_\ell}{\partial X_m} \int_{-\infty}^{\tau} \frac{\langle G_{i\ell}'(\mathbf{k}; \tau, \tau_1) u_{0m}'(\mathbf{k}; \tau_1) u_{0j}'(\mathbf{k}'; \tau) \rangle}{\delta(\mathbf{k} + \mathbf{k}')} d\tau_1, \tag{A76}$$

$$R_{ij}^{(2)} = -\int_{-\infty}^{\tau} \frac{\left\langle G_{i\ell}'(\mathbf{k}; \tau, \tau_1) \frac{D^* u_{0\ell}'(\mathbf{k}; \tau_1)}{DT^*} u_{0j}'(\mathbf{k}'; \tau) \right\rangle}{\delta(\mathbf{k} + \mathbf{k}')} d\tau_1. \tag{A77}$$

Then we may write

$$\frac{\langle u_{1i}'(\mathbf{k}; \tau) u_{0j}'(\mathbf{k}'; \tau) \rangle}{\delta(\mathbf{k} + \mathbf{k}')} = R_{ij}^{(1)} + R_{ij}^{(2)}, \tag{A78}$$

from Eq. (A30) for $\mathbf{u}_1'$ [we may confirm that the third and fourth terms of $\mathbf{I}_1$ in Eq. (A22) give no contribution since it is an odd function of $\mathbf{k}$]. We substitute the perturbational solution (A38) and (A39), and retain the lowest-order contribution in $\hat{Q}$. As a result, we have

$$R_{ij}^{(1)} = -\frac{\partial U_\ell}{\partial X_m}\int_{-\infty}^{\tau}\hat{G}_{i\ell}(\mathbf{k};\tau,\tau_1)\hat{Q}_{mj}(\mathbf{k};\tau,\tau_1)d\tau_1. \tag{A79}$$

The application of the renormalization (A45) to Eq. (A79) leads to

$$R_{ij}^{(1)} = -D_{i\ell}(\mathbf{k})D_{mj}(\mathbf{k})\left(\int_{-\infty}^{\tau}G(k;\tau,\tau_1)Q(k;\tau,\tau_1)d\tau_1\right)\frac{\partial U_\ell}{\partial X_m}, \tag{A80}$$

under the isotropic assumption (A48) and (A49). We combine Eq. (A80) with its counterpart of the second part of the $O(\delta_S)$ term in Eq. (A74), and obtain

$$R_{ij}^{(1)} + R_{ji}^{(1)} = -\left(D_{i\ell}(\mathbf{k})D_{mj}(\mathbf{k}) + D_{j\ell}(\mathbf{k})D_{mi}(\mathbf{k})\right)\frac{\partial U_\ell}{\partial X_m}$$

$$\times\left(\int_{-\infty}^{\tau}G(k;\tau,\tau_1)Q(k;\tau,\tau_1)d\tau_1\right). \tag{A81}$$

Equation (A77) may be evaluated in entirely the same manner. In correspondence to Eq. (A79), we have

$$R_{ij}^{(2)} = -\int_{-\infty}^{\tau}\hat{G}_{i\ell}(\mathbf{k};\tau,\tau_1)\frac{\left\langle\dfrac{D^*w_\ell(\mathbf{k};\tau_1)}{DT^*}w_j(\mathbf{k}';\tau)\right\rangle}{\delta(\mathbf{k}+\mathbf{k}')}d\tau_1. \tag{A82}$$

After Eq. (A49), we write the lowest-order part of G_{ij}, $\hat{G}_{ij}$, as

$$\hat{G}_{ij}(\mathbf{k};\tau,\tau') = D_{ij}(\mathbf{k})\hat{G}(k;\tau,\tau'), \tag{A83}$$

and note

$$D_{ij}(\mathbf{k})w_j(\mathbf{k};\tau) = w_i(\mathbf{k};\tau). \tag{A84}$$

Then we have

$$R_{ij}^{(2)} = -\int_{-\infty}^{\tau}\hat{G}(k;\tau,\tau_1)\frac{\left\langle\dfrac{D^*w_i(\mathbf{k};\tau_1)}{DT^*}w_j(\mathbf{k}';\tau)\right\rangle}{\delta(\mathbf{k}+\mathbf{k}')}d\tau_1, \tag{A85}$$

which gives

$$R_{ij}^{(2)} + R_{ji}^{(2)} = -\int_{-\infty}^{\tau} \hat{G}(k;\tau,\tau_1) \frac{D^*}{DT^*} \frac{\langle w_i(\mathbf{k};\tau_1) w_j(\mathbf{k}';\tau)\rangle}{\delta(\mathbf{k}+\mathbf{k}')} d\tau_1$$

$$= -\int_{-\infty}^{\tau} \hat{G}(k;\tau,\tau_1) \frac{D^* \hat{Q}_{ij}(\mathbf{k};\tau,\tau_1)}{DT^*} d\tau_1. \tag{A86}$$

Under the renormalization (A45), Eq. (A86) results in

$$R_{ij}^{(2)} + R_{ji}^{(2)} = -D_{ij}(\mathbf{k}) \int_{-\infty}^{\tau} G(k,\tau,\tau_1) \frac{DQ(k,\tau,\tau_1)}{DT} d\tau_1, \tag{A87}$$

where use has been made of the replacement

$$\frac{D^*}{DT^*} \to \frac{D}{DT} \tag{A88}$$

since the neglected part is odd in $\mathbf{k}$ and gives no contribution to the final result.

We substitute Eqs. (A75), (A78), (A81), and (A87) into Eq. (A74), and make the replacement

$$\mathbf{X} \to \delta_S \mathbf{x}, \quad T \to \delta_S t. \tag{A89}$$

Then we have [12, A4]

$$R_{ij}(\mathbf{k},\mathbf{x};\tau,t) = D_{ij}(\mathbf{k}) \left(Q(k;\tau,\tau) - \int_{-\infty}^{\tau} G(k;\tau,\tau_1) \frac{DQ(k;\tau,\tau_1)}{Dt} d\tau_1 \right)$$

$$-\left(D_{i\ell}(\mathbf{k}) D_{mj}(\mathbf{k}) + D_{j\ell}(\mathbf{k}) D_{mi}(\mathbf{k})\right) \left(\int_{-\infty}^{\tau} G(k;\tau,\tau_1) Q(k;\tau,\tau_1) d\tau_1 \right) \frac{\partial U_\ell}{\partial x_m}. \tag{A90}$$

Here we should note that the scale parameter δ_S has disappeared automatically.

We rewrite Eq. (A73) as

$$R_{ij} = \int_0^\infty dk \int_{S(k)} R_{ij}(\mathbf{k},\mathbf{x};\tau,t) dS, \tag{A91}$$

where $S(k)$ denotes the surface with k as the radius. From Eq. (5.28) and

$$\int \frac{k_i k_j k_\ell k_m}{k^4} d\mathbf{k} = \frac{1}{15} \left(\delta_{ij}\delta_{\ell m} + \delta_{i\ell}\delta_{jm} + \delta_{im}\delta_{j\ell} \right) \int d\mathbf{k}, \tag{A92}$$

Eq. (A91) with Eq. (A90) is reduced to

$$B_{ij} \equiv R_{ij} - \frac{2}{3} K\delta_{ij} = -\nu_T S_{ij}. \tag{A93}$$

Here the turbulent energy K and the turbulent viscosity ν_T are given by

$$K = \int_0^\infty Q(k;\tau,\tau)d\mathbf{k} - \int_0^\infty d\mathbf{k}\int_{-\infty}^{\tau} G(k;\tau,\tau_1)\frac{DQ(k;\tau,\tau_1)}{Dt}d\tau_1, \tag{A94}$$

$$\nu_T = \frac{7}{15}\int_0^\infty d\mathbf{k}\int_{-\infty}^{\tau} G(k;\tau,\tau_1)Q(k;\tau,\tau_1)d\tau_1, \tag{A95}$$

and the mean velocity-strain tensor S_{ij} is defined by Eq. (4.28). From Eq. (A94), the energy spectrum $E(k)$ is

$$E(k) = 4\pi k^2\left(Q(k;\tau,\tau) - \int_{-\infty}^{\tau} G(k;\tau,\tau_1)\frac{DQ(k;\tau,\tau_1)}{Dt}d\tau_1\right). \tag{A96}$$

Under Eqs. (A55) and (58), Eq. (A96) expresses the nonequilibrium effect on the Kolmogorov spectrum [A14]. Equation (A93) is the so-called turbulent-viscosity representation for the Reynolds stress.

A3.2. Physical-space representation

Equations (A94) and (A95) are written in terms of the velocity correlation $Q(k;\tau,\tau')$ and the Green's function $G(k;\tau,\tau')$ of the $O(1)$ part in the δ_S expansion. The correlation $Q(k;\tau,\tau')$ is related to the energy spectrum $E(k)$ as Eqs. (A55) and (A57), and its low-wavenumber components play the role of reserving the energy supplied from the mean flow. On the other hand, the high-wavenumber components are connected with the energy dissipation process through Eq. (A63). It is generally difficult to express $Q(k;\tau,\tau')$ possessing such a broad role in a compact mathematical form. The inertial range occurring at high Reynolds numbers, however, partially shares some properties with the energy-containing and -dissipation ranges, through the Kolmogorov spectrum, Eq. (A57) with Eq. (A58). We shall make full use of this fortunate situation and reduce Eqs. (A94) and (A95) to one-point expressions in physical space.

We approximate $Q(k;\tau,\tau')$ with the aid of the Kolmogorov spectrum. The simplest expressions for $Q(k;\tau,\tau')$ and $G(k;\tau,\tau')$ leading to the spectrum are Eqs. (A55) and (A56) with Eqs. (A58) and (A59). As the numerical constants in them, we adopt Eqs. (A68) and (A69). We denote the wavenumber characterizing the energy-containing range by k_E. We approximate the integral in wavenumber space by

$$\int_0^\infty dk \to \int_{k_E}^\infty dk, \tag{A97}$$

as in Fig. A2. In correspondence to k_E, we introduce the characteristic length in the energy-containing region, ℓ_E, through

$$\ell_E(\mathbf{x},t) = \frac{2\pi}{k_E(\mathbf{x},t)}. \tag{A98}$$

Here the important point is that these characteristic quantities depend on location and time. In this context, the energy dissipation rate occurring in Eqs. (A58) and (A59), ε, also changes spatially and temporally and may be written as

$$\varepsilon = \varepsilon(\mathbf{x},t). \tag{A99}$$

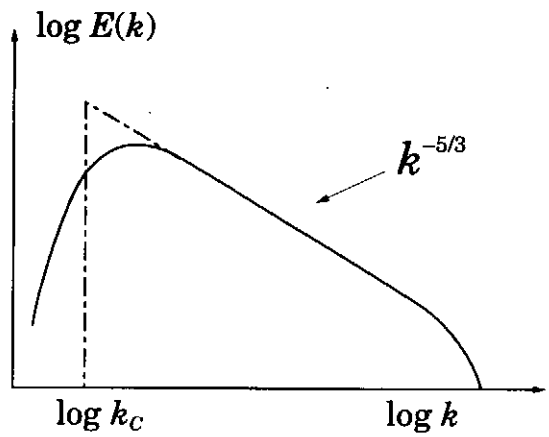

Fig. A2. Inertial-range approximation to the energy spectrum.

We substitute Eqs. (A55) and (A56) into Eq. (A94), and have

$$K = K_O \varepsilon(\mathbf{x},t)^{2/3} \int_{k\geq k_E} k^{-5/3} dk$$

$$-\frac{K_O C_\tau}{4} \int_{k\geq k_E} k^2 \left(2\varepsilon(\mathbf{x},t)^{-1/3} k^{-2/3} \frac{D}{Dt}\left(\varepsilon(\mathbf{x},t)^{2/3} k^{-11/3}\right) dk \right.$$

$$\left. -k^{-5} \frac{D}{Dt}\left(\varepsilon(\mathbf{x},t)^{1/3} k^{2/3}\right)\right) dk. \tag{A100}$$

We make the transformation

$$s = k / k_E, \tag{A101}$$

and note the dependence of k_E on $(\mathbf{x}, t)$. We substitute Eq. (A98) into the resulting expression, and adopt Eqs. (A58) and (A59) as K_O and C_τ in Eq. (A100). As a result, we have

$$K = K\{\ell_E, \varepsilon\} = C_{K1}\varepsilon^{2/3}\ell_E{}^{2/3} - C_{K2}\varepsilon^{-2/3}\ell_E{}^{4/3}\frac{D\varepsilon}{Dt} - C_{K3}\varepsilon^{1/3}\ell_E{}^{1/3}\frac{D\ell_E}{Dt}, \tag{A102}$$

where coefficients C_{Kn} $(n = 1-3)$ are evaluated as

$$C_{K1} = 0.67,\ C_{K2} = 0.058,\ C_{K3} = 0.47. \tag{A103}$$

From the viewpoint of the scale-parameter expansion (A10), the first term of Eq. (A102) is of $O(1)$, whereas the remaining two are of $O(\delta_S)$. Then we solve Eq. (A102) in the perturbational manner based on the first term, and have

$$\ell_E = \ell_E\{K, \varepsilon\} = C_{\ell 1}K^{3/2}\varepsilon^{-1} + C_{\ell 2}K^{3/2}\varepsilon^{-2}\frac{DK}{Dt} - C_{\ell 3}K^{5/2}\varepsilon^{-3}\frac{D\varepsilon}{Dt}, \tag{A104}$$

with

$$C_{\ell 1} = 1.8,\ C_{\ell 2} = 4.4,\ C_{\ell 3} = 2.6. \tag{A105}$$

In the stage of Eq. (A97), k_E was introduced as the unknown lower limit of integral, but it has been related to the observable physical quantities K and ε though Eqs. (A98) and (A104).

We evaluate Eq. (A95) similarly and combine it with the result from the $O(\delta_S{}^2)$ analysis [12, A5, A15]. Then we have

$$\nu_T = \nu_T\{\ell_E, \varepsilon\} = C_{\nu\ell}\varepsilon^{1/3}\ell_E{}^{4/3} - C_{\nu\ell\varepsilon}\frac{\ell_E{}^2}{\varepsilon}\frac{D\varepsilon}{Dt} - C_{\nu\ell\ell}\ell_E\frac{D\ell_E}{Dt}, \tag{A106}$$

where

$$C_{\nu\ell} = 0.054,\ C_{\nu\ell\varepsilon} = 0.011, C_{\nu\ell\ell} = 0.11\ . \tag{A107}$$

The substitution of Eq. (A104) into Eq. (A106) leads to

$$\nu_T = C_{\nu 1}\left(1 - C_{\nu 2}\frac{1}{\varepsilon}\frac{DK}{Dt} + C_{\nu 3}\frac{K}{\varepsilon^2}\frac{D\varepsilon}{Dt}\right)\frac{K^2}{\varepsilon}, \tag{A108}$$

with

$$C_{v1} = 0.12,\ C_{v2} = 1.2,\ C_{v3} = 0.76. \tag{A109}$$

Here only the first term in Eq. (A104) should be used as long as the D/Dt-related terms in Eq. (A106) are dropped. These D/Dt-related terms that are combined with the mean velocity-strain rate S_{ij} are of $O(\delta_S{}^2)$ in the TSDIA analysis. Equation (6.28) with Eq. (6.31) corresponds to Eq. (A108) with the D/Dt-related terms dropped.

As an instance of the theoretical suggestions to turbulence modeling, we mention the modeling of the hydrodynamic version of Eq. (6.13). We perform its $O(\delta_S)$ TSDIA calculation, and have [A16, A17]

$$\mathbf{T}_K = 0.15\frac{K^2}{\varepsilon}\nabla K - 0.047\frac{K^3}{\varepsilon^2}\nabla\varepsilon. \tag{A110}$$

This finding supports the modeling such as Eq. (6.13).

REFERENCES

[A1] Leslie D C 1974 *Developments in the Theory of Turbulence* (Oxford: Clarendon)

[A2] McComb W D 1990 *The Physics of Fluids* (Oxford: Clarendon)

[A3] Lesieur M 1997 *Turbulence in Fluids* (3rd ed.) (Dordrecht: Kluwer)

[A4] Hamba F 1987 J. Phys. Soc. Jpn. **56** 2721

[A5] Okamoto M 1994 J. Phys. Soc. Jpn. **63** 2102

[A6] Kraichnan R H 1959 J. Fluid Mech. **5** 497

[A7] Kraichnan R H 1977 J. Fluid Mech. **83** 349

[A8] Tatsumi T 1980 Adv. Appl. Mech. **20**, 39

[A9] Wyld W H 1961 Ann. Phys. NY **14** 143

[A10] Kraichnan R H 1964 Phys. Fluids **7** 1723

[A11] Kraichnan R H 1965 Phys. Fluids **8** 575

[A12] Nakano T 1972 Ann. Phys. NY **73** 326

[A13] Kaneda Y 1981 J. Fluid Mech. **107** 131

[A14] Yoshizawa A and Nisizima S 1993 Phys. Fluids A **5** 3302

[A15] Yoshizawa A 1994 Phys. Rev. E **49** 4065

[A16] Yoshizawa A 1982 J. Phys. Soc. Jpn. **51** 2326

[A17] Shimomura Y 1998 Phys. Fluids **10** 2636

Recent Issues of NIFS Series

NIFS-694 L.N. Vyachenslavov, K. Tanaka, K. Kawahata,
CO2 Laser Diagnostics for Measurements of the Plasma Density Profile and Plasma Density Fluctuations on LHD Apr. 2001

NIFS-695 T. Ohkawa,
Spin Dependent Transport in Magnetically Confined Plasma: May 2001

NIFS-696 M. Yokoyama, K. Ida, H. Sanuki, K. Itoh, K. Narihara, K. Tanaka, K. Kawahata, N. Ohyabu and LHD experimental group
Analysis of Radial Electric Field in LHD towards Improved Confinement: May 2001

NIFS-697 M. Yokoyama, K. Itoh, S. Okamura, K. Matsuoka, S. -I. Itoh,
Maximum-J Capability in a Quasi-Axisymmetric Stellarator: May 2001

NIFS-698 S-I. Itoh and K. Itoh,
Transition in Multiple-scale-lengths Turbulence in Plasmas: May 2001

NIFS-699 K. Ohi, H. Naitou, Y. Tauchi, O. Fukumasa,
Bifurcation in Asymmetric Plasma Divided by a Magnetic Filter: May 2001

NIFS-700 H. Miura, T. Hayashi and T. Sato,
Nonlinear Simulation of Resistive Ballooning Modes in Large Helical Device: June 2001

NIFS-701 G. Kawahara and S. Kida,
A Periodic Motion Embedded in Plane Couette Turbulence: June 2001

NIFS-702 K. Ohkubo,
Hybrid Modes in a Square Corrugated Waveguide: June 2001

NIFS-703 S.-I. Itoh and K. Itoh,
Statistical Theory and Transition in Multiple-scale-lengths Turbulence in Plasmas: June 2001

NIFS-704 S. Toda and K. Itoh,
Theoretical Study of Structure of Electric Field in Helical Toroidal Plasmas: June 2001

NIFS-705 K. Itoh and S-I. Itoh,
Geometry Changes Transient Transport in Plasmas: June 2001

NIFS-706 M. Tanaka and A. Yu. Grosberg
Electrophoresis of Charge Inverted Macroion Complex: Molecular Dynamics Study: July 2001

NIFS-707 T-H Watanave, H. Sugama and T. Sato
A Nondissipative Simulation Method for the Drift Kinetic Equation: July 2001

NIFS-708 N. Ishihara and S. Kida,
Dynamo Mechanism in a Rotating Spherical Shell: Competition between Magnetic Field and Convection Vortices July 2001

NIFS-709 LHD Experimental Group,
Contributions to 28th European Physical Society Conference on Controlled Fusion and Plasma Physics (Madeira Tecnopolo, Funchal, Portugal, 18-22 June 2001) from LHD Experiment: July 2001

NIFS-710 V.Yu. Sergeev, R.K. Janev, M.J. Rakovic, S. Zou, N. Tamura, K.V. Khlopenkov and S. Sudo
Optimization of the Visible CXRS Measurements of TESPEL Diagnostics in LHD; Aug. 2001

NIFS-711 M. Bacal, M. Nishiura, M. Sasao, M. Wada, M. Hamabe, H. Yamaoka,
Effect of Argon Additive in Negative Hydrogen Ion Sources; Aug. 2001

NIFS-712 K. Saito, R. Kumazawa, T. Mutoh, T. Seki, T. Watari, T. Yamamoto, Y. Torii, N. Takeuchi C. Zhang, Y. Zhao, A. Fukuyama, F. Shimpo, G. Nomura, M. Yokota, A. Kato, M. Sasao, M. Isobe, A.V. Krasilnikov, T. Ozaki, M. Osakabe, K. Narihara, Y. Nagayama, S. Inagaki, K. Itoh, T. Ido, S. Morita, K. Ohkubo, M. Sato, S. Kubo, T. Shimozuma, H. Idei, Y. Yoshimura, T. Notake, O. Kaneko, Y. Takeiri, Y. Oka, K. Tsumori, K. Ikeda, A. Komori, H. Yamada, H. Funaba, K.Y. Watanabe, S. Sakakibara, R. Sakamoto, J. Miyazawa, K. Tanaka, B.J. Peterson, N. Ashikawa, S. Murakami, T. Minami, M. Shoji, S. Ohdachi, S. Yamamoto, H. Suzuki, K. Kawahata, M. Emoto, H. Nakanishi, N. Inoue, N. Ohyabu, Y. Nakamura, S. Masuzaki, S. Muto, K. Sato, T. Morisaki, M. Yokoyama, T. Watanabe, M. Goto, I. Yamada, K. Ida, T. Tokuzawa, N. Noda, K. Toi, S. Yamaguchi, K. Akaishi, A. Sagara, K. Nishimura, K. Yamazaki, S. Sudo, Y. Hamada, O. Motojima, M. Fujiwara,
A Study of High-Energy Ions Produced by ICRF Heating in LHD: Sep. 2001

NIFS-713 Y. Matsumoto, S.-I. Oikawa and T. Watanabe,
Field Line and Particle Orbit Analysis in the Periphery of the Large Helical Device; Sep. 2001

NIFS-714 S. Toda, M. Kawasaki, N. Kasuya, K. Itoh, Y. Takase, A. Furuya, M. Yagi and S. -I. Itoh,
Contributions to the 8th IAEA Technical Committee Meeting on H-Mode Physics and Transport Barriers (5-7 September 2001, Toki, Japan): Oct. 2001

NIFS-715 A. Maluckov, N. Nakajima, M. Okamoto, S. Murakami and R. Kanno,
Statistical Properties of the Particle Radial Diffusion in a Radially Bounded Irregular Magnetic Field; Oct. 2001

NIFS-716 Boris V. Kuteev,
Kinetic Depletion Model for Pellet Ablation; Nov. 2001

NIFS-717 Boris V. Kuteev, Lev D. Tsendin,
Analytical Model of Neutral Gas Shielding for Hydrogen Pellet Ablation: Nov. 2001

NIFS-718 Boris V. Kuteev,
Interaction of Cover and Target with Xenon Gas in the IFE-Reaction Chamber: Nov. 2001

NIFS-719 A. Yoshizawa, N. Yokoi, S.-I Itoh and K. Itoh,
Mean-Field Theory and Self-Consistent Dynamo Modeling: Dec. 2001